VŠB - TECHNICAL UNIVERSITY OSTRAVA
FACULTY OF ELECTRICAL ENGINEERING
AND COMPUTER SCIENCE

Ph.D. THESIS

2019

Tan-Phuoc Huynh

VŠB - TECHNICAL UNIVERSITY OSTRAVA
FACULTY OF ELECTRICAL ENGINEERING
AND COMPUTER SCIENCE
DEPARTMENT OF COMPUTER SCIENCE

Performance enhancement solutions in wireless communication networks

Ph.D. THESIS

Doctoral Study Branch: 2601V018 Communication Technology

Doctoral Study Programme: P1807 Computer Science, Communication Technology and Applied Mathematics

2019 Tan-Phuoc Huynh

FACULTY OF ELECTRICAL ENGINEERING AND COMPUTER SCIENCE
DEPARTMENT OF TELECOMMUNICATIONS

Performance enhancement solutions in wireless communication networks

Ph.D. Thesis; Delivered in May, 2019

Doctoral Study Programme:
P1807 Computer Science, Communication Technology and Applied Mathematics
Doctoral Study Branch: 2601V018 Communication Technology

Ph.D. Student: MSc. Tan-Phuoc Huynh
VŠB - Technical University of Ostrava
Faculty of Electrical Engineering and Computer Science
17. listopadu 2172/15, 708 00 Ostrava, Czech Republic
phuoc.huynh.tan.st@vsb.cz

Supervisor: Prof. Ing. Miroslav Vozňák, PhD.
VŠB - Technical University of Ostrava
Faculty of Electrical Engineering and Computer Science
17. listopadu 2172/15, 708 00 Ostrava, Czech Republic
miroslav.voznak@vsb.cz

OSTRAVA, 2019

DECLARATION

I myself declare that this thesis is conducted as the result of my original research done by myself with the guidance of my supervisor in the Faculty of Electrical Engeneering and Computer Science at VSB - Technical University of Ostrava as a candidate for the Doctor of Communication Technology.
My works included below were carried out under the supervision of Prof. Ing. Miroslav Vozňák, Ph.D. It is noted that this thesis has never been submitted for any other degrees or awards in any other universities or educational institutions.

. . . .
(author's signature)

ACKNOWLEDGEMENT

First and foremost, I would like to express my deepest thankfulness to **my supervisor Prof. Ing. Miroslav Vozňák, Ph.D.** for his encouragement and great support. I appreciate all his contributions of knowledge, time, ideas, and constant support through the process of completion of my thesis. Without his motivation and instructions, the thesis would have been impossible to be done effectively.

I would also like to use the opportunity to send my gratitude to Pham Ngoc Son, Ph.D. for his kindly help during my study. This thesis has improved considerably thanks to the valuable comments and feedback from him. His point and exact suggestions, as well as long discussions, help me to get familiar with the research problems.

I want to thank the members of my research team for creating a perfect, special research atmosphere. They are always willing to ask questions, help and share me all useful information. My deeply thanks come to all my friends: Dr. Lukáš Ševčik and Mr. Jakub Jalowiczor during my study period in VSB - Technical University of Ostrava. Their kindly help, care and motivation gave me strength and helped me up all the trouble.

Finally, I would like to thank my parents, brothers, sisters, and my wife who always encouraged me with love and devoutly supported me. Especially, I am very much thankful to my wife Chau Bich Van for all her love, support, understanding and constant motivation to complete this research work.

. . . .

(author's signature)

ABSTRAKT

V této dizertační práci je provedena studie nových přenosových protokolů pro různé bezdrátové síťové systémy. S využitím matematické analýzy jsme analyzovali a vyhodnotili efektivitu přenosu z hlediska pravděpodobnosti výpadku přes Rayleighův kanál. Teoretické analýzy jsou ověřeny provedenými simulacemi metodou Monte Carlo.

Nejprve došlo ke studii kooperativního přenosu ve dvoucestném dekóduj-a-předej (Two-Way Decode-and-Forward–TWDF) a vícecestném DF schématu s větším počtem přenosových uzlů pro sekundární systém, kdy takto byl získán přístup ke spektru spolu s primárním systémem. Konkrétně jsme navrhli dvoucestné DF schéma se získáváním energie a dvoucestné DF neortogonální schéma s mnohonásobným přístupem (Non-orthogonal Multiple Access–NOMA) s digitálním síťovým kódováním. Kromě toho rovněž zkoumáme bezdrátové systémy s větším počtem přenosových uzlů, kde je přítomen výběr nejlepšího přenosového uzlu pro optimalizaci efektivnosti navrženého schématu. Přenosové protokoly navržených schémat EHAF (Energy Harvesting Amplify and Forward) a EHDF(Energy Harvesting Decode and Forward) jsou společně porovnány v identickém prostředí z pohledu pravděpodobnosti výpadku. Následně, na základě získaných výsledků, jsme dospěli k závěru, že navržená schémata vylepšují výkonnost bezdrátových kooperativních systémů, konkrétně jejich propustnost.

Dále jsme se zaměřili na zkoumání NOMA technologie a navrhli optimální řešení (protokoly) pro urychlení datového přenosu a zajištění QoS v další generaci bezdrátových komunikací. V této práci jsme navrhli dvoucestné DF NOMA schéma (nazýváno jako TWNOMA protokol), ve kterém mezilehlý přenosový uzel napomáhá dvěma zdrojovým uzlům komunikovat mezi sebou. Výsledky simulace a analýzy ukazují, že navržený protokol TWNOMA vylepšuje dosaženou přenosovou rychlost v porovnání s konvenčním dvoucestným schématem používajícím DNC (TWDNC protokol), dvoucestným schématem bez použití DNC (TWNDNC protokol) a dvoucestným schématem v zesil-a-předej (amplify-and-forward) přenosových systémech (TWANC protokol).

Nakonec jsme zvážili využití kombinace NOMA a zabezpečení fyzické vrstvy (Physical Layer Security–PLS) v podpůrné kooperativní kognitivní síti (Underlay Cooperative Cognitive Network–UCCN). Zde je zde zkoumán výběr nejlepšího přenosového uzlu, který užívá NOMA a bere v úvahu PLS pro efektivnější přenos a zabezpečení nové generace bezdrátových sítí.

KLÍČOVÁ SLOVA

Neortogonální mnohonásobný přístup, postupná eliminace rušení, zabezpečení fyzické vrstvy, kooperativní komunikace, dvoucestné schéma, dekóduj-a-předej, oportunistický výběr přenosového uzlu, kognitivní rádio, získávání energie, pravděpodobnost výpadku.

ABSTRACT

In this dissertation thesis, we study the new relaying protocols for different wireless network systems. We analyze and evaluate an efficiency of the transmission in terms of the outage probability over Rayleigh fading channels by mathematical analyses. The theoretical analyses are verified by performing Monte Carlo simulations.

First, we study the cooperative relaying in the Two-Way Decode-and-Forward (DF) and multi-relay DF scheme for a secondary system to obtain spectrum access along with a primary system. In particular, we proposed the Two-Way DF scheme with Energy Harvesting, and the Two-Way DF Non-orthogonal Multiple Access (NOMA) scheme with digital network coding. Besides, we also investigate the wireless systems with multi-relay; the best relay selection is presented to optimize the effect of the proposed scheme. The transmission protocols of the proposed schemes EHAF (Energy Harvesting Amplify and Forward) and EHDF (Energy Harvesting Decode and Forward) are compared together in the same environment and in term of outage probability. Hence, with the obtained results, we conclude that the proposed schemes improve the performance of the wireless cooperative relaying systems, particularly their throughput.

Second, we focus on investigating the NOMA technology and proposing the optimal solutions (protocols) to advance the data rate and to ensure the Quality of Service (QoS) for the users in the next generation of wireless communications. In this thesis, we propose a Two-Way DF NOMA scheme (called a TWNOMA protocol) in which an intermediate relay helps two source nodes to communicate with each other. Simulation and analysis results show that the proposed protocol TWNOMA is improving the data rate when comparing with a conventional Two-Way scheme using digital network coding (DNC) (called a TWDNC protocol), Two-Way scheme without using DNC (called a TWNDNC protocol) and Two-Way scheme in amplify-and-forward(AF) relay systems (called a TWANC protocol).

Finally, we considered the combination of the NOMA and physical layer security (PLS) in the Underlay Cooperative Cognitive Network (UCCN) . The best relay selection strategy is investigated, which uses the NOMA and considers the PLS to enhance the transmission efficiency and secrecy of the new generation wireless networks.

KEYWORDS

Non-orthogonal multiple access, successive interference cancellation (SIC), physical layer security, cooperative communication, Two-Way, decode-and-forward, opportunistic relay selection, cognitive radio (CR), energy harvesting, outage probability.

CONTENTS

LIST OF FIGURES

LIST OF ABBREVIATIONS AND SYMBOLS

Abbreviations

AF	Amplify-and-Forward
AWGNs	Additive White Gaussian Noises
BS	Base Station
CDF	Cumulative Distribution Function
CR	Cognitive Radio
CSI	Channel State Information
DF	Decode-and-Forward
DNC	Digital Network Coding
EH	Energy Harvesting
IoT	Internet of Things
IQI	In-phase and Quadrature-phase Imbalances
NOMA	Non-Orthogonal Multiple Access
OMA	Orthogonal Multiple Access
OPs	Outage Probabilities
pdf	probability density function
PLS	Physical Layer Secuurity
QoS	Quality of Service
RF	Radio Frequency
RX	Receiver
SIC	Successive Interference Cancellation
SINRs	signal-to-Interference-plus-Noise Ratios
SNR	Signal to Noise Ratio
SOPs	Secrecy Outage Probabilities
TX	Transmitter
UCCN	Underlay Cooperative Cognitive Network

1 INTRODUCTION

In recent time, wireless networks have become one of the most common communication methods due to its flexibility in different environments. Besides, many kinds of smart devices and the Internet of Things (IoT) devices are produced. They are predicted to keep rising in the future. Therefore, they will make to surge an increase in amounts of wireless connections. As a result, this tendency is developed in the 5G systems. A major challenge for the wireless system designer is to find the solutions to improve the performance for reliable transmission, high data rate (i.e. bandwidth) and security.

To deploy above problems, in this thesis, we introduce the new NOMA technology and apply the cooperative relay methods: Two-Way cooperative relay, relay selection to propose the relay protocols to enhance the efficiency in the wireless communication systems. Besides, we have also proposed the NOMA in the UCCN with PLS to increase security transmission and improve the bandwidth for wireless communication systems. The concepts of this Section are presented as follows.

1.1 Backgrounds

1.1.1 NOMA technology

The NOMA has been recently received significant attention from the researches in wireless systems as a promising technique to achieve enhanced spectrum efficiency of the fifth generation (5G) mobile network [1, 2, 3, 4, 5, 6]. In the NOMA technique, the users can share both time and frequency resources and only adjust their power allocation ratios. The users with better channel conditions can serve as relays to enhance the system performance by using SIC [7, 8]. This technology improves the limitation of orthogonal multiple access (OMA) . Figure 1.1 is denoted the difference between the NOMA and OMA. The OMA technique is known as Time division multiple access (TDMA), and orthogonal frequency-division multiple access (OFDMA). In TDMA technology, the users share the same frequency channel by dividing the signal into different time slots. The users communicate in quick sequence, one after the other, each using their assigned time slots. With the OFDMA, the multi-user is contacted via orthogonal frequency-division multiplexing (OFDM) technique, in which subcarrier frequencies are chosen so that the subcarriers are orthogonal to each other [8].

In figure 1.1 (a), the characteristic NOMA scheme is considered with a single-cell downlink scenario in which a single base station (BS) connects to two users (U_1, U_2) directly. The BS always transmits the signals to the U_1 and U_2 at the same time, the total power also distributes two users. It is assumed that each user has a private antenna. The variances of Zero-mean Additive White Gaussian Noises (AWGNs) are equal, denoted similarly as N_0. All channels are designated to flat and block Rayleigh fading. The Channel State Information (CSI) regarding the BS to U_1, U_2 are known at the BS and the U_1,

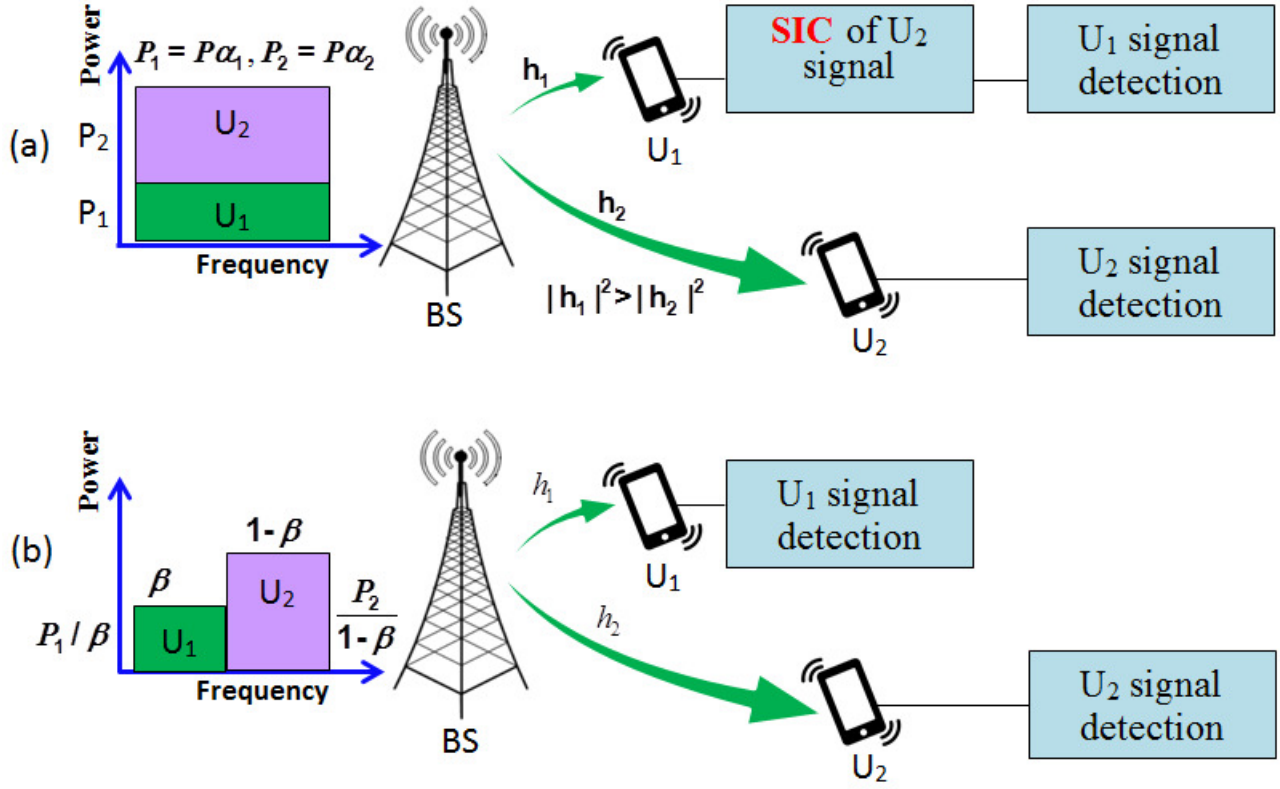

Figure 1.1: Multiple access schemes for a two-user scenario (a) NOMA (b) OMA.

U_2. In NOMA, the channel condition is presented as $|h_1|^2 > |h_2|^2$. This is a condition to the user U_2 always holds the weakest instantaneous channel [9]. The operation principle of the above simple NOMA scheme is presented as follows
Firstly, the BS broadcasts the information x_S [9] to two users in which x_S is given by

$$x_s = \sqrt{\alpha_1 P} x_1 + \sqrt{\alpha_2 P} x_2, \tag{1.1}$$

where P is the power at BS that are distributed to user U_1, user U_2. The α_1 and α_2 are the power allocation coefficients, x_1 and x_2 are the messages sending to user U_1 and user U_2. Following the principle of the NOMA and in Figure 1.1, we assume that $\alpha_2 > \alpha_1$ with $\alpha_1 + \alpha_2 = 1$.
The received signal at user U_i, $i \in (1, 2)$ can be represented as

$$y_i = h_i x_s + n_i. \tag{1.2}$$

Firstly, user U_1 performs SIC to decode the signal x_2 from (1.1) for user U_2 and removes this signal. So user U_1 receives the signal x_1, and is given as

$$y_1 = \sqrt{\alpha_1 P} x_1 h_1 + n_1. \tag{1.3}$$

Because user U_2 does not use SIC, the signal is decoded directly. The signal received at user U_2 is expressed as follows

$$y_2 = \sqrt{\alpha_1 P} h_2 x_1 + \sqrt{\alpha_2 P} h_2 x_2 + n_2, \tag{1.4}$$

where n_i denote the AWGNs at the user U_i with the same variance N_0, $E\{|x_i|^2\} = 1$ ($E\{x\}$ is denoted for the expectation process of x).
From the formulas (1.3), (1.4) and applying the Shannon formula, the achievable data rate for user U_1 and user U_2 are given by

$$R_1 = \log_2 \left(\frac{1 + \alpha_1 P |h_1|^2}{N_0} \right). \tag{1.5}$$

$$R_2 = \log_2 \left(1 + \frac{\alpha_2 P |h_2|^2}{\alpha_1 P |h_2|^2 + N_0} \right), \tag{1.6}$$

In this thesis, we apply the NOMA technology to investigate two protocols model and denote for improving the performance of the wireless communication system. The details of the NOMA technology are presented in Chapter 6 and Chapter 7.

1.1.2 Cooperative communication DF, AF

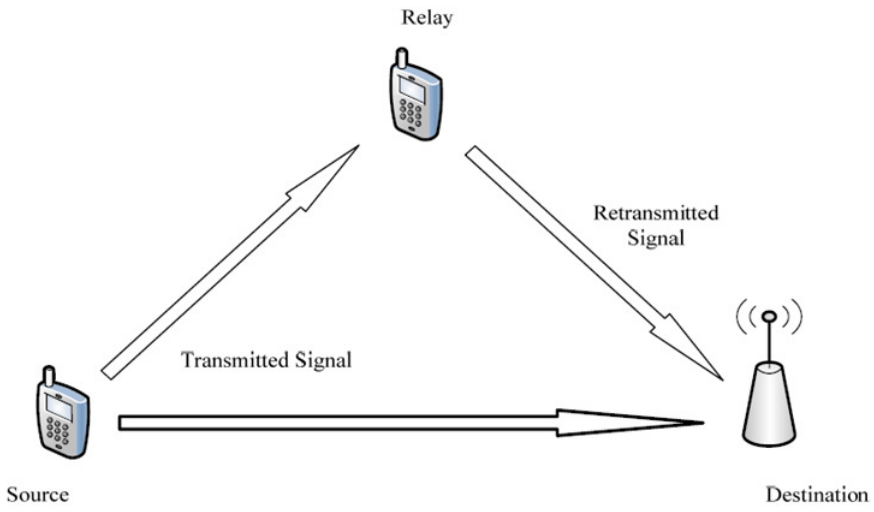

Figure 1.2: Cooperative communication.

In order to advance the transmitting signals in the fading environment, avoid the limited power of the wireless communication devices, the useful solution to increase diversity capacity and improve range of wireless communication is to use the cooperative communication [10, 11, 12, 13, 14]. The wireless communication is mainly depended on communication technology that is most functional in terms of mobile access. Since its

initiation, it has gone through many developmental phases to satisfy the increasing requirement of its wide range of applications.

Figure 1.2 shows a brief description of the concept of cooperative communication. There are two mobile users interacting with the same destination. Each mobile node has one antenna and cannot independently set up spatial diversity. When the distance from Source to Destinations is very far, or there are disadvantages to the fading environment, the relays will help wireless source nodes in forwarding their data to destinations.

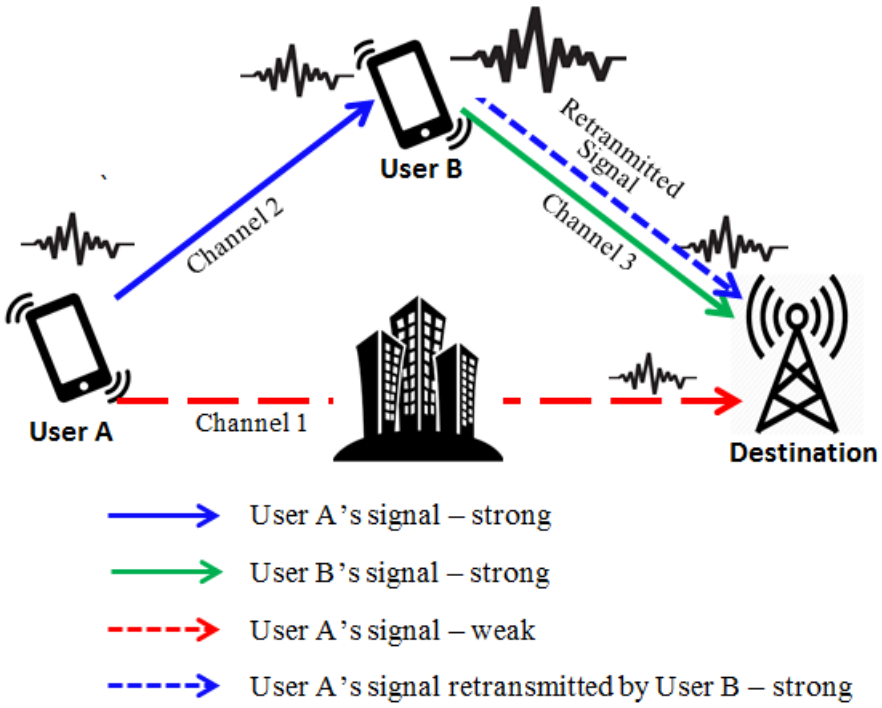

Figure 1.3: Amplify and Forward.

In this thesis, we assume that wireless devices are used to perform as source and relay nodes; however, without the loss of generality, any other wireless devices can also be used in cooperative communication. There are different types of cooperative communication protocols which could be outlined. These include the AF and DF protocols.

In AF, Figure 1.3 illustrates a simple cooperative signaling method which immediate user B helps to forward the signal of user A to the Destination. In this figure, user A sends its messages to the user B. Then the collected signal at user B is amplified and re-transmitted to the BS [15-21].

With DF, there are many authors studied in [22-29]. The procedure of this technique is given in figure 1.4. The received signal from the user A is decoded then re-encoded and forwarded to the destination station by the user B. The DF method helps data security in transmission among users.

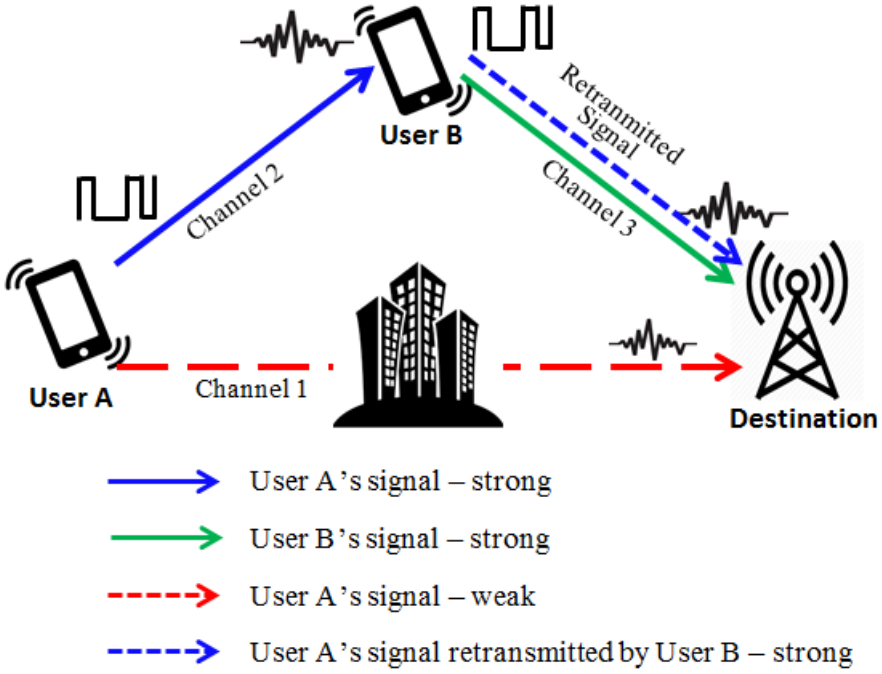

Figure 1.4: Decode and Forward.

1.1.3 Two-Way Cooperative Networks

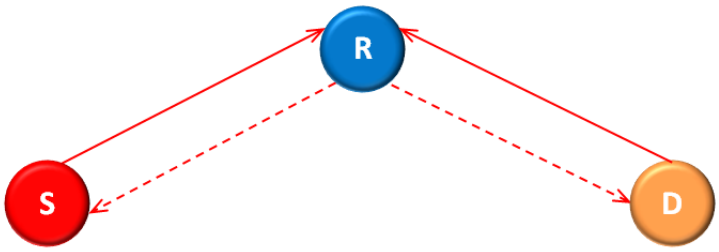

Figure 1.5: Two-Way Cooperative communication.

Two-Way cooperative relaying is essential to increase diversity capacity and thus to improve the range of wireless communication. Due to the ability to enhance data rate and cutting down the consumed energy of the network [30-40], Two-Way cooperative relaying has become an interesting case study. Problem importance being it takes four phases in common one-way relaying to transfer different messages between two sources, those are links S-R, R-S, D-R, and R-D respectively. Therefore, the performance operation of the system in the traditional one-way relaying system is not optimal efficiency, while Two-Way relaying only takes two phases or three phases in the transmitting signal. Therefore, Two-Way relaying scheme improves the performance of the system. As in figure 1.5, During the first (broadcast) phase, the source nodes S_1 and S_2 broadcast their packets x_1 and x_2 to the relay R. In the second (cooperation) phase, the relay R decodes the packets

x_1 and x_2 based on the channel gains, and then, the relay combines the packets x_1,x_2 together by using an XOR operation ($x = x_1 \oplus x_2$) [30] before broadcasting the coded x to the source nodes S_1 and S_2. At source S_1, the signal is also decoded by an XOR method $x_1 \oplus x = x_1 \oplus x_1 \oplus x_2 = x_2$, the result S_1 received the signal x_2 from source S_2. Similarly, the source S_2 take the signal x_1 from source S_1 by $x_2 \oplus x = x_2 \oplus x_1 \oplus x_2 = x_1$. Because of this efficiency, so many researches focus on the Two-Way relaying system as a potential solution to widen the coverage and to manipulate the diversity characteristic of wireless networks.

1.1.4 Relay Selection Methods

In cooperative communication systems as shown in figure 1.6, selecting a proper relay is a difficult choice. One of several reasons is that, if any of the channel links, such as the source-relay link or destination-relay link experiences deep fading, the performance cannot be as good as we expected. Subsequently, the outcome may be lead to the wastage of limited systems resources if the selected relay is not satisfactory. Some researchers in [44, 45, 46] have seen that the principle of choosing relay can maximize or minimize the desired purpose of each transmission. Throughput, error rate, signal to noise ratio (SNR) and transmission power are some main desired purposes of the function. In summary, the main reason for relay selection or allocation is to enhance cooperating as shown in Figure 1.7. However, if the number of relays is increased, it may be lead to the overhead and complexity in the system. Consequently, to reach a high efficient result, we must introduce a balance in relay selection because all relays may not have good channel conditions. Another promising challenge is synchronization among participating relays.

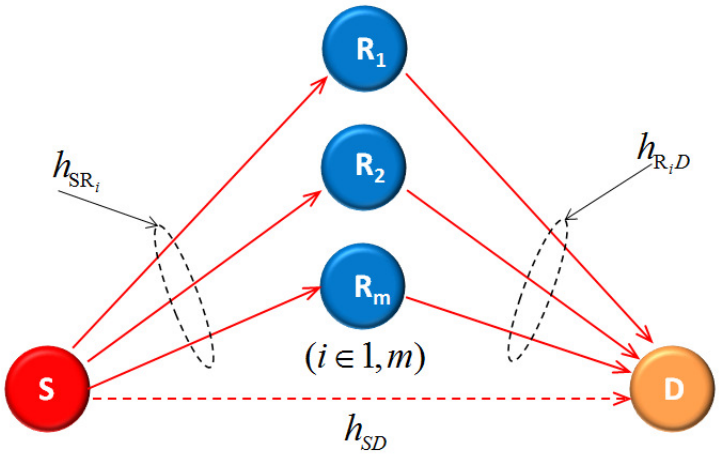

Figure 1.6: Cooperative communication with M Relays.

This method is very important. It is used to find the best relay to help the optimal system. There are two relay selection methods, namely, Opportunistic relay selection method and Partial relay selection [46].

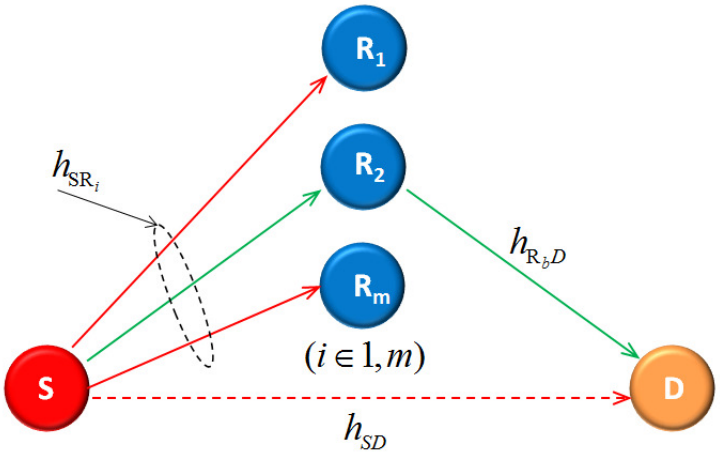

Figure 1.7: Cooperative communication with Best Relay.

- Opportunistic relay selection method:

There are the authors to research this method. They have proposed the only best relay is selected to forward the data from source to the destination. The opportunistic relay selection considers the signal quality balance between two links at every relay. The opportunistic relay selection method is given as

$$\mathrm{R}_b = \arg \max_{i=1,2,\ldots,M} \left\{ \min \left(\gamma_{\mathrm{S,R}_i}, \gamma_{\mathrm{R}_i,\mathrm{D}} \right) \right\}. \tag{1.7}$$

- Partial relay selection method:

The best Partial relay selection strategy is based on the maximum channel gain of the links at either the source-relay or the relay-destination, this method is presented by the formula as follows,

$$\mathrm{R}_b = \arg \max_{i=1,2,\ldots,M} \left(\gamma_{\mathrm{S,R}_i} \right), \tag{1.8}$$

where: $\gamma_{\mathrm{S,R}_i}$ and $\gamma_{\mathrm{R}_i,D}$ are defined as the Signal-to-Noise Ratio, R_b is the relay best.

1.2 Related works

1.2.1 Energy Harvesting (EH)

In recent times, in order to develop the green communication based on the superiority over classical grid-powered and battery-based devices, EH devices have become one of the most interesting research fields [48, 49, 50, 51, 52]. There are many power sources from different environments such as Radio Frequency (RF) , solar, wind, sea wave, thermoelectric effects or other physical phenomena. There had been many types of research about renewable energy such as solar and wind, but the power from the ambient RF signal is a new and promised solution to transfer data and energy at the same time. In general, to preserve

the long-term operation of wireless sensor networks, we usually have to replace the limited lifetime batteries in a large number of sensor nodes. However, RF-based energy could be a promised replacement of energy resources of low-power wireless sensor networks. Therefore, EH could solve the limited lifetime of the battery. Another tendency about wireless power transmission is the incorporation of the traditional cooperative networks and the energy harvesting technology to lengthen the lifetime and the coverage range [53, 54, 55]. As we had known in cellular networks and Wireless LAN, the mobile devices do not have long continuous working time because of the batteries issue. Also, the applications on these devices also drain the battery capacity quickly. As a result, in the scenario that the relay nodes in the communication network do not have the private energy sources, energy harvesting technology can be a proper solution. Two following receiver architectures is used to enable wireless energy harvesting and information processing at the energy constrained relay in wireless AF relaying networks.

-Power splitting receiver: Figure 1.8 shows Power splitting architecture. Power splitting receiver detects a part of the received RF power to harvest energy and the remaining part of the RF power to process the information signals. Power splitting receiver is studied to improve the throughput of wireless communication systems [56].

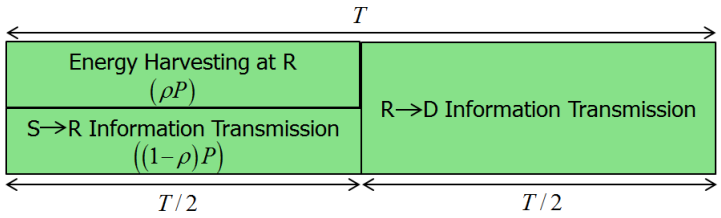

Figure 1.8: Power Splitter Architecture.

-Time switching receiver: Transmitted RF signals are separated into two intervals [58]. The first interval is used to provide energy for the receiver. The second interval is used to transmit the desired information.

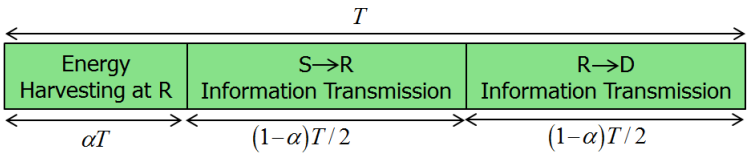

Figure 1.9: Time Switching Architecture.

1.2.2 Physical Layer Security (PLS)

Wireless and mobile networks are rapidly extending, so the security of information transfer is an important problem. It needs to increase in research and development. In recent

years, PLS has been investigated in lots of papers [59-63]. The article in [59] considered the secrecy wireless communication with the same cipher keys to connect between the source and destination nodes. In [60], the authors evaluate optimal power allocation for secure multiuser communication in cooperative relaying networks. Nowadays, there are many studied PLS to apply for 5G network [61, 62, 63]. The combination of cooperative communication and PLS is an effective approach to overcome the disadvantages of the fading environment as well as to increase the security capacity of the wireless network. In addition, the security performance of wireless mobile sensor networks is studied and applied for the smart city [64].

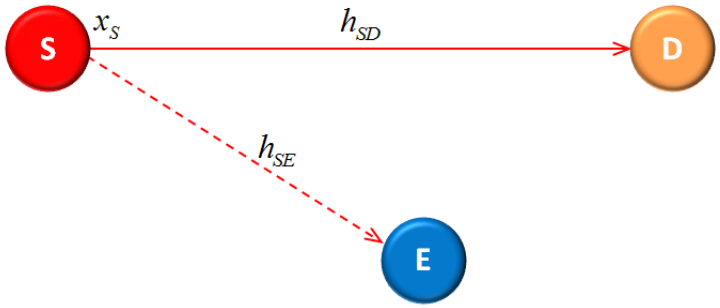

Figure 1.10: A simple system model of a direct transmission under physical layer security.

Figure 1.10 presents a simple system model of a direct transmission under PLS in which a source node S transmits its packets x_S to a destination node D. Eavesdropper node E is always wiretap to get data from node S. In Figure 1.10, secure communication is implemented if the capacity of the desired channel is larger than that of the eavesdropping channel, and is given by formula as follows

$$[ASR = \{R_{SD} - R_{SE}\}^{+} \tag{1.9}$$

where R_{SD} is the achievable data rate of link S-D and R_{SE} is the obtainable data rates of wiretapped link S-E. They are denoted by mathematical formula as following

$$R_{SE} = \frac{1}{2}\log_2\left(1 + SNR_{SE}\right) = \frac{1}{2}\log_2\left(1 + \frac{\gamma|h_{SE}|^2}{N_0}\right), \tag{1.10}$$

$$R_{SD} = \frac{1}{2}\log_2\left(1 + SNR_{SD}\right) = \frac{1}{2}\log_2\left(1 + \frac{\gamma|h_{SD}|^2}{N_0}\right), \tag{1.11}$$

The PLS method is shown in Chapter 7.

1.2.3 Underlay Cooperative Cognitive Network (UCCN)

The underlay cognitive radio was considered in [65, 66, 67] to increase the transmission in wireless communication. In cooperative cognitive network, the secondary user is permitted to use the licensed spectrum bands so that any interference created is always small than the maximum of the interference power level at the primary user). The underlay CR network is studied throughout figure1.11 where an ST transmits its signal to an SR using the licensed spectrum band of the primary network. Both PR and SR of the primary will have designed signals with the same spectrum band. In order to reduce the affection of interference to PR, the ST has to adjust its transfer power P_{ST} before transmitting its signal x_S.

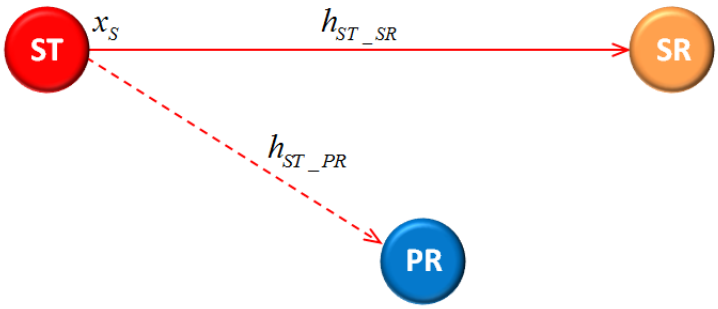

Figure 1.11: A simple system model of underlay CR network.

Therefore, this adjust is denoted by formula $P_{ST} \leq \frac{I_{th}}{|h_{ST\_PR}|^2}$, where $|h_{ST\_PR}|^2$ is channel gain of link ST-SR, and I_{th} is the maximum interference threshold at the PR. Due to restraint of the transmit power in the underlay CR network, the transmission signal will be decreased in fading environments. To overcome this disadvantage, many researchers [68, 69] investigated the cooperative transmissions in the secondary network under interference constraints, so that transmitted signals from ST to SR were good than with the support of secondary relays.

1.3 Thesis Organization

The structure of the thesis is as follows:

- Chapter 1 introduces to thesis with background concepts. Besides that, the detail Related works and the thesis organization are also denoted.
- Chapter 2 presents the state-of-the-art of all the related research works in this thesis.
- Chapter 3 consists of our primary goals in the thesis.
- Chapter 4 presents a Two-Way scheme to increase channel quality and diversity capacity.
- In Chapter 5 implements the best relay selection method in energy-harvesting cooperation scheme to improve the efficient performance and throughput.

- Chapter 6 focuses on the NOMA technology in Two-Way Decode-and-Forward scheme with DNC to enhance spectrum efficiency.
- In Chapter 7, we examine the security of UCCN Using NOMA to improve the system performance and secrecy performance.
- Chapter 8 draws conclusions from our works and also suggests some possible directions for future research.

2 STATE OF THE ART

2.1 The performance enhancement solutions in wireless communication networks

There are many studies about wireless communication [10, 11, 12, 13]. One of the most attracting aspects is optimizing the efficiency of the network. Studying about cooperative communication has become a highlighted subject for researching and applying in other to enhance the capability of wireless communication. Cooperative relaying is essential to increase diversity capacity and thus to improve the range of wireless communication. The aim of the cooperative relaying is to help wireless source nodes to transmit their data to destinations. During the first (broadcast) phase, the source node broadcasts its data to relays while the second (cooperation) phase, the relays help the source to forward the received data to the destination. In other to transfer data from the source to the destination through the relay, cooperative methods are considered as AF and DF [15-24]. The DF technique is more complex than the AF because the relays must successfully decode the received data signals first and then forward the recoded signals to the destination node. The AF technique does not require the decoding operation at the relays, but it creates more noises due to the amplification characteristic of the signals plus noises.

In recent years, Two-Way cooperative communication is investigated to increase diversity capacity and thus to improve the range of wireless communication [30]. In Two-Way schemes, many methods are proposed for enhancing the diversity capacity, secrecy capacity, ... They are known as the power transmission policies for the energy harvesting [33], the performance of NOMA-based cooperative relaying systems [7, 87, 89], the optimal relay transmission policy [31].

In addition, wireless networks having multiple-relay are also studied broadly. The relay selection method and the optimal relay selection [45, 46, 47] are applied to advance the performance of the system. It helps the users to transmit data quickly.

In order to prolong the lifetime and expand the coverage of the network, there is a new research trend on wireless power transfer, which is combining the EH technology and the conventional cooperative networks [48]. Concerning cellular networks and WLAN, because the fast growth multimedia applications consume much energy, the batteries in mobile devices have limited operation time. EH techniques have become a further important role in wireless powered communication networks, in which the relay nodes are assumed not to have an internal energy source.

There are many study cases in cooperative relay networks about EH [74, 75, 76, 77, 78, 79]. The researchers in [76] studied the throughput maximization with the assumptions of both causal and non-causal knowledge of the harvested energy for the EH two-hop AF relaying network. Besides, the authors assumed that the channel state information is well recognized before the data is transmitted to the destination by the collaboration of the

single relay node and the transmitter.

In [79], the author studied transmission power policies for the EH Two-Way relay channel which maximize the sum-throughput. The EH relay can perform AF, DF, compress-and-forward, or compute-and-forward relaying. Due to intermittent energy availability, the channel calls for relaying strategies that adapt to varying transmit powers.

The above researches show that the performance of the system has improved and they have been deployed in the wireless communications. However, they have not been the best solutions for the development of the fifth generation (5G) yet.

2.2 The NOMA solutions for applying the fifth generation (5G) mobile network.

With the NOMA technique, the users can share both time and frequency resources. This sharing is implemented by adjusting its power allocation ratio. The users with better channel conditions can serve as relays to enhance the system performance by using successive interference cancellation (SIC) [7, 8]. So, it is not only considered to apply for increasing amounts of the wireless connections, transmitting data traffic, data rate and the consumed energy in the next generation of wireless communications but also helps to improve the system throughput and transmit lower latency in wireless communications. There are many studied cases regard combinations of cooperative relaying and NOMA [87, 88, 89]. The researchers in [88] studied the performance of NOMA-based cooperative relaying systems. These are the filed which has attracted increasing interests recently to improve the throughput of future 5G wireless networks. Besides that, the authors researched the NOMA technique combining with the PLS in [101, 102]. In [101], the authors solved the problem of maximizing the minimum confidential information rate among users subject to the secrecy outage constraint and instantaneous transmit power constraint. Cooperative NOMA systems with the PLS were investigated in [102] in cases of both AF and DF operations. The PLS and NOMA have recently received great attention from the researches in wireless system fields as a promising technique to achieve enhanced spectrum efficiency of the fifth generation (5G) mobile network. The PLS is very important for data transmissions. It helps safety for the source nodes to communicate with each other. In addition, the underlay cognitive radio networks applying NOMA technique and security principle is also proposed by some authors in [103-108]. In [103] a cooperative transmission scheme was proposed for a downlink NOMA in CR systems and this research exploited the maximal spatial diversity. The authors in [108] studied secure communication in cognitive DF relay networks in which a pair of cognitive relays is opportunistically selected for security protection against eavesdroppers. The above solutions help to enhance the significant performance of wireless communication. Nevertheless, the authors have not considered the Two-Way DF scheme using NOMA, also have not examined a combination of the NOMA with PLS in the UCCN yet.

3 GOALS OF DISSERTATION THESIS

This Session, we denote the particular goals of the research. There are three goals in the thesis. The details are shown as follows

3.1 Goal 1: Design and deploy Multi-relay AF, DF scheme to improve the performance and throughput for the wireless communication networks.

With the backgrounds, we proposed the system models which are based on the network coding technique, Two-Way scheme, multi-relay scheme, relay selection technique, and energy harvesting technique for performance enhancement solutions in wireless communication networks. In particular, we design and deploy two new protocols such as Energy-Harvesting Cooperation Scheme with Best Relay Selections Under I/Q Imbalance; Two-Way DF Scheme with Energy Harvesting from Intermediate Relaying Station. The achievable results are presented as follow:
In the first protocol, we have researched the throughput performance. The achievable result being the throughput performance of the proposed protocols EHAF and EHDF is improved when compared with that of a non-selection cooperation scheme. In addition, because of the optimal relay selection approach, we have figured out that, the system model with three relays achieves the better throughput than the system model with one relay in both protocols, so the proposed protocol EHDF is more efficient than the EHAF protocol.
The second proposed protocol, we have investigated the performance of the Two-Way DF scheme by applying digital network coding and energy harvesting. Due to collect energy from the source nodes, the system performance obtained the good diversity performance of signal transmission between two source nodes.

3.2 Goal 2: Implement proposed Two-Way NOMA protocols to increase the spectral efficiency and overcome disadvantages of the fading environment.

In this goal, we proposed a Two-Way cooperation scheme with multiple wireless relays in which the best relay uses the non-orthogonal multiple access (NOMA) to improve the system performance in 5G wireless networks (called a TWNOMA protocol). We applied digital network coding (DNC) technique to compress received data from source nodes. The system performance has analyzed and evaluated in terms of exact closed-form outage probability over Rayleigh fading channels. The theoretical analyses have also validated by performing Monte Carlo simulations.

For the results of research, we have developed a new protocol model based on NOMA technique for Performance enhancement solutions in wireless communication networks.

In this protocol, the efficiency transmission has improved because we applied both the NOMA technique and the DNC technique to compensate for the loss of the bandwidth. Besides, the spectral efficiency of the proposed protocol was best when the relay was located at the midpoint between the sources. Finally, by using the NOMA technology, the system has overcome the disadvantages of the fading environment.

3.3 Goal 3: Design expanded NOMA protocol to advance the secrecy system.

In this part, with the inheritance from the goal 2, we have developed and extended operation protocol based on NOMA technique combining with Physical Layer Security in Underlay Cooperative Cognitive Networks for performance enhancement in wireless communication networks.

We have researched the best relay selection strategies by three types of relay selection criteria. With the analyzing and evaluating results, we have seen that the system increased the security as well as the spectrum efficiency. Besides, due to applying the NOMA technique, the performance of system and bandwidth have achieved higher efficiency. Finally, the result of the proposed system has obtained well security performance when eavesdropper node E moved far from the source and cooperative relay.

4 PRESENTS A TWO-WAY SCHEME TO INCREASE CHANNEL QUALITY AND DIVERSITY CAPACITY.

Today, many wireless devices, IoT and smart devices are developed quickly. So, we need to have the solutions to expand the scope of the networks and the energy for these devices. In this chapter, we proposed the Two-Way cooperative relaying scheme with the energy harvesting to denote these problems. As we know, Two-Way cooperative relaying is essential to increase diversity capacity and thus to improve the range of wireless communication. The aim of the cooperative relaying is to help wireless source nodes to transmit their data to destinations. During the first (broadcast) phase, the source nodes broadcast their data to relays while in the second (cooperation) phase, the relays help the sources to forward the received data to the destinations. In order to transfer data from the sources to the destinations through the relays, cooperative solutions are considered as AF and DF techniques [HTP02], [32, 70, 71, 73]. With energy harvesting helps the system to improve throughput performance and prolong the lifetime of the wireless networks.

4.1 Motivation

It has been many researches about energy harvesting in cooperative network [31, 74, 75, 76, 77]. In [74] based on the presumption of both causal and non-causal knowledge of the harvested energy in the energy harvesting two-hop AF relaying network, the authors researched the throughput maximization. Furthermore, before the data is transmitted to the destination through the single relay node and the transmitter, an assumption has been made that channel state information was well identified.

Besides, the researchers in [78] examined the power transmission policies for the energy harvesting Two-Way scheme to find out the optimal the sum throughput. The research has been observing the energy harvesting relay can operate AF, DF, compress-and-forward, or compute-and-forward relaying.

Most of all above researchers have assumed that the source nodes have enough energy in the first phase of the transmission processes. In the other hand, in [79], the source nodes are insufficient energy for operation in the one-way scheme. There is no study about Two-Way relaying networks with finite energies at the source and the destination nodes.

Due to the emerged idea, in this Chapter, we proposed an intermediate relay supplies the power and transfers the signals to two source nodes in Two-Way energy-harvesting scheme (called a TWEH protocol). The relay applies digital network coding to compress received data from the source nodes. There are two significant assumptions given follow. Initially, we presume that both sources have not enough energy to send as well as to receive the data. As a result, each source has to harvest energy from the RF signals of the relay. For instance, in real wireless systems, source nodes sometimes lack the power

to send and receive messages from other sources while original stations relays have full energy. In our assumption, the sources node can be charged their battery by using the power from the RF signals of the relay with full energy (original stations). And then these source nodes have enough energy to operate.
The second, we examine and compare the proposed TWEH protocol with a conventional Two-Way DF scheme without using digital network coding and energy harvesting (called a TWNEH protocol).

In this Chapter, we evaluate the system performances with reference to exact closed-form outage probabilities (OPs) of the Two-Way DF schemes. There are four superiorities extracted from simulation results: 1) the proposed TWEH protocol outperforms the Two-Way decode-and-forward scheme without using digital network coding and energy harvesting (TWNEH protocol); 2) The sum OPs of the protocols TWEH and TWNEH are smallest when the relay is located at the midpoint of the two sources; 3) the proposed TWEH protocol achieves the higher performance at the higher energy conversion efficiencies and the smaller target data rates; 4) The theoretical expressions correspond with the Monte Carlo simulation results.

This research is constructed as follows: Section 4.2 illustrates a Two-Way system model with the energy harvesting architecture and operation principles of the proposed TWEH protocol; Section 4.3 studies and measures the exact OPs of the source nodes, and figures out the sum OPs of the protocols TWEH and TWNEH; In Section 4.4, we hand out the simulation results; and Section 4.5 is about our summarization and conclusions.

4.2 System model

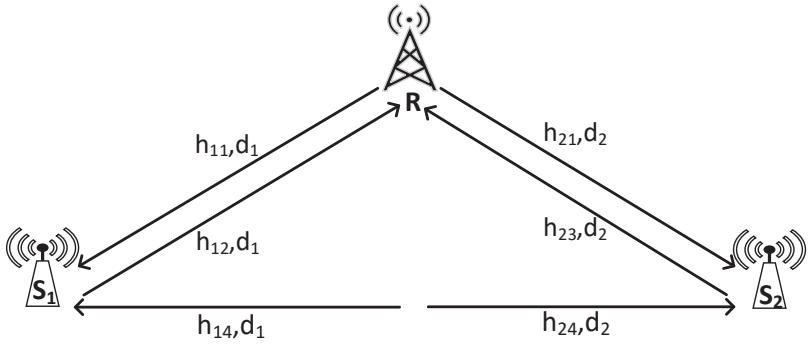

Figure 4.1: System model of a Two-Way DF energy-harvesting scheme

As shown in Figure 4.1, in this Section, we study a system model of a Two-Way DF with the energy-harvesting scheme, in which consists of a relay R and two source nodes S_1 and S_2. The S_1 and S_2 are the energy harvesting source nodes. In this scheme, we consider that two sources S_1 and S_2 are insufficient energy in the transmitting-receiving process

of the pilot messages in the preparing phase, and two sources collect energy from the RF signals of the relay R. Then, the messages of two source nodes S_1 and S_2 are carried to the intermediate relay node R. We have four presumptions as follow. First thing, each node has a single antenna. Then, variances of Zero-mean White Gaussian Noises (AWGNs) are equal, denoted similarly as N_0. Next, all channels are aimed to flat and block Rayleigh fading. Finally, Channel State Information (CSI) is perceived at the source nodes S_1 and S_2 [80].

In Figure 4.1, let h_{1i} and h_{2i} are Rayleigh fading channel coefficients, where $i \in \{1, 2, 3, 4\}$. The distances of link R-S_1 and R-S_2 are d_1, d_2, respectively. The random variables $g_{1i} = |h_{1i}|^2$ and $g_{2i} = |h_{2i}|^2$ have exponential distributions with the parameters $\lambda_1 = d_1^\beta$ and $\lambda_2 = d_2^\beta$, respectively, where β is a path-loss exponent. The Cumulative Distribution Function (CDF) and probability density function (pdf) of random variables g_{ji} are expressed as $F_{g_{ji}}(x) = 1 - e^{-\lambda_i x}$ and $f_{g_{ji}}(x) = \lambda_i e^{-\lambda_i x}$, respectively, where $j \in \{1, 2\}$.

As the above assumptions, the fading channel h_{ji} stays intact during a block time T, and is independent and identically assigned between two consecutive block times.

The operation principle of the Two-Way DF with the energy-harvesting scheme (called the TWEH protocol)[HTP05] is divided into four time slots. In the first time slot, an energy-provided packet of the relay is carried to two source nodes. The second time slot, S_1 and S_2 harvest the energy from the relay R, and then S_1 sends an information-carrying packet x_1 to the relay. Similar to S_1, S_2 also dispatches an information carrying packet x_2 to the relay R in the third time slot. Finally, in the last time slot, a coded packet is based on digital network coding by an XOR operation ($x = x_1 \oplus x_2$) [HTP04] is transmitted to the source nodes S_1 and S_2.
In the next Section, we will discuss the mathematical expressions and the outage probability analyses of the protocols TWEH and TWNEH [HTP05].

4.3 Outage Probability Analysis

We assume that a node decodes the received packet successfully if its achievable data rate is larger than a target data rate threshold R_t. The assumption is aimed to analyze the outage probability of the Two-Way DF schemes (the TWEH and TWNEH protocols).

4.3.1 The TWEH protocol

Because of the symmetry of the system model in Figure 4.1, the outage probability of the two source nodes S_1 and S_2 is calculated in the same way. Therefore, we only calculate the outage probability of S_1, and then infer the outage probability of S_2.

At the first phase point of the block time T, the energy signal e of the relay R is transmitted to the source nodes S_1 and S_2 with a transmission power P, where $E\{|e|^2\} = 1$ ($E\{x\}$ is notated for the expectation process of x). The energy carried signals received at

the source nodes Sj are given, respectively, as

$$y_{S_j}^{(1)} = \sqrt{P} h_{j1} e + n_{S_j}, \tag{4.1}$$

where n_{S_j} represent the AWGNs at receiving antennas of the source nodes Sj, respectively, with the same variance N_0. The harvested energies at the source nodes Sj over a time interval T are obtained from (4.1), as

$$E_{S_j} = P|h_{j1}|^2 T\eta_j, \tag{4.2}$$

where η_i is defined as the energy conversion efficiencies at the nodes Sj, $0 < \eta_j \leq 1$. The source nodes Sj are considered having the same construction, and η_j are constant, denoted as $\eta_j = \eta$.

In the second phase, the relay R receives the signal from the source node S_1, and is shown as

$$y_R^{(2)} = \sqrt{P_{S_1}} h_{12} x_1 + n_R. \tag{4.3}$$

The power P_{S_1} in (4.3) can be achieved from the harvested energy E_{S_1} as in (4.2) for sending the signal x_1 to the cooperative relay R over a time interval T as follows

$$P_{S_1} = \frac{E_{S_1}}{T}. \tag{4.4}$$

Replacing E_{S_1} at formula (4.2) into (4.4), we have the formula as:

$$P_{S_1} = P|h_{11}|^2 \eta. \tag{4.5}$$

At the third time slot, by calculating the same way, the following formula is shown for the received signal at the relay R from the source node S_2 as

$$y_R^{(3)} = \sqrt{P_{S_2}} h_{23} x_2 + n_R. \tag{4.6}$$

Similar to formula (4.4), we have the power P_{S_2} which is represented as follows

$$P_{S_2} = P|h_{21}|^2 \eta. \tag{4.7}$$

The received SNR_{S_2R} at the relay R which decode the signal x_2 is achieved as follows

$$SNR_{S_2R} = \frac{P_{S_2}|h_{23}|^2}{N_0} = \frac{P\eta|h_{21}|^2|h_{23}|^2}{N_0} = \gamma\eta g_{21} g_{23}, \tag{4.8}$$

where γ is denoted as a transmit SNR,$\gamma = \frac{P}{N_0}$. Hence, we have the achievable data rate at the relay R to decode the information signal x_2 of the source S_2, is given as:

$$R_{S_2R} = \frac{1}{4}\log_2\left(1 + SNR_{S_2R}\right), \tag{4.9a}$$

where a ratio ¼ denotes for four time slots of the operation in the proposed TWEH protocol .

Replacing the SNR_{S_2R} from (4.8) into (4.9a), R_{S_2R} is expressed as:

$$R_{S_2R} = \frac{1}{4}\log_2\left(1 + \gamma\eta g_{21} g_{23}\right) \tag{4.9b}$$

After the relay R received the packets x_1 and x_2 in the second time slot, the relay R codes these signals by using the digital network coding as $x = x_1 \oplus x_2$. The next, the signal x will be sent to the source nodes Sj in the last time slot, and are shown respectively, as

$$y_{S_j}^{(4)} = \sqrt{P} h_{j4} x + n_{S_j}. \tag{4.10}$$

Base on the (4.10), the received SNR_{RS_1} at the source S_1 for decoding the information signal x is obtained from (4.10) as follows

$$SNR_{RS_1} = \frac{P|h_{14}|^2}{N_0} = \gamma g_{14}. \tag{4.11}$$

Using formula SNR_{RS_1} in (4.11), the achievable data rate at the source node S_1 from the transmission x of the relay R is given as:

$$R_{RS_1} = \frac{1}{4}\log_2\left(1 + SNR_{RS_1}\right). \tag{4.12a}$$

Replacing SNR_{RS_1} the from (4.11) into (4.12a), the following result is shown as

$$R_{RS_1} = \frac{1}{4}\log_2\left(1 + \gamma g_{14}\right). \tag{4.12b}$$

Using formulas (4.9b) and (4.12), we calculate the outage probability of the source node S_1 in which the source node S_1 does not receive signal from the source node S_2. The outage probability of the source node S_1 is achieved by a math equation as follows

$$P_{TWEH}^{out\_S_1} = \underbrace{\Pr[R_{S_2R} < R_t]}_{\Pr 1} + \underbrace{\Pr[R_{S_2R} \geq R_t, R_{RS_1} < R_t]}_{\Pr 2} \tag{4.13}$$

Pr1 is solved by replacing formula (4.9b) into the equation of Pr1 in (4.13) and is represented as follows

$$\Pr 1 = \Pr\left[\frac{1}{4}\log_2\left(1 + \gamma\eta g_{21} g_{23}\right) < R_t\right] = \int_0^\infty f_{g_{21}}(x) F_{g_{23}}\left(a/x\right) dx, \tag{4.14a}$$

where $a = \frac{2^{4R_t}-1}{\gamma\eta}$, Using the pdf and CDF of the random variables g_{21} and g_{23} into (4.14a), we have a closed form expression of Pr1 as

$$\Pr 1 = \int_0^\infty \lambda_2 e^{-\lambda_2 x}\left(1 - e^{-\lambda_2\left(a/x\right)}\right) dx = 1 - u_1 \times K_1(1, u_1), \tag{4.14b}$$

where $u_1 = 2\lambda_2\sqrt{a}$ and $K_1(.)$ is the modified Bessel function [112, eq.(8.432.6)].

Similar to Pr1, Pr2 is calculated by replacing the formula (4.9b) and (4.12b) into the formula of Pr2 in (4.13), Pr2 is solved as

$$\begin{aligned}\Pr 2 &= \Pr\left[\tfrac{1}{4}\log_2\left(1 + \gamma\eta g_{21} g_{23}\right) \geq R_t, \tfrac{1}{4}\log_2\left(1 + \gamma g_{14}\right) < R_t\right] \\ &= \underbrace{\Pr\left[\frac{1}{4}\log_2\left(1 + \gamma\eta g_{21} g_{23}\right) \geq R_t\right]}_{\Pr 2.1} \underbrace{\times \Pr\left[\frac{1}{4}\log_2\left(1 + \gamma g_{14}\right) < R_t\right]}_{\Pr 2.2}.\end{aligned} \tag{4.15}$$

From (4.21), the probability Pr2.1 and Pr2.2 is solved respectively, as follows

$$\Pr 2.1 = 1 - \Pr\left[\frac{1}{4}\log_2\left(1+\gamma\eta g_{21}g_{23}\right) < R_t\right] = 1 - \Pr 1 = u_1 \times K_1(1,u_1). \tag{4.16}$$

$$\Pr 2.2 = \Pr\left[g_{14} < \frac{2^{4R_t}-1}{\gamma}\right] = \Pr\left[g_{14} < a\eta\right] = F_{g_{14}}\left(a\eta\right) = 1 - e^{-\lambda_1 a\eta}. \tag{4.17}$$

From (4.16) and (4.17), Pr2 is obtained as follows:

$$\Pr 2 = \Pr 2.1 \times \Pr 2.2 = u_1 \times K_1(1,u_1) \times \left(1 - e^{-\lambda_1 a\eta}\right). \tag{4.18}$$

Finally, from (4.14b) and (4.18), we have the outage probability of the source node S_1 $P_{TWEH}^{out\_S_1}$ is obtained in the closed-form expression as

$$P_{TWEH}^{out\_S_1} = \Pr 1 + \Pr 2 = 1 - u_1 \times e^{-\lambda_1 a\eta} \times K_1(1,u_1). \tag{4.19}$$

Similarly, the outage probability $P_{TWEH}^{out\_S_2}$ of the source node S_2 in the TWEH protocol is inferred by changing λ_2 to λ_1 and vice versa as

$$P_{TWEH}^{out\_S_2} = 1 - u_2 \times e^{-\lambda_2 a\eta} \times K_1(1,u_2), \tag{4.20}$$

where $u_2 = 2\lambda_1\sqrt{a}$.

The sum OPs $P_{TWEH}^{out\_sum}$ in the TWEH protocol is obtained as

$$P_{TWEH}^{out\_sum} = P_{TWEH}^{out\_S_1} + P_{TWEH}^{out\_S_2} = 2 - u_1 \times e^{-\lambda_1 a\eta} \times K_1(1,u_1) - u_2 \times e^{-\lambda_2 a\eta} \times K_1(1,u_2). \tag{4.21}$$

4.3.2 The TWNEH protocol

In this Section, we present the TWNEH protocol which the two source nodes S_1 and S_2 are sufficient energy. Two source nodes do not need to harvest the energy from the relay R in the first time slot. Because the operation principle of the TWNEH protocol is also performed in four time slots, so the outage probability of the source node S_1 in the TWNEH protocol is similar to the TWEH protocol, and is expressed as

$$P_{TWNEH}^{out\_S_1} = \underbrace{\Pr[R_{S_2R}^{NEH} < R_t]}_{\Pr 3} + \underbrace{\Pr[R_{S_2R}^{NEH} \geq R_t, R_{RS_1}^{NEH} < R_t]}_{\Pr 4}, \tag{4.22}$$

where $R_{S_2R}^{NEH}$ and $R_{RS_1}^{NEH}$ are achievable data rates at the relay R and the source node S_1, respectively.

In the TWNEH protocol, the sum energy equals to $4 \times T \times P_{NEH}$, where P_{NEH} is the same power of the nodes S_1, S_2 and R, whereas the sum energy in the TWEH is $2 \times T \times P$. With fair comparison purpose about used energy, we set as $4 \times T \times P_{NEH} = 2 \times T \times P$, then $P_{NEH} = P/2$.

The achievable data rates at the relay R and the source node S_1 to decode the information signal x_2 of the source node S_2 are given, respectively, as:

$$R_{S_2R}^{NEH} = \frac{1}{4}\log_2\left(1 + SNR_{S_2R}^{NEH}\right) = \frac{1}{4}\log_2\left(1 + \frac{\gamma g_{23}}{2}\right). \tag{4.23}$$

$$R_{RS_1}^{NEH} = \frac{1}{4}\log_2\left(1 + SNR_{RS_1}^{NEH}\right) = \frac{1}{4}\log_2\left(1 + \frac{\gamma g_{14}}{2}\right). \tag{4.24}$$

By replacing the $R_{S_2R}^{NEH}$ from (4.23) into the formula of Pr3 in (4.22), Pr3 is obtained as follows

$$\begin{aligned}\Pr 3 &= \Pr\left[\tfrac{1}{4}\log_2\left(1 + \tfrac{\gamma g_{23}}{2}\right) < R_t\right] = \Pr\left[g_{23} < 2^{\frac{2^{4R_t}-1}{\gamma}}\right] \\ &= \Pr\left[g_{23} < 2a\eta\right] = F_{g_{23}}\left(2a\eta\right) = 1 - e^{-2\lambda_2 a\eta}.\end{aligned} \tag{4.25}$$

The Pr4 is calculated similar to the Pr3. The Pr4 are achieved by replacing the $R_{S_2R}^{NEH}$ from (4.23) and $R_{RS_1}^{NEH}$ from (4.24) into the Pr4 in (4.22) as

$$\Pr 4 = \left[1 - \Pr\left(g_{23} < 2\frac{2^{4R_t}-1}{\gamma}\right), \Pr\left(g_{14} < 2\frac{2^{4R_t}-1}{\gamma}\right)\right] = e^{-2\lambda_2 a\eta} \times \left(1 - e^{-2\lambda_1 a\eta}\right). \tag{4.26}$$

Finally, the $P_{TWNEH}^{out\_S_1}$ is achieved the closed-form expression as

$$P_{TWNEH}^{out\_S_1} = \Pr 3 + \Pr 4 = 1 - e^{-(\lambda_1+\lambda_2)2a\eta}. \tag{4.27}$$

Due to identical effects of the relay R on the transfer signal between the source node S_1 and S_2 in the TWNEH protocol, the outage probability $P_{TWNEH}^{out\_S_2}$ of the source node S_2 is equal to $P_{TWNEH}^{out\_S_1}$ and the sum OPs $P_{TWNEH}^{out\_sum}$ in the TWNEH protocol is $2 \times P_{TWNEH}^{out\_S_1}$.

4.4 Simulation Results

In this Section, we use the Monte Carlo simulations to check the exact theoretical analyses of the system performance. The parameters for analysis is set as, the path-loss exponent β equal to 3, in the two-dimensional plane, the SNR on the x-axis is defined as SNR $= P/N_0$. Besides, we set the coordinates of S_1, S_2, and R as S_1 (0, 0), S_2 (1, 0) and R (x, y), respectively, satisfying $0 < x < 1$. Therefore, we have the distances $d_1 = \sqrt{x^2 + y^2}$ and $d_2 = \sqrt{(1-x)^2 + y^2}$.

Figure 4.2 shows the sum OPs of the protocols TWEH and TWNEH versus the SNR (dB). We consider the values with x = 0.5, y=0, $R_t = 1$ (bit/s/Hz) and $\eta = 0.9$. Due to the symmetric network model, the OPs of the source nodes S_1 and S_2 are identical. We can see that in Figure 4.2, the sum OPs of the source nodes S_1 and S_2 in both protocols decrease when the SNRs increase because the harvested energies as in formulas (4.21) and (4.27), the decoding capacities at the nodes S_1, S_2 and R are larger at the higher SNRs. Furthermore, because the proposed TWEH protocol applies the digital network coding to compensate the loss of the bandwidth for the energy harvesting phase (the first time

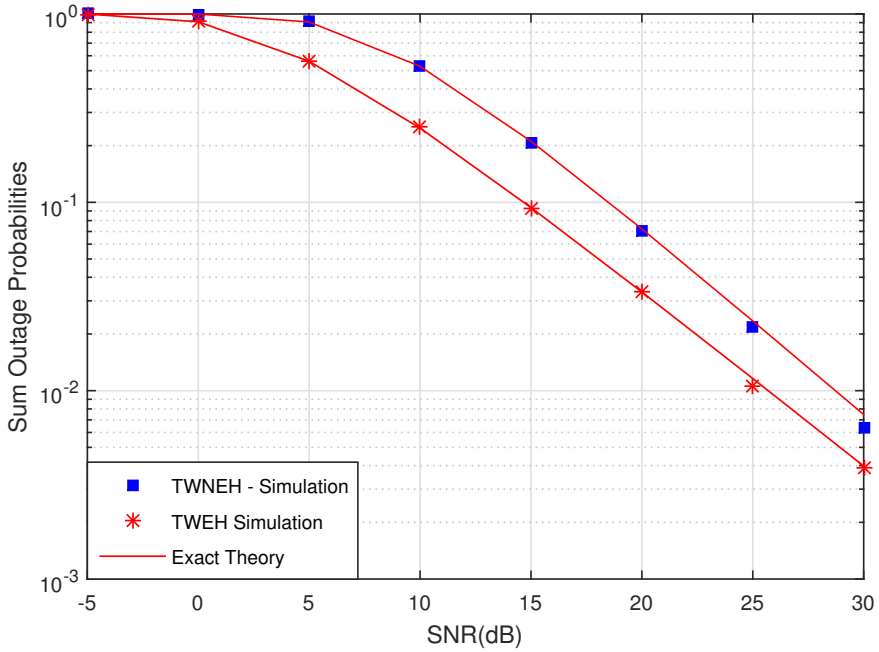

Figure 4.2: The sum OPs of the source nodes S_1 and S_2 in the protocols TWEH and TWNEH versus SNR (dB) when x=0.5, R_t= 1 (bit/s/Hz), $\eta = 0.9$

slot), the performance of the proposed TWEH protocol exceeds the conventional TWNEH protocol. Lastly, we can see that the simulation results match well to the theoretical results. Thus, we can confirm that the derived formulas during analyzing are accurate.

In Figure 4.3 presents sum OPs of the protocols TWEH and TWNEH versus the location of relay x on x-axis, when SNR = 10 (dB), R_t = 1 (bit/s/Hz), and x moves from 0.1 to 0.9. In Figure 4.3, the sum OPs of the TWEH protocol is also smaller than that of the TWNEH protocol. Hence, the proposed TWEH protocol with the digital network coding outperforms the TWNEH protocol, and concurrently, achieves higher bandwidth utilization efficiency. In addition, the performance of both protocols is best when the relay is located at the midpoint of the sources S1 and S2. At this point, the proposed TWEH protocol can balance the energy harvesting operations and the decoding capacities.

Figure 4.4 presents the sum OPs versus η of the protocols TWEH and TWNEH with R_t = 1(bit/s/Hz), x= 0.5, y=0, η is moved from 0.1 to 1, and the SNR values are set to 10 and 20 (dB). As shown in Figure 4.4, the sum OPs of the TWEH protocol is smaller than the sum OPs of the TWNEH protocol at SNR=10 dB. At SNR = 20 dB, the sum OPs values of the TWEH protocol is larger than sum OPs of the TWNEH protocol when $\eta < 0.2$(small energy conversion efficiency). However, when the value of the energy conversion efficiency increases from 0.2 to 1, the sum OPs of the TWEH protocol also decrease and smaller than the sum OPs of the TWNEH protocol. Because the proposed TWEH protocol apply the energy harvesting, the performance system is good than the

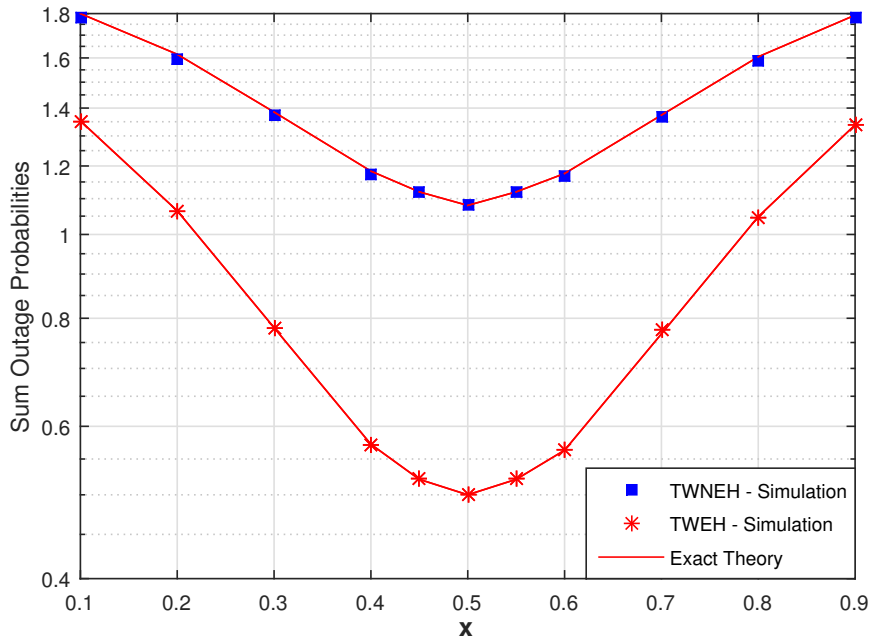

Figure 4.3: Sum OPs of the protocols TWEH and TWNEH versus location of relays x on x-axis, when SNR = 10 (dB), $\eta = 0.9$, $R_t = 1$ (bit/s/Hz), and x moves from 0.1 to 0.9.

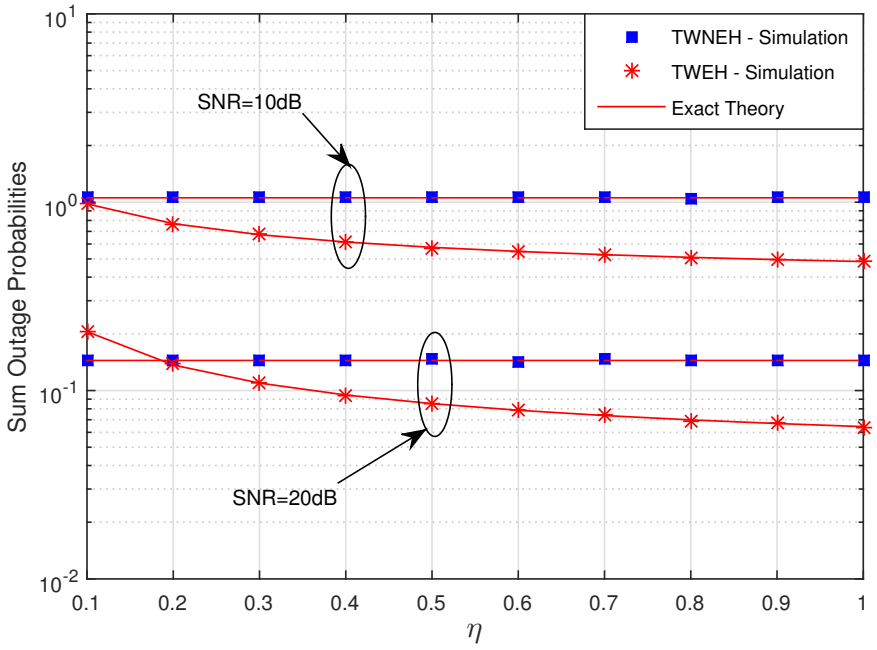

Figure 4.4: The sum OPs of the scheme in the TWEH and TWNEH protocols versus η when x=0.5, y=0, $R_t = 1$ (bit/s/Hz) and SNR is considered at 10 and 20 (dB).

TWNEH protocol does not apply the energy harvesting.

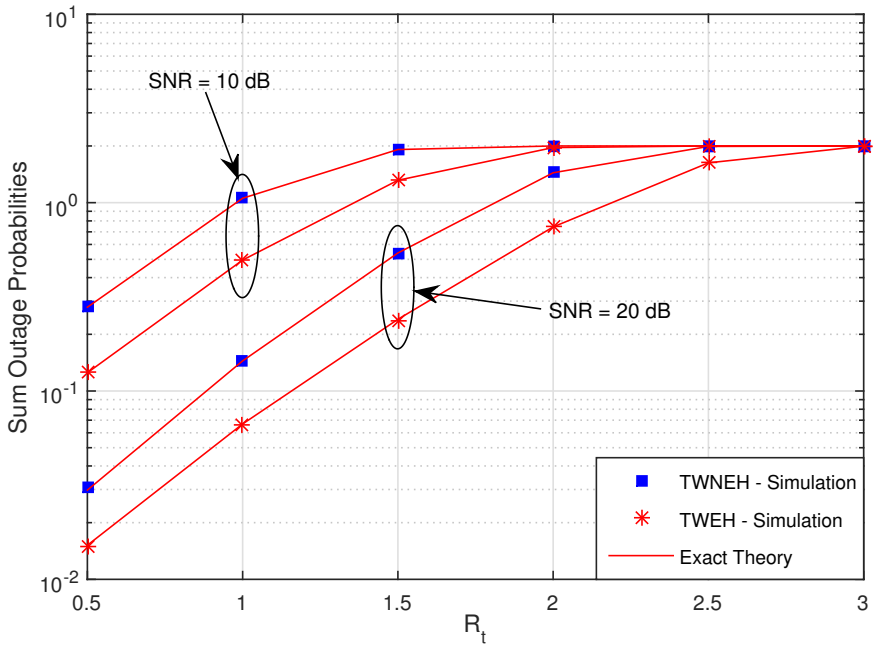

Figure 4.5: The sum OPs of the scheme in the TWEH and TWNEH protocols versus R_t when x=0.5, y=0, and SNR is considered at 10 and 20 (dB).

In Figure 4.5, the sum OPs of the proposed TWEH is compared with the TWNEH protocol via R_t when x=0.5, y=0, SNR values are set to 10 (dB) and 20 (dB). The Fingure 4.5 illustrates the target data rate R_t goes up, the system performance of the protocols TWEH and TWNEH decreases and then moves to the worst regions (about $R_t > 2.5$).

4.4.1 Conclusions

In this research, we introduce the Two-Way energy-harvesting model (called the TWEH protocol) in which the intermediate relay performs two roles: supporting energy to two source nodes in the initial system and implementing the digital network coding to compress received data from the source nodes. In the offered TWEH protocol, to have enough energy to transmit and receive the data, each source has to collect energy from the RF signals of the relay. The system performance of the proposed protocol is gauged by the exact closed-form outage probability expressions and is verified by the Monte Carlo simulation method. The outcomes show that the proposed TWEH protocol has higher performance when compared with the conventional Two-Way DF scheme without using digital network coding and energy harvesting (called the TWNEH protocol). It also shows that when the relay is placed at the midpoint of the two sources, both protocols attain the lowest sum OPs. Moreover, when applying the TWEH protocol, the performance of the system obtains efficient and maintain the long-term time operation for transmission.

5 IMPLEMENTS THE BEST RELAY SELECTION METHOD IN ENERGY-HARVESTING COOPERATION SCHEME.

In Chapter 4, we research the TWEH protocol with only one relay to help the transfer signal between two source nodes and improve throughput performance of wireless systems. In this Chapter, to advance in the longer lifetime operation and enhance the throughput performance of wireless networks, we propose an energy-harvesting cooperation scheme in which relays suffer in-phase and quadrature-phase imbalances (IQI) and harvest energy from a wireless transmit source [HTP02].

5.1 Motivation

In recent time, widening the range and rising the diversity capacity of wireless communication are effected by cooperative relaying. The cooperative communication supports the data transmission from the wireless source nodes to the destinations. Therefore, many researchers propose cases of cooperative networks under the impact of IQI [82, 83]. The IQI pertains to the phase and/or amplitude mismatch between the in-phase (I) and quadrature (Q) signals at the transmitter (TX) and receiver (RX) sides. Most researches about IQI have only investigated the performance analysis and baseband compensation that base on the single hop communication systems. The performance analysis of AF dual-hop relaying, where IQI affects both the TX and RX front ends of the relay node [82].

Most of the above researchers, the authors have not presented the energy-harvesting cooperation scheme with the best relay selection under IQI yet. In this Chapter, we propose a dual-hop DF and AF relaying networks in which the best relay selection collects the energy under the impact of IQI.

The Chapter is summarized as follows. Firstly, an energy-harvesting cooperative multi-relay scheme is proposed. We apply the opportunistic relay selection method to find a best relay for the EHAF protocol and partial relay selection to have a best relay for the EHDF protocol. These best relays suffer the IQI. Secondly, the exact closed-form throughput over Rayleigh fading channels are derived and are confirmed by Monte Carlo simulations. Thirdly, the proposed EHDF protocol outperforms the proposed EHAF protocol. Finally, the throughput performance of the two protocols also improves when the number of cooperative relay increase.

This Chapter is presented as follows: Section 5.2 considers a dual-hop DF and AF cooperative relaying scheme in which the multiple wireless energy harvesting relay nodes under impact of IQI; The throughput performance analyses of the proposed EHDF and EHAF protocols are described in Section 5.3; Section 5.4 is presented the simulation results are presented; Section 5.5 summarizes our conclusions.

5.2 System model

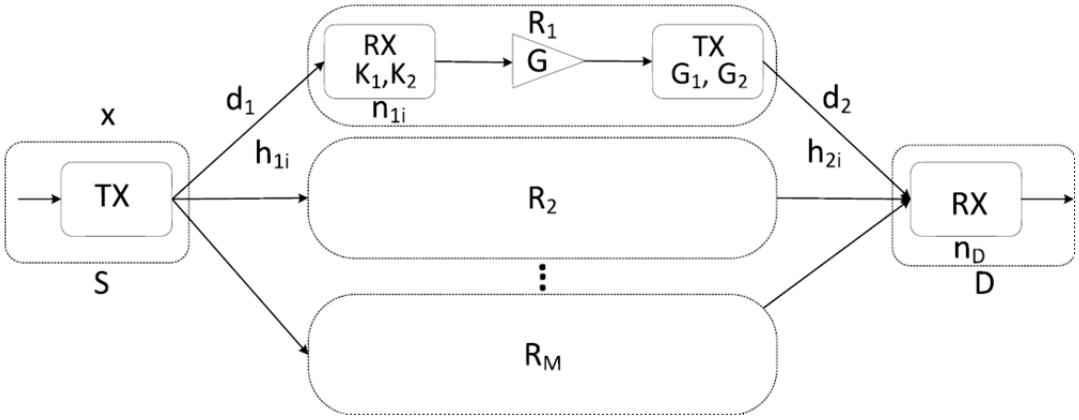

Figure 5.1: dual-hop DF and AF relaying model with M energy-harvesting relays under IQI.

We propose two kinds of cooperative relays, namely DF and AF in which M energy-harvesting relays denoted as with i = 1, 2, . . ., M. As shown in Figure 5.1, a source node S and a destination node D are assumed having a single antenna, and transmittance is forced in the half-duplex mode where transmitting and receiving works do not happen concurrently. Assuming that there is no connection between the source S and destination D directly, which the transmission signal from the source S and destination D is just via relays R_i because of deep shadowing. In addition, the relays R_i suffer the impact of the IQI.

In the proposed scheme, we consider two phases to transfer a single data. In the first phase, the source S transfers the signal to the relays R_i, and then, the relays harvest energy from the RF signals of the source S. In the second stage, the signal is carried to the destination through relays R_i. The next, relays R_i apply two methods to process the received signals: amplify and forward to the destination D (called the EHAF protocol), and decode and forward to the destination D (called the EHDF protocol). In this Chapter, the best relay of two proposed protocols EHAF and EHDF is found by basing on the end-to-end SINRs.

The mathematical equations for the throughput analyses of the two protocols EHDF and EHAF will be considered in the next Section.

5.3 Throughput performance analyses

In this Section, we define the h_{1i} and the h_{2i} as Rayleigh channel factors of the $S - R_i$ link and the $R_i - D$ link, respectively. Besides, let $n_{1i} \sim CN(0, N_1)$ and $n_D \sim CN(0, N_2)$ as the complicated Gaussian noises at the relays R_i and D.
Two proposed protocols EHDF and EHAF which the throughput based on the research

in [48], is described as follows

$$\tau_{\mathrm{X}} = (1 - \mathrm{P}_{out}^{X})(1-\alpha)\mathrm{R}/2 \tag{5.1}$$

where: P_{out}^{X} are the OPs of the protocols X, X $\in \{\mathrm{EHAF}, \mathrm{EHDF}\}$, R is defined as a target data rate and is related to a threshold SINRs γ_0 as $R = \log_2(1 + \gamma_0)$. and α is described as time-switching coefficient with $0 < \alpha < 1$.
In the first phase, the source S transmits its signals to the relays R_i. Then, the received baseband signals at the relays R_i of the proposed EHAF and EHDF protocols after down shift and under effects of RX I/Q mismatch can be presented as

$$y_{X\_SR_i} = K_1(h_{1i}x + n_{1i}) + K_2(h_{1i}x + n_D)^* \tag{5.2}$$

where x is the transmit signal of the source node S with average transfer energy $\mathrm{E}\{|x|^2\} = P$ ($\mathrm{E}\{z\}$ is an expectation expression of z), and

$$K_1 \triangleq (1 + g_T^{e^{j\varphi_T}})/2 \tag{5.3}$$

$$K_2 \triangleq (1 - g_T^{e^{j\varphi_T}})/2 \tag{5.4}$$

The TX magnitude and phase mismatch in (5.3-5.4) is performed g_T and φ_T.
The mirror data introduced by the IQI is often assigned as $(h_{1i}x + n_{1i})^*$ terms in Eq. (5.2). From (5.2) and [48], the power is gotten from the collected energy in the time $(1-\alpha)T/2$ for forwarding the processed signal to the destination D as

$$P_{R_i} = \frac{(|K_1|^2 + |K_2|^2)\, 2\alpha\eta P|h_{1i}|^2}{(1-\alpha)} \tag{5.5}$$

The relays R_i tranfer the signal to the destination D by amplifing (the EHAF protocol) or decoding (the EHDF protocol) in the second time slot.

5.3.1 The EHAF protocol

In this Section, we consider the operation principle of the proposed EHAF protocol. After the signals are broadcasted to the relay R_i from the source S, they will be magnified at the baseband level by the relay R_i with a magnification coefficient G, the next, converted up the radio frequency level (RF), and then, transferred to the destination D. Under TX IQI at the relay R_i[HTP03], the received baseband signal at the destination D is presented as

$$y_{EHAF\_R_iD} = h_{2i}(G_1(G\, y_{EHAF\_SR_i}) + G_2^*(G\, y_{EHAF\_SR_i})^*) + n_D \tag{5.6}$$

where

$$G_1 \triangleq (1 + g_R^{e^{j\varphi_R}})/2 \tag{5.7}$$

$$G_2 \triangleq (1 - g_R^{e^{j\varphi_R}})/2 \tag{5.8}$$

$$G = \sqrt{\frac{P_{R_i}}{F(|h_{1i}|^2 P + N_i)}} \tag{5.9}$$

In (5.7-5.8), g_R and φ_R denote the RX magnitude and phase mismatch.
Replacing the formulas (5.2), (5.9) into (5.6), and after some manipulations, the end-to-end SINRs is achieved as

$$\gamma_{EHAF\_R_iD} = \frac{aPP_{R_i}|h_{1i}|^2|h_{2i}|^2}{\begin{array}{l}\{bPP_{R_i}|h_{1i}|^2|h_{2i}|^2 + aN_1P_{R_i}|h_{2i}|^2 + \\ bN_1P_{R_i}|h_{2i}|^2 + N_2P|h_{1i}|^2 + N_1N_2\}\end{array}} \tag{5.10}$$

where $a = {A^2}/{F}$, $b = {B^2}/{F}$, $c = a + b$, $A \triangleq K_1G_1 + K_2^*G_2^*$; $B \triangleq K_1G_2 + K_2^*G_1^*$,
$F \triangleq (|K_1|^2 + |K_2|^2)(|G_1|^2 + |G_2|^2)$
Replacing the P_{R_i} in (5.5) into (5.10), we have the following result:

$$\gamma_{EHAF\_R_iD} = \frac{(2a\alpha\eta P^2(|K_1|^2 + |K_2|^2)|h_{1i}|^4|h_{2i}|^2)}{\left\{\begin{array}{l}(2b\alpha\eta P|h_{1i}|^4|h_{2i}|^2) + (2a\alpha\eta N_1P|h_{1i}|^2|h_{2i}|^2) \\ + (2b\alpha\eta N_1P|h_{1i}|^2|h_{2i}|^2) + (N_2P|h_{1i}|^2(1-\alpha) + N_1N_2(1-\alpha)\end{array}\right\}} \tag{5.11}$$

We base on the maximum of the end-to-end SINRs to find the best relay R_{b_1}, and is expressed as

$$R_{b_1} = \arg \max_{i \in \{1,2,\ldots,M\}} \gamma_{EHAF\_R_iD} \tag{5.12}$$

A math equation presents the outage probability of the EHAF protocol as follows

$$\begin{aligned} P_{out}^{EHAF} &= \Pr\left[\gamma_{EHAF\_R_{b_1}D} < \gamma_0\right] = \Pr\left[\max_{i=1,2,\ldots,M}(\gamma_{EHAF\_R_iD}) < \gamma_0\right] \\ &= \prod_{i=1}^{M} \Pr\left[\gamma_{EHAF\_R_iD} < \gamma_0\right] = \prod_{i=1}^{M} \Pr\left[w_{2i} < \frac{\omega w_{1i} + \psi}{u w_{1i}^2 - v w_{1i}}\right] \end{aligned} \tag{5.13}$$

Applied the proposition in [48], the expression P_{out}^{EHAF} is given as:

$$P_{out}^{EHAF} = \left[1 - \lambda_1 \int_{v/u}^{\infty} e^{-(\lambda_1 x + \lambda_2 \frac{\omega x + \psi}{(ux^2 - vx)})} dx\right]^M \tag{5.14}$$

$$\approx \left[1 - e^{-\frac{\lambda_1 v}{u}} \mu K_1(\mu)\right]^M, \text{ (SINRs approximation)}$$

where

$$\begin{aligned} \omega &= \gamma_0 N_2 P(1-\alpha) \\ \psi &= \gamma_0 N_1 N_2 (1-\alpha) \\ u &= 2a\alpha\eta P^2 \left(|K_1|^2 + |K_2|^2\right) - 2b\alpha\eta\gamma_0 P^2 \\ v &= 2a\alpha\eta P - 2b\alpha\eta\gamma_0 P \end{aligned}$$

5.3.2 The EHDF protocol

From (5.2), the SINRs at the relays R_i is achieved as follows

$$\gamma_{EHDF\_SR_i} = \frac{|K_1|^2 P |h_{1i}|^2}{|K_2|^2 P |h_{1i}|^2 + (|K_1|^2 + |K_2|^2) N_1} \tag{5.15}$$

After the decoded signal, this signal will be forward to the destination D by the relays R_i. The received signal at the destination D with the TX IQI at the relays R_i is shown as

$$y_{EHDF\_R_iD} = G_1(h_{2i}x + n_D) + G_2(h_{2i}x + n_D)^* \tag{5.16}$$

The next, the SINRs $\gamma_{EHDF\_R_iD}$ at the destination D is represented as

$$\begin{aligned} \gamma_{EHDF\_R_iD} &= \frac{|G_1|^2 P_{R_i} |h_{2i}|^2}{|G_2|^2 P_{R_i} |h_{2i}|^2 + (|G_1|^2 + |G_2|^2) N_2} \\ &= \frac{2\alpha\eta P |G_1|^2 |h_{1i}|^2 |h_{2i}|^2}{\left\{\left(2\alpha\eta P |G_2|^2 |h_{1i}|^2 |h_{2i}|^2\right) + (|G_1|^2 + |G_2|^2) N_2 (1-\alpha)\right\}} \end{aligned} \tag{5.17}$$

We calculate similar to the EHAF protocol, the best relay R_{b_2} in proposed EHDF protocol is given as follows

$$R_{b_2} = \arg \max_{i \in \{1,2,\ldots,M\}} \min \left(\gamma_{EHDF\_SR_i},\ \gamma_{EHDF\_R_iD}\right) \tag{5.18}$$

From formula (5.18), the outage probability of the EHDF protocol is achieved as

$$\begin{aligned} P_{out}^{EHDF} &= \Pr\left[\max_{i \in \{1,2,\ldots,M\}} \min \begin{pmatrix} \gamma_{EHDF\_SR_i}, \\ \gamma_{EHDF\_R_iD} \end{pmatrix} < \gamma_0\right] \\ &= \prod_{i=1}^{M} \Pr\left[\min \begin{pmatrix} \gamma_{EHDF\_SR_i}, \\ \gamma_{EHDF\_R_iD} \end{pmatrix} < \gamma_0\right] \\ &= \prod_{i=1}^{M} \left[1 - \Pr\left[\begin{array}{l} \min(\gamma_{EHDF\_SR_i}, \\ \gamma_{EHDF\_R_iD}) > \gamma_0 \end{array}\right]\right] \\ &= \prod_{i=1}^{M} \Pr\left[1 - \underbrace{\Pr\left[\begin{array}{l} (\gamma_{EHDF\_SR_i} > \gamma_0, \\ \gamma_{EHDF\_R_iD}) > \gamma_0 \end{array}\right]}_{\Phi}\right] \end{aligned} \tag{5.19}$$

The Φ in (5.19) is solved as

$$\begin{aligned} \Phi &= \Pr\left(w_{1i} > m, w_{2i} > \tfrac{o}{(p-q)w_{1i}}\right) \\ &= \begin{cases} \Pr\left[w_{1i} > m, w_{2i} > \frac{o}{(p-q)w_{1i}}\right], & p > q \\ \Pr\left[w_{1i} > m\right], & p \le q \end{cases} \\ &= \begin{cases} \lambda_1 \int_m^{\infty} e^{-(\lambda_1 x + \lambda_2 \frac{t}{x})} dx, & p > q \\ e^{-\lambda_1 m}, & p \le q \end{cases} \end{aligned} \tag{5.20}$$

where $m = \frac{\left(|K_1|^2+|K_2|^2\right)N_1\gamma_0}{(|K_1|^2-|K_2|^2\gamma_0)P}$;
$w_{1i} = |h_{1i}|^2$; $o = (|G_1|^2 + |G_2|^2)\, N_1(1-\alpha)\gamma_0$
$p = |G_1|^2 2\alpha\eta P$; $q = |G_2|^2 2\alpha\eta P\gamma_0$
The integral in Φ (5.20) is complex, and solving of this integral is not practical. However, we can find the values of Φ by using the numerical method.

5.4 Simulation results

Similar to the simulation results in Section 4.4 of Chapter 4, the system performance of the proposed protocols EHAF and EHDF is also analyzed and evaluated by using the exact theoretical analyses and the Monte Carlo simulations of the throughput. Besides, the coordinates of S, D, and R_i are set the same with (0, 0), (1, 0) and (x, y), respectively, satisfying $0 < x < 1$. Hence, $d_1 = \sqrt{x^2 + y^2}$ and $d_2 = \sqrt{(1-x)^2 + y^2}$. The IQI parameters are set to $20\log10(g_T) = 20\log10(g_R) = 1.58$dB. In addition, the SINRs on the x-axis is defined as $\gamma = \frac{P}{N_i} \quad \{i \in 1, 2\}$.

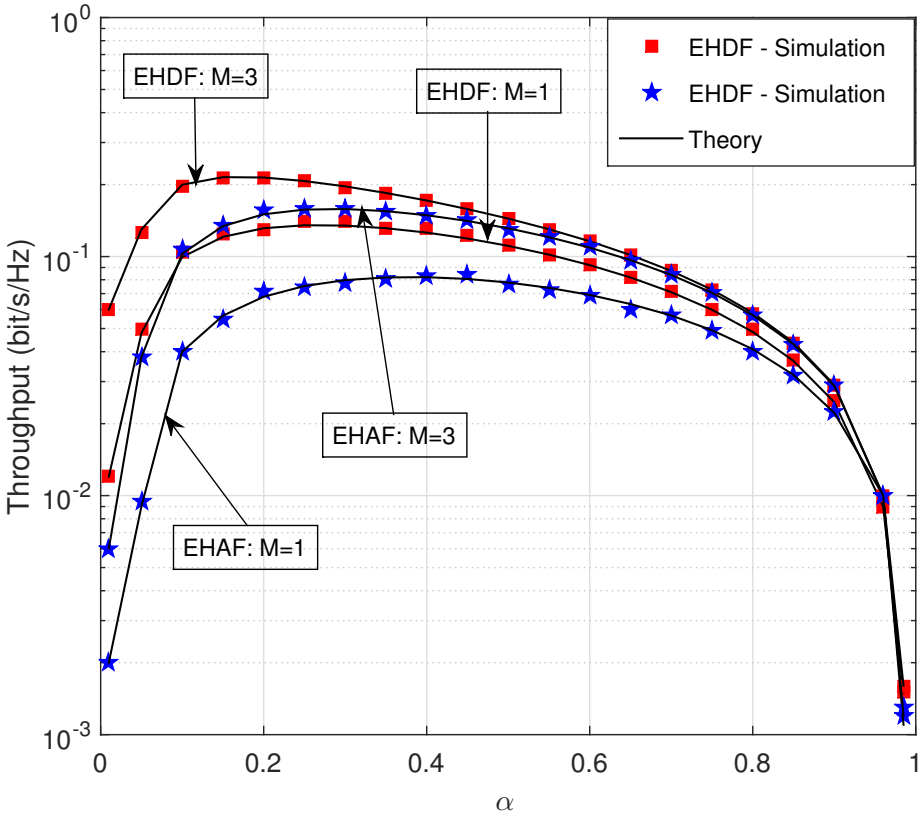

Figure 5.2: The throughput at the destination in the protocols EHDF and EHAF versus when the IQI parameters: 20 log10 (g_T) = 20 log10 (g_R) = 1.58dB and $\varphi_T = \varphi_R = 10^0$, η =0.9.

Figure 5.2 shows the throughput performance of two proposed protocols EHDF and

EHAF via the α with the values are considered as $d_1 = d_2 = 1$, SINR=5(dB), η=0.9 and $0<\alpha<1$. In this Figure, the throughput performance of in both EHDF and EHAF protocol increases by time-switching coefficient α and then throughput performance decreases when α increases. Besides, the throughput performance obtains the largest when values α get to an optimal value. These optimal values can be obtained by the Golden Section Search (GSS) method in [85] with a minimal interval 10^{-3}. Particularly, the optimal values in the EHDF protocol are approximately 0.27 and 0.17 when the number of relays, M, is set to 1 and 3, respectively. In EHAF protocol, the optimal value $\alpha = 0.39$ when M=1 and $\alpha = 0.29$ when M=3. As shown in Figure 5.2, the results show that the throughput performance achieves the optimal at the ideal value α. Besides, because of applying the best relay selection method, we have seen that, the system model has 3 relays, the throughput performance achieves the better than the system model has 1 relay in both proposed protocols. In addition, due to the impact of IQI noise in the propose system, the throughput performance will descend by α. Finally, the throughput performance of the EHDF protocol is greater than that of the EHAF protocol.

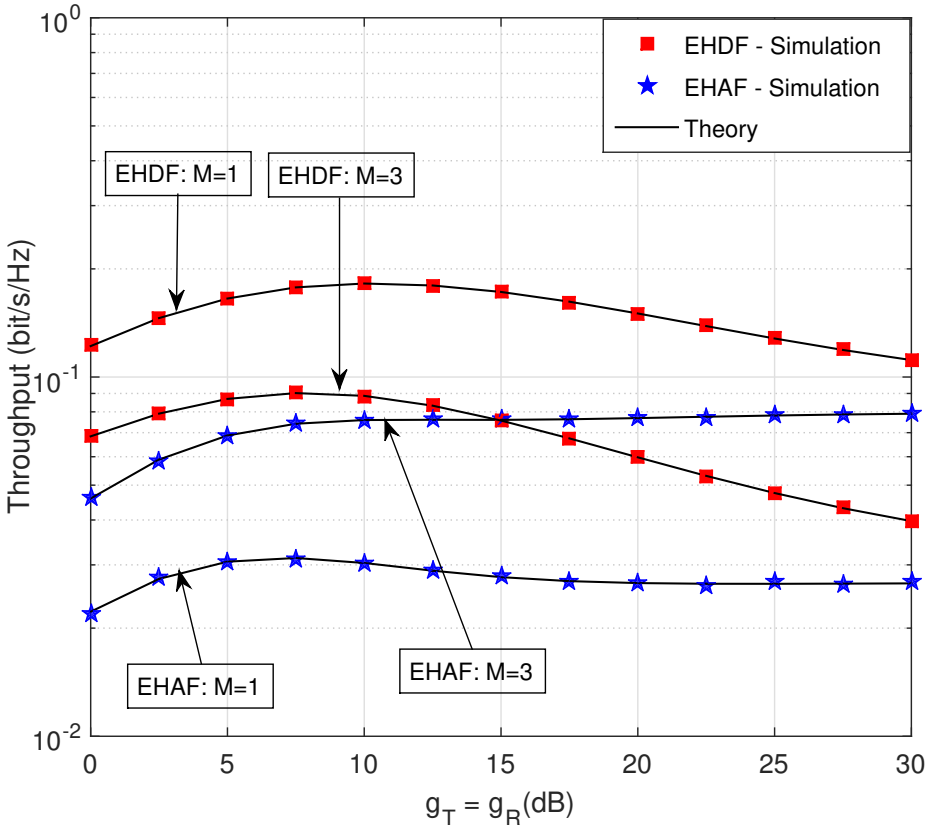

Figure 5.3: The throughputs in the protocols EHDF and EHAF versus the IQI parameters g_T= g_R(dB) and $\varphi_T = \varphi_R$= 10^0, η =0.9.

Figure 5.3 illustrates the throughput performances vesus the IQI parameters $g_T = g_R$(dB). In the asymmetric network scheme, we set parameters values φ_T= φ_R=10^0, η=0.9,

the IQI from 0 (dB) to 30 (dB). The parameters α are set to the optimal values α_{opt_AF} and α_{opt_DF} at each value of the g_T . It can be seen that when the IQI parameters values increase, the throughput performances of both protocols EHDF and EHAF decrease.

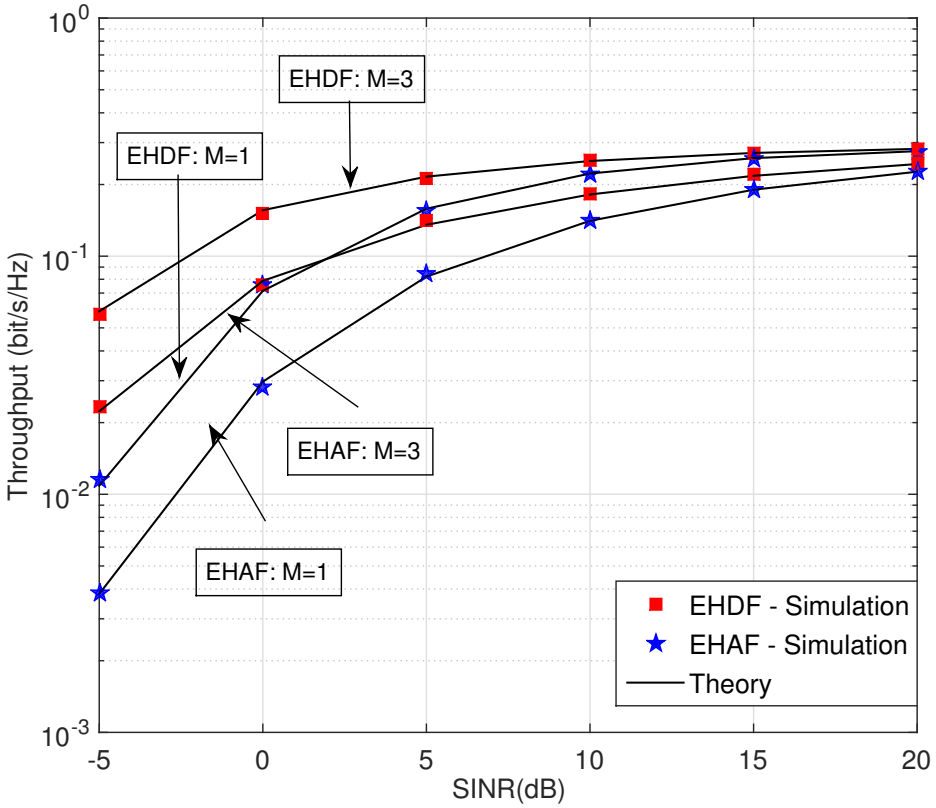

Figure 5.4: The throughput at the destination in the protocols EHDF and EHAF versus SINR when the IQI parameters: 20 log10 (g_T)=20log10 (g_R) = 1.58dB and $\varphi_T = \varphi_R = 10^0$, η=0.9.

Figure 5.4 compares the throughput performance between the EHDF and EHAF protocol versus SINR (dB) when α is set to the optimal valuesα_{opt_AF} and α_{opt_DF} at each value of the SINR(dB), respectively. The throughput performance of two proposed protocols increases when the SINRs values increase. Besides, we can see that the throughput of the EHDF protocol is efficiency the throughput of the EHAF protocol.

Lastly, the simulation results in two proposed protocols EHDF and EHAF fit well to the theoretical results. Hence, we can conclude that the formulas of throughput performance analysis are precise.

5.5 Conclusion

In this research, we presented a system model having M relays to transfer the signal between two sources together under the impact of IQI. To enhance the performance of the

system, we applied the best relay selection basing on end-to-end SINRs and using energy-harvesting from a wireless transmit source in both AF (called an EHAF protocol) and DF (called an EHDF protocol) cooperation methods. The system performance has analyzed and examined in terms of exact closed-form throughput over Rayleigh fading channels. The results have shown that the proposed EHDF protocol obtained higher throughput performance the proposed EHAF protocol. Furthermore, when the system model had the number of relays increases, the throughput performance of the two proposed protocols was also improved.

6 THE NOMA TECHNOLOGY IN TWO-WAY DECODE-AND-FORWARD SCHEME WITH DNC

In Chapter 4, we investigated the Two-Way cooperative relaying with energy harvesting. We have proof that it has the advantage of increasing diversity capacity and improving the performance of wireless communication. However, with the development of wireless devices, the demand for always available connectivity and transfer data quickly increasing steadily, so we need the solutions to resolve the speed up data rate, the QoS efficiently. The NOMA technique is one of the optimal solutions to improve these problems. [HTP01], [HTP04].

6.1 Motivation

It has been many research the combinations of cooperative relaying and NOMA [7, 88, 89, 90]. In [80], the performance of NOMA-based cooperative relaying systems had been studied and the performance of NOMA schemes in AF relay systems had been investigated in [90]. In order to improve the throughput of future 5G wireless networks, the NOMA has been recently received great attention from the researches and has been becoming an interesting topic.

The majority of researchers have not to focus on the Two-Way DF using NOMA. Because of the emerged idea, in this study, we introduce the Two-Way DF scheme to enhance the spectrum efficiency and improve the speed transfer data in which an transitional relay applies the NOMA technique and uses the DNC solution to compress received data from the source nodes (called a TWNOMA protocol) [HTP04].

The particular goal of this paper can be summarized as follows. Initially, we introduce a Two-Way DF cooperative relaying scheme in which relay applies NOMA technology to enhance the system performance for the wireless networks. Then, Monte Carlo simulation is used to derive and to confirm the exact closed-form sum OPs over Rayleigh fading channels. Lastly, the proposed TWNOMA protocol surpasses the conventional protocols, namely, Two-Way scheme using DNC (TWDNC), Two-Way scheme without using DNC (TWNDNC) and Two-Way AF scheme (TWANC).

The details of research are organized as follows:a Two-Way DF NOMA system model is described in Section 2; Section 3 presents the exact OPs of the source nodes in the proposed TWNOMA protocol; the simulation results are shown in Section 4; and Section 5 summarizes our conclusions.

6.2 System model

As shown in Figure 6.1, in this part, a Two-Way DF NOMA model in which relay R using SIC in NOMA is proposed called as a TWNOMA protocol. Particularly, the system

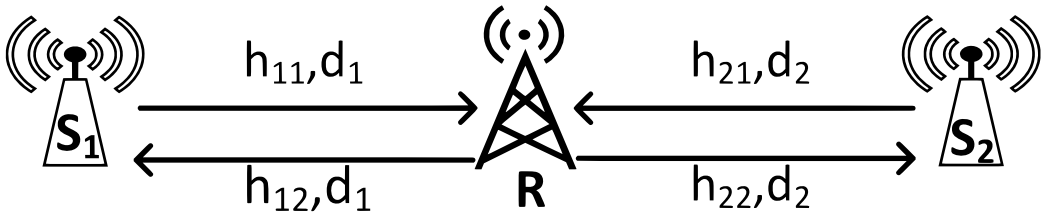

Figure 6.1: System model of a Two-Way DF NOMA scheme

consists of two source nodes S_1, S_2 and intermediate relay R. The S_1 propagates the signal x_1 to S_2 and S_2 transits the signal x_2 to S_1, where $E\{|x_1|^2\} = 1$, $E\{|x_2|^2\} = 1$,($E\{x\}$ is notated for the expectation process of x).
There are four assumptions given as follows. Firstly, the variances of Zero-mean AWGNs are equal, represented namely N_0. Secondly, all channels are designated to flat and block Rayleigh fading. Thirdly, all the nodes in the system have a private antenna.. Finally, Channel State -Information (CSI) are known at all the source nodes[30, 87].

In Figure 6.1, the parameters for analysis are the same way in Section 4.2 of the Chapter 4. Particularly, (h_{1i}, d_1) and (h_{2i}, d_2) are Rayleigh fading channel coefficients and the link distances of S_1-R, S_2-R respectively, where $i \in \{1, 2\}$. The random variables $g_{1i} = |h_{1i}|^2$ and $g_{2i} = |h_{2i}|^2$ have exponential distributions with the parameters $\lambda_1 = d_1^\beta$ and $\lambda_2 = d_2^\beta$, respectively, where β is a path-loss exponent. The Cumulative Distribution Function (CDF) and probability density function (pdf) of random variables g_{ji} are expressed as $F_{g_{ji}}(x) = 1 - e^{-\lambda_i x}$ and $f_{g_{ji}}(x) = \lambda_i e^{-\lambda_i x}$, respectively, where $j \in \{1, 2\}$.

The operation principle of the TWNOMA protocol is divided into two timeslots based on a time division channel model. In the beginning timeslot, the source nodes S_1 and S_2 transmit their packets x_1 and x_2 to the relay R. In the next timeslot, the relay R applies the NOMA to decode one after another the packets x_1 and x_2 based on the channel gains, and then uses the DNC by an XOR operation ($x = x_1 \oplus x_2$) before broadcasting the coded x to the source nodes S_1 and S_2.

6.3 Outage Probability Analysis

In this Section, some assumptions are given as. The source nodes S_1, S_2 and the relay R use the transmit power P the same, a node successfully decodes the received packet if its achievable data rate is larger than or equal a target data rate R_t.

The transmission signal between source node S_1 and source node S_2 consist of two phases. In the first phase, two source nodes S_1, S_2 transfer their signal to each other through relay R. So, the relay R gets the signals from S_1, S_2 are given as

$$y_R = \sqrt{P}h_{11}x_1 + \sqrt{P}h_{21}x_2 + n_R \tag{6.1}$$

In the second time slot, the relay R sends the received signals $x = x_1 \oplus x_2$ to at the sources S_1 and S_2 are given as

$$y_{S_k} = \sqrt{P} h_{k2} x + n_{S_k},\ k \in \{1, 2\} \tag{6.2}$$

where n_R and n_{S_k} denote the AWGNs at the nodes R and S_k respectively, with the same variance N_0.

This Chapter, due to proposing the Two-Way scheme, we consider two conditions of channel gain to calculate the outage probability as follow:

The condition $g_{11} > g_{21}$

Based on researches about the NOMA in [1, 2, 3, 4, 5], by applying SIC technology in the NOMA first the relay R decodes x_1 from (6.1) [HTP01], then x_2 will be decoded without the component $\sqrt{P} h_{11} x_1$ in (6.1). The received Signal-to-Noise Ratios (SNRs) $SNR^1_{S_1R}$ and $SNR^1_{S_2R}$ at the relay R for decoding the information signal x_1 and x_2 are obtained, respectively, as follows

$$SNR^1_{S_1R} = \frac{P|h_{11}|^2}{P|h_{21}|^2 + N_0} = \frac{\gamma g_{11}}{\gamma g_{21} + 1} \tag{6.3}$$

$$SNR^1_{S_2R} = \frac{P|h_{21}|^2}{N_0} = \gamma g_{21} \tag{6.4}$$

where γ is defined as a transmit SNR, $\gamma = \frac{P}{N_0}$.

The outage probability of the source node S_2 without receiving signal x_1 happens when the achievable data rates of links S_1-R and R-S_2 are small than the threshold Rt, and represented as follows,

$$\begin{aligned} P^{out\_S_2{}^1}_{TWNOMA} = & \underbrace{\Pr\left[R^1_{S_1R} < R_t\right]}_{\Pr 1.1} \\ & + \underbrace{\Pr\left[R^1_{S_1R} \geq R_t, R^1_{RS_2} < R_t\right]}_{\Pr 1.2} \end{aligned} \tag{6.5}$$

where $R^1_{S_1R}$ and $R^1_{RS_2}$ are given as

$$\begin{aligned} R^1_{S_1R} &= \tfrac{1}{2}\log_2\left(1 + SNR^1_{S_1R}\right) \\ &= \tfrac{1}{2}\log_2\left(1 + \tfrac{\gamma g_{11}}{\gamma g_{21}+1}\right) \end{aligned} \tag{6.6}$$

$$R^1_{RS_2} = \frac{1}{2}\log_2\left(1 + SNR^1_{RS_2}\right) = \frac{1}{2}\log_2\left(1 + \gamma g_{22}\right) \tag{6.7}$$

The probability Pr1.1 at (6.5) is manipulated and calculated as

$$\begin{aligned}\Pr 1.1 &= [g_{11} > g_{21}, g_{11} < \theta g_{21} + \theta/\gamma] \\ &= \Pr[g_{21} < g_{11} < \theta g_{21} + \theta/\gamma] \\ &= \begin{cases} \int_0^{\infty} f_{g_{21}}(x)[-F_{g_{11}}(x) + F_{g_{11}}(\theta x + \theta/\gamma)] \\ \qquad\qquad\qquad\qquad , 1-\theta < 0 \\ \int_0^{a} f_{g_{21}}(x)[-F_{g_{11}}(x) + F_{g_{11}}(\theta x + \theta/\gamma)] \\ \qquad\qquad\qquad\qquad , 1-\theta > 0 \end{cases} \end{aligned} \tag{6.8a}$$

where $\theta = 2^{2Rt} - 1$, $a = \frac{\theta}{(1-\theta)\gamma}$

By applying the pdf of the random variable g_{21} and the CDF of the random variable g_{11}, Pr1.1 obtained a closed form expression as

$$\Pr 1.1 = \begin{cases} \frac{\lambda_2}{\lambda_1+\lambda_2} - \frac{\lambda_2 e^{-\lambda_1\theta/\gamma}}{\lambda_2+\lambda_1\theta}, & 1-\theta < 0 \\ \frac{\lambda_2}{\lambda_1+\lambda_2}\left(1 - e^{-(\lambda_1+\lambda_2)a}\right) & 1-\theta > 0 \\ -\frac{\lambda_2 e^{-\lambda_1\theta/\gamma-(\lambda_2+\lambda_1\theta)a}}{\lambda_2+\lambda_1\theta} \times \left(e^{(\lambda_2+\lambda_1\theta)a} - 1\right) & \end{cases} \tag{6.8b}$$

Calculating similar to the Pr1.1, Pr1.2 in (6.5) is also is solved as

$$\Pr 1.2 = \Pr[g_{11} > g_{21}, g_{11} \geq \theta g_{21} + \theta/\gamma, g_{22} < \theta/\gamma]$$

$$\begin{aligned} &= \begin{cases} \Pr[g_{11} \geq \theta g_{21} + \theta/\gamma, g_{22} < \theta/\gamma], & 1-\theta < 0 \\ \Pr[g_{11} \geq \theta g_{21} + \theta/\gamma, \\ \quad g_{21} < \theta g_{21} + \theta/\gamma, g_{22} < \theta/\gamma], & 1-\theta > 0 \\ + \Pr[g_{21} \geq \theta g_{21} + \theta/\gamma, \\ \quad g_{11} > g_{21}, g_{22} < \theta/\gamma] & \end{cases} \\ &= \begin{cases} \int_0^{\infty} \left(\begin{array}{l} f_{g21}(x)(1 - F_{g_{11}}(\theta x + \theta/\gamma) \\ \times F_{g_{22}}(\theta/\gamma)\, dx \end{array} \right), 1-\theta < 0 \\ \int_0^{a} \left(\begin{array}{l} f_{g_{21}}(x)\,[1 - F_{g_{11}}(\theta x + \theta/\gamma] \\ \times F_{g_{22}}(\theta/\gamma) dx \end{array} \right) \\ \quad + \int_a^{\infty} \left(\begin{array}{l} f_{g_{21}}(x)\,[1 - F_{g_{11}}(x)] \\ \times F_{g_{22}}(\theta/\gamma) dx \end{array} \right), & 1-\theta > 0 \end{cases} \\ &= \begin{cases} \left(1 - e^{\lambda_2\theta/\gamma}\right) \frac{\lambda_2 e^{-\lambda_1\theta/\gamma}}{\lambda_2+\lambda_1\theta} & , \quad 1 < \theta \\ \lambda_2 \left(1 - e^{-\lambda_2\theta/\gamma}\right) \times & \\ \left\{ \begin{array}{l} \left(\frac{e^{-\lambda_1\theta/\gamma - a\lambda_2 - a\lambda_1\theta}}{\lambda_2+\lambda_1\theta}\right) \\ \times \left(e^{(\lambda_2+\lambda_1\theta)a} - 1\right) + \frac{e^{-(\lambda_2+\lambda_1)a}}{\lambda_1+\lambda_2} \end{array} \right\}, & 1 > \theta \end{cases} \end{aligned} \tag{6.9}$$

With the probabilities Pr1.1 in (6.8b) and Pr1.2 in (6.9) in hand, the closed-form expression is denoted for the outage probability of the source node S_2 in the TWNOMA protocol in (6.5) is obtained in the closed-form expression.
Similarly, the outage probability of the source node S_1 in the TWNOMA protocol in also the condition $g_{11} > g_{21}$ is expressed by a math expression as follows

$$\begin{aligned} P_{TWNOMA}^{out\_{S_1}^1} = & \underbrace{\Pr\left[R_{S_2R}^1 < R_t\right]}_{\Pr 2.1} \\ & + \underbrace{\Pr\left[R_{S_2R}^1 \geq R_t, R_{RS_1}^1 < R_t\right]}_{\Pr 2.2} \end{aligned} \tag{6.10}$$

where $R_{RS_2}^1$ and $R_{RS_1}^1$ are expressed respectively, as
$R_{RS_2}^1 = \frac{1}{2}\log_2(1+\gamma g_{22})$ and $R_{RS_1}^1 = \frac{1}{2}\log_2(1+\gamma g_{12})$. Hence, the probabilites Pr2.1 and Pr2.2 are also solved easily as follows

$$\begin{aligned} \Pr 2.1 &= \Pr[g_{1,1} > g_{21}, g_{21} < \theta/\gamma] \\ &= \int_0^{\theta/\gamma} f_{g_{21}}(x)(1 - F_{g_{11}}(x))dx \\ &= \frac{\lambda_2}{\lambda_1+\lambda_2}(1 - e^{-\theta/\gamma(\lambda_1+\lambda_2)}) \end{aligned} \tag{6.11}$$

$$\begin{aligned} \Pr 2.2 &= \Pr[g_{11} > g_{21}, g_{21} > \theta/\gamma, g_{12} < \theta/\gamma] \\ &= F_{g_{12}}(\theta/\gamma) \times \int_{\theta/\gamma}^{\infty} f_{g_{21}}(x)(1 - F_{g_{11}}(x))dx \\ &= \left(1 - e^{-\lambda_1\theta/\gamma}\right)\frac{\lambda_2}{\lambda_2+\lambda_1}e^{-(\lambda_1+\lambda_2)\theta/\gamma} \end{aligned} \tag{6.12}$$

From (6.11) and (6.12), the outage probability $P_{TWNOMA}^{out\_{S_1}^1}$ is solve successfully.

The condition $g_{11} \leq g_{21}$

The system model of the TWNOMA protocol is researched in the symmetric characteristic. Therefore, the outage probabilities of the source nodes S_1 and S_2 are inferred easily by changes parameters λ_1 as λ_2. The outage probabilities are expressed as $P_{TWNOMA}^{out\_{S_1}^2} = \Pr 3.1 + \Pr 3.2$ and $P_{TWNOMA}^{out\_{S_2}^2} = \Pr 4.1 + \Pr 4.2$, where the closed-form results are shown as:

$$\Pr 3.1 = \begin{cases} \frac{\lambda_1}{\lambda_1+\lambda_2} - \frac{\lambda_1 e^{-\lambda_2\theta/\gamma}}{\lambda_1+\lambda_2\theta} & , 1-\theta < 0 \\ \frac{\lambda_1}{\lambda_1+\lambda_2}\left(1 - e^{-(\lambda_1+\lambda_2)a}\right) & \\ -\frac{\lambda_1 e^{-\lambda_2\theta/\gamma-(\lambda_1+\lambda_2\theta)a}}{\lambda_1+\lambda_2\theta} & , 1-\theta > 0 \\ \times\left(e^{(\lambda_1+\lambda_2\theta)a} - 1\right) & \end{cases} \tag{6.13}$$

$$\Pr 3.2 = \begin{cases} \left(1-e^{-\lambda_1\theta/\gamma}\right)\frac{\lambda_1 e^{-\lambda_2\theta/\gamma}}{\lambda_1+\lambda_2\theta} & , \ 1-\theta<0 \\ \lambda_1\left(1-e^{-\lambda_1\theta/\gamma}\right)\left(\frac{e^{-\lambda_2\theta/\gamma-a\lambda_1-a\lambda_2\theta}}{\lambda_1+\lambda_2\theta}\right) & \\ \times\left(e^{(\lambda_1+\lambda_2\theta)a}-1\right) & , \ 1-\theta>0 \\ +\lambda_1\left(1-e^{-\lambda_1\theta/\gamma}\right)\left(\frac{e^{-(\lambda_2+\lambda_1)a}}{\lambda_1+\lambda_2}\right) & \end{cases} \tag{6.14}$$

$$\Pr 4.1 = \frac{\lambda_1}{\lambda_1+\lambda_2}\left(1-e^{-\theta/\gamma(\lambda_1+\lambda_2)}\right) \tag{6.15}$$

$$\Pr 4.2 = \left(1-e^{-\lambda_2\theta/\gamma}\right)\frac{\lambda_1}{\lambda_2+\lambda_1}e^{-(\lambda_2+\lambda_1)\theta/\gamma} \tag{6.16}$$

Finally, with the formulas in (6.8b), (6.9), (6.11), (6.12), (6.13),(6.14), (6.15) and (6.16), the sum outage probabilities $P_{TWNOMA}^{out\_sum}$ of the proposed TWNOMA protocol are obtained and are expressed in the closed form.

$$\begin{aligned} P_{TWNOMA}^{out\_sum} &= P_{TWNOMA}^{out\_S_1^1} + P_{TWNOMA}^{out\_S_2^1} + P_{TWNOMA}^{out\_S_1^2} + P_{TWNOMA}^{out\_S_2^2} \\ &= 1 - \frac{1}{\lambda_1+\lambda_2}\left[\begin{array}{l} \lambda_2\left(1-e^{-(2\lambda_1+\lambda_2)\theta/\gamma}\right) \\ +\lambda_1\left(1-e^{-(\lambda_1+2\lambda_2)\theta/\gamma}\right) \end{array}\right] \\ &+ \begin{cases} 1-\frac{\lambda_2 e^{-(\lambda_1+\lambda_2)\theta/\gamma}}{\lambda_2+\lambda_1\theta}-\frac{\lambda_1 e^{-(\lambda_1+\lambda_2)\theta/\gamma}}{\lambda_1+\lambda_2\theta} & , \ 1-\theta<0 \\ \left(1-e^{-(\lambda_1+\lambda_2)a}\right)-\frac{\lambda_2 e^{-\lambda_1\theta/\gamma-(\lambda_2+\lambda_1\theta)a}}{\lambda_2+\lambda_1\theta}\left(e^{(\lambda_2+\lambda_1\theta)a}-1\right)-\frac{\lambda_1 e^{-\lambda_2\theta/\gamma-(\lambda_1+\lambda_2\theta)a}}{\lambda_1+\lambda_2\theta}\left(e^{(\lambda_1+\lambda_2\theta)a}-1\right) & \\ \lambda_2\left(1-e^{-\lambda_2\theta/\gamma}\right)\left\{\left(\frac{e^{-\lambda_1\theta/\gamma-a\lambda_2-a\lambda_1\theta}}{\lambda_2+\lambda_1\theta}\right)\left(e^{(\lambda_2+\lambda_1\theta)a}-1\right)+\frac{e^{-(\lambda_2+\lambda_1)a}}{\lambda_1+\lambda_2}\right\}+ & \\ \lambda_1\left(1-e^{-\lambda_1\theta/\gamma}\right)\left\{\left(\frac{e^{-\lambda_2\theta/\gamma-a\lambda_1-a\lambda_2\theta}}{\lambda_1+\lambda_2\theta}\right)\left(e^{(\lambda_1+\lambda_2\theta)a}-1\right)+\frac{e^{-(\lambda_2+\lambda_1)a}}{\lambda_1+\lambda_2}\right\} & , \ 1-\theta>0 \end{cases} \end{aligned} \tag{6.17}$$

6.4 Simulation Results

In this Section, we analyzed and evaluated the system performance of the TWNOMA protocol. The exact theoretical analyses results have verified by the Monte Carlo simulations. In the two-dimensional plane, we set the S_1, S_2, and R at positions as S_1 (0, 0), S_2 (1, 0) and R (x, y), respectively, satisfying $x \in (0, 1)$. Therefore, we had $d_1 = \sqrt{x^2+y^2}$ and $d_2 = \sqrt{(1-x)^2+y^2}$. The path-loss exponent β is assumed equal 3.

In this research, we compared the simulation and analysis results of the proposed TWNOMA protocol with the TWANC protocol [17], the TWDNC protocol and the TWNDNC protocol [30]. We considered these protocols having the same energy E for comparing fairly between protocols TWNOMA, TWANC, TWDNC, and TWNDNC.

Figure 6.2 illustrate the sum OPs of two source nodes S_1 and S_2 via E/N_0 (dB) when the parameters for analysis in the network model are set with $x = 0.2$, $y = 0$, $R_t = 1$ (bit/s/Hz). We can see that in Figure 6.2, the sum outage probabilities of the source nodes S_1 and S_2 in the protocols decrease when the E/N_0 raises due to the large transmit powers. Besides, because the proposed TWNOMA protocol uses both SIC technique in the

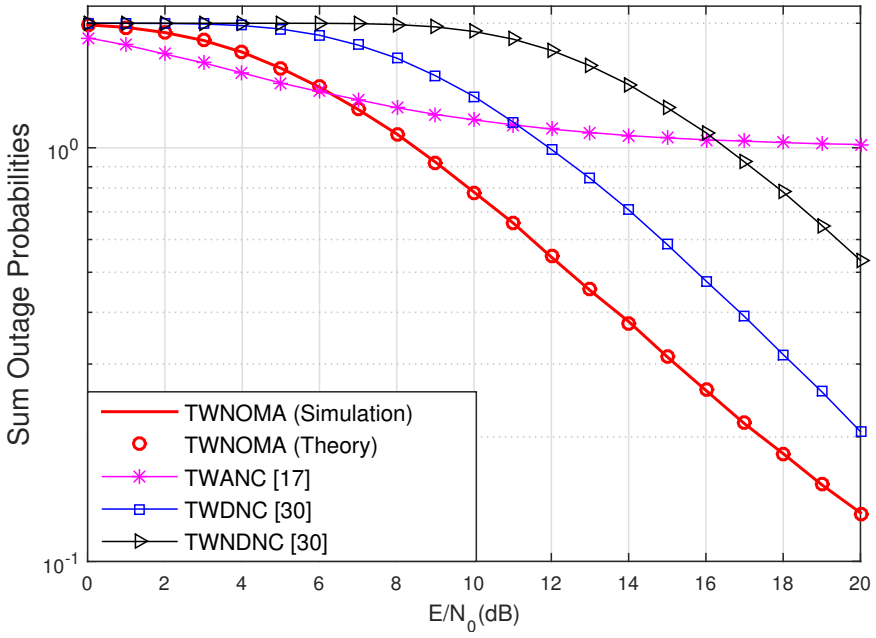

Figure 6.2: The sum OPs of the source nodes S_1 and S_2 versus E/N_0 (dB) when x=0.2, $R_t = 1$ (bit/s/Hz).

NOMA and the DNC technique to compensate the loss of the bandwidth, the performance of the proposed TWNOMA protocol outperforms the conventional protocols TWANC, TWDNC, and TWNDNC . Lastly, the theoretical results match well to simulation results of the proposed TWNOMA protocol. Hence, we conclude that the derived formulas are accurate during analysis.

Figure 6.3 presents sum OPs versus the position x of the relay on x-axis, when the parameters are set as follow, $E/N_0 = 10$ (dB), $R_t = 1$ (bit/s/Hz), and x moves from 0.1 to 0.9. In Figure 6.3, we can see that the performance of the proposed TWNOMA protocol is best when the relay is located at the point $x_1 = 0.3$ and $x_1 = 0.7$ between the sources S_1 and S_2. It mean that, if the relay R is set at these position, the performance of system is achieved the best efficiency. Besides, the sum OPs of the proposed TWNOMA protocol is also smaller than that of the protocols TWANC, TWDNC, and TWNDNC. Therefore, the proposed TWNOMA protocol with the NOMA and DNC techniques exceed the other protocols, and simultaneously, achieves higher bandwidth utilization efficiency.

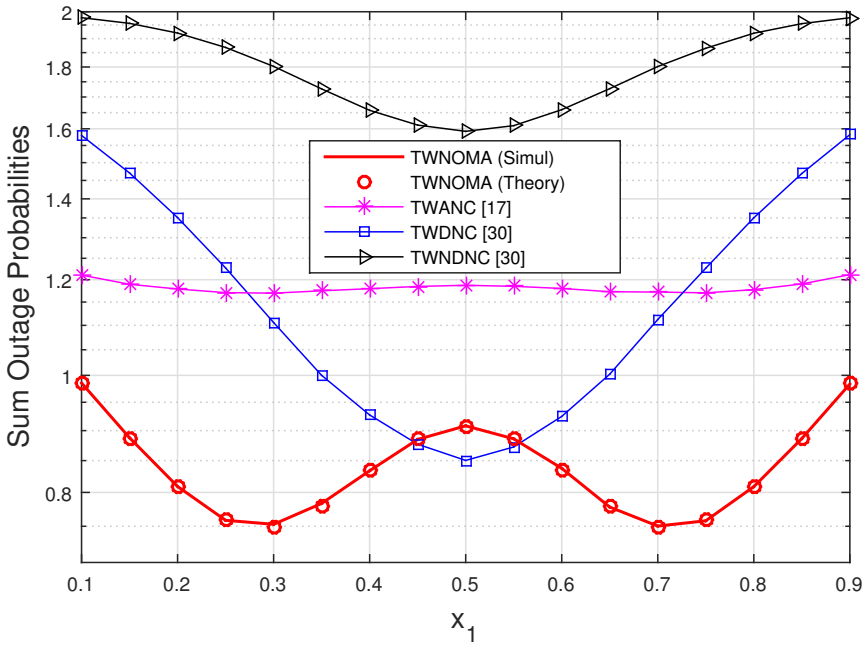

Figure 6.3: The sum OPs versus location x of the relay on x-axis, when $E/N_0 = 10$ (dB), $R_t = 1$ (bit/s/Hz), and x_1 moves from 0.1 to 0.9.

6.5 Conclusions

In this research, the Two-Way DF NOMA scheme (called the TWNOMA protocol) was proposed. The intermediate relay applied SIC in the NOMA technology to detect the received and transmitted signals. The system performance was analyzed, evaluated and obtained closed-form exact for SOPs over Rayleigh fading channels. The research results shown that the proposed TWNOMA protocol improved performance when it was compared with the conventional Two-Way DF scheme using DNC (called the TWDNC protocol), Two-Way DF scheme without using DNC (called the TWNDNC protocol) and Two-Way AF scheme (called the TWANC protocol). Besides, we can see that the proposed protocol achieved the best performance if the relay was set at two optimal positions between two source nodes. Lastly, we obtained the closed-form exact for the sum OPs and matched well with the Monte Carlo simulation results.

7 THE SECURITY OF UCCN USING NOMA TO IMPROVE THE SYSTEM PERFORMANCE AND SECRECY PERFORMANCE

Inheritance from Chapter 6, this chapter, we suggested the NOMA scheme with PLS to enhance the spectral efficiency and the security capacity of the wireless network.

7.1 Motivation

Today, the security is one of the important problems to save the data of users. So, there are many types of research to the PLS [98, 101]. The research in [98] investigated the secrecy performance of the cooperative network using the relay selection method under the impact of co-channel. The other authors in [101] studied the secrecy performance of multiple DF relaying under the effect of correlated fading and using the optimal relay selection method. Besides, the NOMA technology combining with the PLS was researched in [102, 103]. In [102], the authors presented the problem of maximizing the minimum confidential information rate among users subject to the secrecy outage constraint and instantaneous transmits power constraint. The NOMA with the PLS in AF and DF cooperation network were also investigated in [103].

In addition, NOMA technique in underlay cognitive radio networks was proposed by some authors in [104, 105, 106, 107]. In [104], A downlink NOMA in CR systems has been researched to exploit the optimal spatial diversity. The studies in [108, 109, 110] given many security principles. The authors in [109] researched the secrecy communication in cognitive DF relay networks in which a pair of cognitive relays is opportunistically selected for security protection against eavesdroppers. The authors in [110] presented the tradeoffs between reliability and secrecy in cooperative cognitive radio networks with the NOMA technology.

All of the above researchers, the authors have not presented to combine between the NOMA technology and PLS in the UCCN yet. So, in this Chapter, we propose a NOMA cooperative relay scheme for UCCN in which the best relay helps to DF and transfer two signals x_1 and x_2 two destination nodes D_1 and D_2 respectively, under impact wiretapping of a node eavesdropper. In this Chapter, we give three strategies to choose the best relay. In the first and second strategy, the best relay selection is based on maximizing the value of the channel gains from the links R_i-D_1, R_i-D_2, respectively. Remain of strategy is applied by the minimum value of the channel gains from R_i-E link. After finding the best relay, we examine the efficient secrecy of the transmissions x_1 and x_2 in the proposed UCCN-NOMA scheme in terms of the secrecy outage probabilities(SOPs) over Rayleigh fading channels to enhance the spectrum efficiency and secure communication.

The chapter is summarized with the main contributions as follows. Firstly, we propose a DF-formed cooperation UCCN scheme in which the best relay uses the NOMA and

considers the PLS to enhance the system performance in 5G wireless networks. Secondly, the SOPs over Rayleigh fading channels are derived and are confirmed by Monte Carlo simulations. Thirdly, the secrecy performances of the transmissions x_1 and x_2 in three best relay selection strategies are compared with each other in the proposed UCCN-NOMA system. The rest of this Chapter organized as follows: Section 7.2 presents a UCCN system model in which the best relay applying the NOMA technology collaborating with the PLS and operation principles of the suggested system; Section 7.3 analyzes and evaluates the secrecy outage probabilities of the messages x_1 and x_2 in the proposed UCCN-NOMA system; Section 4 shows the simulation results; and Section 5 outlines our conclusions.

7.2 System model

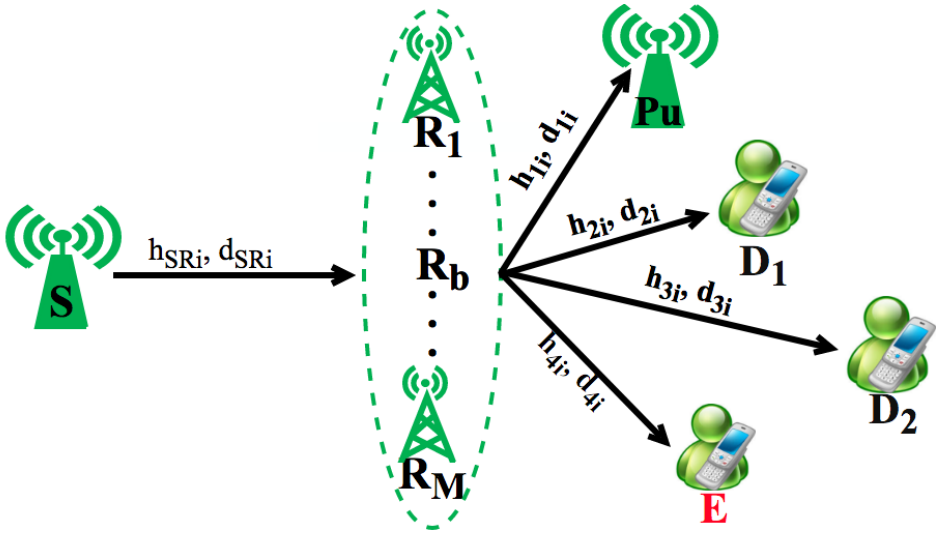

Figure 7.1: System model of a UCCN-NOMA scheme considering PLS.

In this Section, in Figure 7.1 was considered a wireless cooperative scheme for a UCCN. The cooperative scheme uses the NOMA principle to improve spectral performance. It contains one source node S transfer the messages to two destination nodes D_1, D_2 through multi-wireless relay nodes under impact by one eavesdropper node E to wiretap the signals. As shown in this figure, we assume that the source S and two destination nodes are not transmitted directly which the intermediate relays help to carry the messages to D_1 and D_2 with illegal presence of the eavesdropper E. In system model, we assumed the distance from R_i to D_2 link is farther than distance from R_i to D_1. Besides, the source node S sent its packets to two nodes D_1 and D_2 shown as x_1 is sent to D_1, x_2 is sent to D_2. To obtain optimal performance, we considered applying the NOMA technology and the relay selection technique to find out the best relay to support the two nodes D_1 and D_2 can receive quickly. Three kinds of relay selection were given as follow, the first strategy and second strategy were calculated to base on the maximum channel gain of the links R_i -

D_1 and R_i - D_2, respectively. The remaining strategy was presented by minimum channel gain of the link R_i-E.

Some assumptions are denoted as follows. The first, the source S and two destination nodes D_1 and D_2 have a private antenna. Secondly, variances of Zero-mean AWGNs are equal, presented the same N_0. Thirdly, all channels are designated to flat and block Rayleigh fading. Finally, the Channel State Information (CSI) regarding the S-E, S-R_i, and R_i-E channels are known at the source node S and the destination nodes D_1 and D_2 [96].

In Figure 7.1, we define the parameters for analysis as follow. The h_{SR_i}, h_{ji} are Rayleigh fading channel coefficients which is fixed during a block time T, and are the variables independent and identically distributed between two continuous block times. The d_{SR_i}, d_{ji} are the link distances of S-R_i, R_i-D_k, R_i-E, and R_i-Pu respectively, where $j \in \{1, 4\}$, $i \in \{1, M\}$, and $k \in \{1, 2\}$. Hence, the random variables $g_{ji} = |h_{ji}|^2$ has exponential distribution with the parameter $\lambda_j = d_{ji}^{\beta}$, where β is a path-loss exponent. The respectively distances of R_i-D_k, R_i-E, and R_i-Pu have represented in the figure 7.1. The Cumulative Distribution Function (CDF) and probability density function (pdf) of random variables g_{ji} are expressed as $F_{g_{ji}}(a) = 1 - e^{-\lambda_j a}$ and $f_{g_{ji}}(a) = \lambda_j e^{-\lambda_j a}$, respecctively.

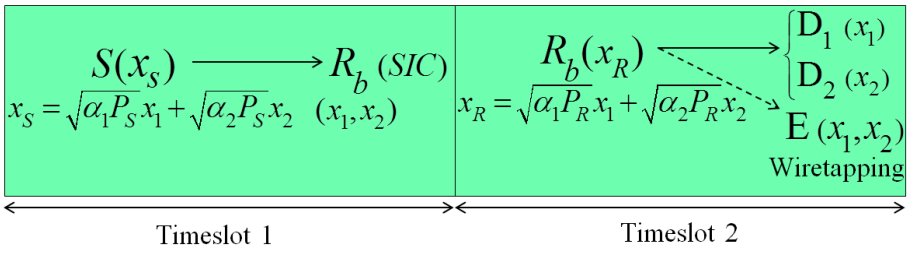

Figure 7.2: Operation diagram of the proposed system.

As shown in Figure 7.2, the operation principle of the proposed NOMA scheme in UCCN is presented within two timeslots. The first timeslot, the source node S sends its signal x_s which consists messages x_1 and x_2 through the best relay R_b, with $E\{|x_1|^2\} = 1, E\{|x_2|^2\} = 1$ ($E\{x\}$ is denoted for the expectation process of x). The message x_s is created by the superposition coding method. The strategy for finding the best relay R_b [HTP02] will be presented in the next section. The best relay R_b applies the SIC in NOMA technology to decode the messages x_1 and x_2 sequentially based on the allocated powers to the messages x_1 and x_2 at the source node S. In remaining timeslot, the best relay R_b combines the messages x_1 and x_2 to the coded signal x_R by the superposition coding. Then, the message x_R is sent to the destinations D_1 and D_2. The eavesdropper E is always wiretapping the message x_R in the wireless environment.

7.3 Secrecy Outage Probability (SOP) Analysis

In this section, the security performance for the eavesdropping of the messages x_1 and x_2 in the proposed UCCN-NOMA system is analyzed and exploited. With the assumption that a node decodes the received packet successfully and safely if its achievable secrecy capacity is larger than a target secrecy capacity SC_{th}.

The message x_s is the superposition coding [HTP04]. It is created by the source node S and is sent to to all of the relay R_i in first timeslot. The message x_s is shown by

$$x_s = \sqrt{\alpha_1 P_s} x_1 + \sqrt{\alpha_2 P_s} x_2, \tag{7.1}$$

where P_s is the power at source node S, the α_1 and α_2 are the power allocation coefficients, and x_1 and x_2 are the messages sending to D_1 and D_2. Following the operation principle of the NOMA, the power allocation coefficients are define as $\alpha_1 > \alpha_2$ with $\alpha_1 + \alpha_2 = 1$. The message received at the relay R_i is shown as follow

$$y_{SR_i}^{x_{1,2}} = x_s h_{SR_i} + n_{R_i} = \sqrt{\alpha_1 P_s} h_{SR_i} x_1 + \sqrt{\alpha_2 P_s} h_{SR_i} x_2 + n_{R_i}, \tag{7.2}$$

where n_{R_i} denote the AWGNs at the relay R_i with the same variance N_0.

In the operation principle of NOMA scheme, after the relay R_i received the signal from (7.1), it decodes the signal x_1 and removes it using the SIC, and then the signal x_2 will be decoded and forward to D_2 without the component $\sqrt{\alpha_1 P_s} h_{SR_i} x_1$ in (7.2). So the signal received at R_i after decoding x_1 is illustrated as follows

$$y_{SR_i}^{x_2} = \sqrt{\alpha_2 P_s} x_2 h_{SR_i} + n_{R_i}. \tag{7.3}$$

In the second phase, the messages received at the users D_1 and D_2 related to links R_i-D_1 and R_i-D_2, respectively, can be shown as

$$y_{R_i D_1}^{x_1} = \sqrt{\alpha_1 P_R} h_{2i} x_1 + \sqrt{\alpha_2 P_R} h_{2i} x_2 + n_{D_1}. \tag{7.4}$$

$$y_{R_i D_2}^{x_2} = \sqrt{\alpha_2 P_R} x_2 h_{3i} + n_{D_2}. \tag{7.5}$$

where n_{D_k}denote the AWGNs at the user D_k with the same variance N_0, P_R is a transmit power of the relay R_i.

Similar as above, the eavesdropper E also wiretaps the messages x_1 and x_2 from R_i, respectively, the received signals at eavesdropper E are achieved as follows

$$y_{R_i E}^{x_1} = \sqrt{\alpha_1 P_s} x_1 h_{4i} + \sqrt{\alpha_2 P_s} x_2 h_{4i} + n_E. \tag{7.6}$$

$$y_{R_i E}^{x_2} = \sqrt{\alpha_2 P_s} x_2 h_{4i} + n_E. \tag{7.7}$$

where n_E denote the AWGNs at the eavesdropper E with the same variance N_0.

In the UCCN, because of the impact the interference constraint at the Pu node, the relay R_i have to adjust their transmitting powers less than a threshold value, I_{th} [111]. The maximum powers of the relays R_i are given, respectively,

$$P_R = \frac{I_{th}}{|h_{1i}|^2} = \frac{I_{th}}{g_{1i}}. \tag{7.8}$$

The received SINRs at the users D_1 and D_2 for decoding the information messages x_1 and x_2 are calculated by the formulas in (7.4) and (7.5) and are achieved, respectively, as follows

$$SINR_{R_iD_1}^{x_1} = \frac{P_R\alpha_1 g_{2i}}{P_R\alpha_2 g_{2i} + N_0}. \tag{7.9}$$

$$SINR_{R_iD_2}^{x_2} = \frac{P_R\alpha_2 g_{3i}}{N_0}. \tag{7.10}$$

Similarly, the received SINRs at the node E for eavesdropping the information signal x_1 of D_1 and signal x_2 of D_2 from the relay R_i are obtained, respectively, as follows

$$SINR_{R_iE}^{x_1} = \frac{P_R\alpha_1 g_{4i}}{P_R\alpha_2 g_{4i} + 1} = \frac{Q\alpha_1 g_{4i}}{Q\alpha_2 g_{4i} + g_{1i}}. \tag{7.11}$$

$$SINR_{R_iE}^{x_2} = \frac{P_R\alpha_2 g_{4i}}{N_0} = \frac{Q\alpha_2 g_{4i}}{g_{1i}}. \tag{7.12}$$

The formulas (7.11) and (7.12) is found by the formulas (7.6) and (7.7).
Using the Shannon capacity formula, the achievable rates of the links R_i–Y are formulated as

$$R_{R_iY}^{x_k} = \frac{1}{2}\log_2(1 + SINR_{R_iY}^{x_k}), \tag{7.13}$$

where the number 1/2 is ratio that data transmission is split into two time slots, and $Y \in \{E, D_k\}$.

Hence, we calculate the secrecy capacity of proposed system for the R_i-D_k communication can be presented as

$$SC_w = \left[SC_{R_{bw}D_k}^{x_k} - SC_{R_{bw}E}^{x_k}\right]^+, \tag{7.14}$$

where $[x]^+ = \max(0, x)$; $w \in \{1, 3\}$; $SC_{R_{bw}D_k}^{x_k}$ are the secrecy capacities from the the relay R_i to the destination D_k are given, respectively, as

$$SC_{R_{bw}D_k}^{x_k} = \max(0, R_{R_{bw}D_k}^{x_k} - R_{R_{bw}E}^{x_k}). \tag{7.15}$$

7.3.1 The sum SOP of the secrecy transmission in the proposed UCCN-NOMA system with the best relay selection, called as ST1 case.

To calculate the sum SOPs, we have to find out the best relay R_{b_1}. In this case (ST1), the best relay R_{b_1} achieve by calculating the maximum channel of the R_i-D_1 link. Hence, we find the SOPs of the ST1 case in which the destination nodes D_1 and D_2 does not

get signal safely from the source node S through R_{b_1} under the malicious attempt of the eavesdropper E. And then, the sum SOPs is compared with the sum SOPs in the ST2 and ST3 case in the section 7.3.2 and 7.3.3. The best relay R_{b_1} obtained as follows

$$R_{b_1} = \arg \underbrace{\max}_{i=1...M} |h_{R_i D_1}|^2 = \underbrace{\max}_{i=1...M} |h_{2i}|^2 = g_{2b_1} \tag{7.16}$$

From formula of R_{b_1} in (7.16), the CDF and pdf of the random variables $g_{2b_1}$is obtained respective, as

$$\begin{aligned} F_{g_{2b_1}}(a) &= \Pr\left(g_{2b_1} < a\right) = \Pr\left[\underbrace{\max}_{i=1...M} g_{2i} < a\right] \\ &= \prod_{i=1}^{M}\left(1 - e^{-\lambda_2 a}\right) = \left(1 - e^{-\lambda_2 a}\right)^M \end{aligned} \tag{7.17}$$

$$f_{g_{2b_1}}(a) = \frac{\partial F_{g_{2b_1}}(a)}{\partial a} = M\lambda_2 e^{-\lambda_2 a}\left(1 - e^{-\lambda_2 a}\right)^{M-1}. \tag{7.18}$$

The first, we perform the SOP at destination node D_1 in the ST1 case in which the node D_1 does not receive signal safely from the R_{b_1} under the malicious attempt of the eavesdropper E, and is denoted by a math equation as follows

$$P_{\mathrm{ST1}}^{out\_D_1} = \mathrm{P_r}\left(SC_{R_{b_1}D_1}^{x_1} < SC_{th}\right). \tag{7.19}$$

Replacing formula (7.15) into (7.19), $P_{\mathrm{ST1}}^{out\_D_1}$ is achieved as

$$P_{\mathrm{ST1}}^{out\_D_1} = \Pr\left(R_{R_{b_1}D_1}^{x_1} - R_{R_{b_1}E}^{x_1} \le SC_{th}\right) \tag{7.20}$$

Substituting formula (7.13) into (7.20), $P_{\mathrm{ST1}}^{out\_D_1}$ is expressed as

$$\begin{aligned} P_{\mathrm{ST1}}^{out\_D_1} &= \Pr\left[\tfrac{1}{2}\log_2\left(1 + SINR_{R_{b_1}D_1}^{x_1}\right) < \tfrac{1}{2}\log_2\left(1 + SINR_{R_{b_1}E}^{x_1}\right) + SC_{th}\right] \\ &= \Pr\left[\tfrac{1}{2}\log_2\left(1 + \tfrac{P_R\alpha_1 g_{2b_1}}{P_R\alpha_2 g_{2b_1}+1}\right) < \tfrac{1}{2}\log_2\left(1 + \tfrac{P_R\alpha_1 g_{4b_1}}{P_R\alpha_2 g_{4b_1}+1}\right) + SC_{th}\right] \\ &= \Pr\left[\tfrac{P_R\alpha_1 g_{2b_1}}{P_R\alpha_2 g_{2b_1}+1} < \theta + (\theta+1)\left(\tfrac{P_R\alpha_1 g_{4b_1}}{P_R\alpha_2 g_{4b_1}+1}\right)\right], \end{aligned} \tag{7.21}$$

where $\theta = 2^{2SC_{th}} - 1$.

In this part, we examine the worst case in which the node E can get the data of D_1 with the best conditions. From formula (7.21), we have an upper constraint of the $P_{\mathrm{ST1}}^{out_D_1}$as follows

$$\begin{aligned} P_{\mathrm{ST1}}^{out\_D_1} \le P_{\mathrm{ST1}}^{out\_upper} &= \Pr\left[\tfrac{P_R\alpha_1 g_{2b_1}}{P_R\alpha_2 g_{2b_1}+1} < \theta + (\theta+1)\left(P_R\alpha_1 g_{4b_1}\right)\right] \\ &= \Pr\left[g_{4b_1} > \tfrac{g_{2b_1}g_{1b_1}}{(\theta+1)\left(Q\alpha_2 g_{2b_1}+g_{1b_1}\right)} - \tfrac{\theta g_{1b_1}}{(\theta+1)Q\alpha_1}\right] \\ &= \int_0^\infty f_{g_{1b_1}}(x)\Pr\left[g_{4b_1} > \frac{g_{2b_1}x}{(\theta+1)\left(Q\alpha_2 g_{2b_1}+x\right)} - \frac{\theta x}{(\theta+1)Q\alpha_1}\right]dx \\ &= \int_0^\infty f_{g_{1b_1}}(x)\left(\mathrm{A_1}+\mathrm{A_2}\right)dx, \end{aligned} \tag{7.22}$$

where $P_R = \frac{I_{th}}{g_{1i}}$, $Q = \frac{I_{th}}{N_0}$, $\mathrm{A}_1 = \Pr\left[g_{4b_1} > \frac{g_{2b_1}x}{(\theta+1)(Q\alpha_2 g_{2b_1}+x)} - \frac{\theta x}{(\theta+1)Q\alpha_1}\right]$,

$\mathrm{A}_2 = \mathrm{P_r}\left[g_{4b_1} > \frac{g_{2b_1}x}{(\theta+1)\left(\alpha_2 Q g_{2b_1}+x\right)} - \frac{\theta x}{(\theta+1)Q\alpha_1}; \frac{g_{2b_1}x}{(\theta+1)\left(\alpha_2 Q g_{2b_1}+x\right)} > \frac{\theta x}{(\theta+1)Q\alpha_1}\right]$,

in order to solve the $P_{\mathrm{ST1}}^{out\_upper}$ in (7.22), we apply two Lemmas as follows

Lemma 1: The A_1 is achieved by a closed-form expression as follows

$$\mathrm{A}_1 = \begin{cases} 1 & ,\alpha_1 \le \alpha_2\theta \\ \left(1 - e^{-\lambda_2\psi x}\right)^M & ,\alpha_1 > \alpha_2\theta, \end{cases} \tag{7.23}$$

where $\psi = \frac{\theta}{Q(\alpha_1 - \theta\alpha_2)}$.

Proof: The proof of Lemma 1 is provided in Appendix A1.

Lemma 2: The following expression is valid of A_2

$$\mathrm{A}_2 = \begin{cases} 0 & ,\alpha_1 \le \theta\alpha_2 \\ \int\limits_{\psi x}^{\infty} f_{g_{2b_1}}(y)\, e^{-\lambda_4\left(\frac{xy}{(\theta+1)(\alpha_2 Q y + x)} - \frac{\theta x}{(\theta+1)Q\alpha_1}\right)} dxdy & ,\alpha_1 > \theta\alpha_2. \end{cases} \tag{7.24}$$

Proof: The proof of Lemma 2 is presented clearly in Appendix A2.

The exact upper expression $P_{\mathrm{ST1}}^{out\_upper}$ of the SOP $P_{\mathrm{ST1}}^{out\_D_1}$ is provided in a following Theorem.

Theorem 1: The upper expression $P_{\mathrm{ST1}}^{out\_upper}$ is obtained by the expression as

$$P_{\mathrm{ST1}}^{out\_upper} = \begin{cases} 1 & ,\alpha_1 \le \theta\alpha_2 \\ \left(\lambda_1 \sum\limits_{t=0}^{M} (-1)^t C_M^t \times \frac{1}{(\lambda_1 + \lambda_2\psi t)} + \frac{\lambda_1\lambda_2 M}{\alpha_2 Q} \times \mathrm{I}_1\right) & ,\alpha_1 > \theta\alpha_2, \end{cases} \tag{7.25}$$

where $\mathrm{I}_1 = \int\limits_0^{\infty}\int\limits_{px}^{\infty} \left[\begin{array}{l} \exp\left(-\lambda_1 x + nx - \frac{\lambda_4 x}{(\theta+1)\alpha_2 Q} + \frac{\lambda_2 x}{\alpha_2 Q}\right) \\ \times \exp\limits_{px}^{\infty} \exp\left(\frac{\lambda_4 x^2}{(\theta+1)\alpha_2 Q z} - \frac{\lambda_2 z}{\alpha_2 Q}\right)\left(1 - \exp(-\frac{\lambda_2(z-x)}{\alpha_2 Q})\right)^{M-1} \end{array}\right] dzdx.$

and $n = \frac{\lambda_4\theta}{(\theta+1)\alpha_1 Q}$.

Proof: Substituting Lemma 1 and Lemma 2 into (7.22), $P_{\mathrm{ST1}}^{out_upper}$is shown in two cases as

-When $\alpha_1 \le \theta\alpha_2$:

$$P_{\mathrm{ST1}}^{out\_upper} = \int\limits_0^{\infty} f_{g_{1b_1}}(x)(1+0)dx = \int\limits_0^{\infty} \lambda_1 e^{-\lambda_1 x} dx = 1. \tag{7.26a}$$

-When $\alpha_1 > \theta\alpha_2$:

$$P_{\mathrm{ST1}}^{out\_upper} = \left(\underbrace{\int\limits_0^{\infty} f_{g_{1b_1}}(x)\left(1 - e^{-\lambda_2 x\psi}\right)^M dx}_{\mathrm{A}_3} + \underbrace{\int\limits_0^{\infty} f_{g_{1b_1}}(x) \int\limits_{\psi x}^{\infty} f_{g_{2b_1}}(y)\, e^{-\lambda_4\varphi} dxdy}_{\mathrm{A}_4} \right), \tag{7.26b}$$

where $\varphi = \frac{xy}{(\theta+1)(\alpha_2 Qy+x)} - \frac{\theta x}{(\theta+1)\alpha_1 Q}$.
The A_3 in (7.26b) is calculated as

$$\begin{aligned} A_3 &= \int_0^\infty f_{g_{1b_1}}(x)(1-e^{-\lambda_2\psi x})^M dx = \int_0^\infty \lambda_1 e^{-\lambda_1 x}\left(1-e^{-\lambda_2\psi x}\right)^M dx \\ &= \lambda_1 \sum_{t=0}^{M}(-1)^t C_M^t \int_0^\infty e^{-(\lambda_1+\lambda_2\psi t)x} dx = \lambda_1 \sum_{t=0}^{M}(-1)^t C_M^t \times \frac{1}{(\lambda_1+\lambda_2\psi t)}, \end{aligned} \tag{7.27}$$

where $C_m^n = \frac{(m)!}{n!(m-n)!}$.
The A_4 in (7.26b) is presented as

$$\begin{aligned} A_4 &= \int_0^\infty f_{g_{1b_1}}(x)\, dx \int_{\psi x}^\infty f_{g_{2b_1}}(y)\, e^{-\lambda_4\varphi} dy \\ &= \int_0^\infty \lambda_1 e^{-\lambda_1 x} \int_{\psi x}^\infty M \times \lambda_2 e^{-\lambda_2 y}\left(1-e^{-\lambda_2 y}\right)^{M-1} e^{-\lambda_4\varphi} dx dy \\ &= \lambda_1\lambda_2 M \int_0^\infty \exp\left(-x\left(\lambda_1 - \frac{\lambda_4\theta}{(\theta+1)\alpha_1 Q}\right)\right) \\ &\quad \times \int_{\psi x}^\infty \exp\left(\frac{-\lambda_4 xy}{(\theta+1)(\alpha_2 Qy+x)} - \lambda_2 y\right) \times (1-\exp(-\lambda_2 y))^{M-1} dx dy, \end{aligned} \tag{7.28}$$

By setting $z = \alpha_2 Qy + x$, the A_4 in (7.28) is given as

$$\begin{aligned} A_4 &= \frac{\lambda_1\lambda_2 M}{\alpha_2 Q} \int_0^\infty \int_{px}^\infty \left[\begin{array}{l} \exp\left(-\lambda_1 x + nx\right) \\ \times \exp\left(\frac{-\lambda_4 x(z-x)}{(\theta+1)\alpha_2 Qz} - \frac{\lambda_2(z-x)}{\alpha_2 Q}\right) \times \left(1-\exp(-\frac{\lambda_2(z-x)}{\alpha_2 Q})\right)^{M-1} \end{array} \right] dz dx \\ &= \frac{\lambda_1\lambda_2 M}{\alpha_2 Q} \int_0^\infty \int_{px}^\infty \left[\begin{array}{l} \exp\left(\lambda_1 x + nx - \frac{\lambda_4 x}{(\theta+1)\alpha_2 Q} + \frac{\lambda_2 x}{\alpha_2 Q}\right) \times \exp\left(\frac{\lambda_4 x^2}{(\theta+1)\alpha_2 Q z} - \frac{\lambda_2 z}{\alpha_2 Q}\right) \\ \times \left(1-\exp(-\frac{\lambda_2(z-x)}{\alpha_2 Q})\right)^{M-1} \end{array} \right] dz dx, \end{aligned} \tag{7.29}$$

where $p = \alpha_2 Q\psi + 1$.
Replacing A_3 in (7.27) and A_4 in (7.29) into (7.26b), the $P_{\mathrm{ST1}}^{out\_upper}$ is given as

$$P_{\mathrm{ST1}}^{out\_upper} = \left(\lambda_1 \sum_{t=0}^{M}(-1)^t C_M^t \times \frac{1}{(\lambda_1+\lambda_2\psi t)} + \frac{\lambda_1\lambda_2 M}{\alpha_2 Q} \times \mathrm{I}_1\right). \tag{7.30}$$

From obtained results in formulas (7.30) and (7.26a), the Theorem 1 in (7.25) is proven successfully.

Secondly, we find the SOP at destination node D_2 in the ST1 case in which the node D_2 does not receive message safely from the source node S through the best relay R_{b1} under the malicious attempt of the eavesdropper E as follows

$$P_{\mathrm{ST1}}^{out\_D_2} = \Pr\left(SC_{R_{b_1}D_2}^{x_2} < SC_{th}\right). \tag{7.31}$$

Replacing formula (7.15) into (7.31), $P_{\mathrm{ST1}}^{out\_D_2}$ is obtained as

$$P_{\mathrm{ST1}}^{out\_D_2} = \Pr\left(R_{R_{b_1}D_2}^{x_2} - R_{R_{b_1}E}^{x_2} \leq SC_{th}\right). \tag{7.32}$$

Substituting the formula (7.13), $P_R = \frac{I_{th}}{g_{1i}}$, $Q = \frac{I_{th}}{N_0}$ into (7.32), $P_{\mathrm{ST1}}^{out\_D_2}$ is expressed as

$$\begin{aligned} P_{\mathrm{ST1}}^{out\_D_2} &= \mathrm{P_r}\left[\tfrac{1}{2}\log_2\left(1 + SINR_{R_{b_1}D_2}^{x_2}\right) - \tfrac{1}{2}\log_2\left(1 + SINR_{R_{b_1}E}^{x_2}\right) < SC_{th}\right] \\ &= \Pr\left[\tfrac{1}{2}\log_2\left(1 + \tfrac{P_R\alpha_2 g_{3b_1}}{N_0}\right) - \tfrac{1}{2}\log_2\left(1 + \tfrac{P_R\alpha_2 g_{4b_1}}{N_0}\right) < SC_{th}\right] \\ &= \Pr\left[g_{3b_1} < \tfrac{\theta g_{1b_1}}{Q\alpha_2} + (\theta+1)g_{4b_1}\right]. \end{aligned} \tag{7.33}$$

The math equation in (7.33) is achieved the close-form expression by applying the pdf of the random variables g_{1b_1}, g_{4b_1} and the CDF of the random variable g_{3b_1}, and given as

$$\begin{aligned} P_{\mathrm{ST1}}^{out\_D_2} &= \int_0^\infty\int_0^\infty \Pr\left[g_{3b_1} < \frac{\theta x}{Q\alpha_2} + (\theta+1)y\right] f_{g_{1b_1}}(x) f_{g_{4b_1}}(y)\, dxdy \\ &= 1 - \int_0^\infty\int_0^\infty \lambda_1 e^{-\lambda_1 x}\lambda_4 e^{-\lambda_4 y} e^{-\lambda_3\left(\frac{\theta x}{Q\alpha_2} + (\theta+1)y\right)}\, dxdy \\ &= 1 \; - \; \frac{\lambda_1\lambda_4}{\left(\lambda_1 + \frac{\lambda_3\theta}{Q\alpha_2}\right)(\lambda_4 + \lambda_3(\theta+1))}. \end{aligned} \tag{7.34}$$

Finally, from formulas (7.25) and (7.34), the sum SOPs in ST1 case is constrained by the upper expression as

$$\begin{aligned} Sum\, P_{\mathrm{ST1}}^{out} &= P_{ST1}^{out\_D_1} \; + \; P_{ST1}^{out\_D_2} \\ &\leq \begin{cases} 1 + \left(1 \; - \; \frac{\lambda_1\lambda_4}{\left(\lambda_1 + \frac{\lambda_3\theta}{Q\alpha_2}\right)(\lambda_4 + \lambda_3(\theta+1))}\right) & , \alpha_1 \leq \theta\alpha_2 \\ \left(\lambda_1 \sum\limits_{t=0}^{M} (-1)^t C_M^t \times \frac{1}{(\lambda_1 + \lambda_2\psi t)} + \frac{\lambda_1\lambda_2 M}{\alpha_2 Q} \times \mathrm{I}_1\right) + \left(1 \; - \; \frac{\lambda_1\lambda_4}{\left(\lambda_1 + \frac{\lambda_3\theta}{Q\alpha_2}\right)(\lambda_4 + \lambda_3(\theta+1))}\right) & , \alpha_1 > \theta\alpha_2. \end{cases} \end{aligned} \tag{7.35}$$

7.3.2 The SOP of the secrecy transmission in the proposed UCCN-NOMA system with the best relay selection, called as ST2 case.

We have the best relay R_{b_2} by calculating the same way the best relay R_{b_1} but based on maximum channel gain of the R_i-D_2 link. Then, we calculate the sum SOPs of the nodes D_1, D_2 in the ST2 case.

The best relay R_{b_2} is presented as follows

$$R_{b_2} = \arg \underbrace{\max}_{m=1\ldots M} |h_{R_m D_2}|^2 = \underbrace{\max}_{m=1\ldots M} |h_{3i}|^2 = g_{3b_2} \tag{7.36}$$

The CDF and pdf of the random variable $g_{3b_2}$is expressed similar as (7.17) and (7.18) and is shown as $F_{g_{3b_2}}(a) = \left(1 - e^{-\lambda_3 a}\right)^M$, $f_{g_{3b_2}}(a) = M\lambda_3 e^{-\lambda_3 a}\left(1 - e^{-\lambda_3 a}\right)^{M-1}$.
The SOP at destination D_2 in the ST2 case happens when the destination D_2 does not receive signals x_2 safely from the source node S, and is expressed by a math expression as follows

$$P_{\mathrm{ST2}}^{out\_D_2} = \Pr\left(SC_{R_{b_2}D_2}^{x_2} < SC_{th}\right) \tag{7.37}$$

Replacing formula (7.15) into (7.37), the$P_{\mathrm{ST2}}^{out_D_2}$ is calculated as

$$P_{\mathrm{ST2}}^{out\_D_2} = \Pr\left(R_{R_{b_2}D_2}^{x_2} - R_{R_{b_2}E}^{x_2} \le SC_{th}\right) \tag{7.38}$$

Substituting formula (7.13) , $P_R = \frac{I_{th}}{g_{1i}}$,$Q = \frac{I_{th}}{N_0}$ into (37), $P_{\mathrm{ST2}}^{out\_D_2}$ is expressed as

$$\begin{aligned} P_{\mathrm{ST2}}^{out\_D_2} &= \Pr\left[\tfrac{1}{2}\log_2\left(1 + SINR_{R_{b_2}D_2}^{x_2}\right) - \tfrac{1}{2}\log_2\left(1 + SINR_{R_{b_2}E}^{x_2}\right) < SC_{th}\right] \\ &= \Pr\left[\tfrac{1}{2}\log_2\left(1 + \tfrac{P_R\alpha_2 g_{3b_2}}{N_0}\right) - \tfrac{1}{2}\log_2\left(1 + \tfrac{P_R\alpha_2 g_{4b_3}}{N_0}\right) < SC_{th}\right] \\ &= \Pr\left[g_{3b_2} < \tfrac{\theta g_{1b_2}}{Q\alpha_2} + (\theta+1)g_{4b_2}\right] \end{aligned} \tag{7.39}$$

By calculating similar to (7.33), the probability $P_{\mathrm{ST2}}^{out_D_2}$in (7.39) is obtained the close-form as follows

$$\begin{aligned} P_{\mathrm{ST2}}^{out\_D_2} &= \int_0^\infty\int_0^\infty \Pr\left[g_{3b_2} < \frac{\theta x}{Q\alpha_2} + (\theta+1)y\right] f_{g_{1b_2}}(x) f_{g_{4b_2}}(y)\, dxdy \\ &= \int_0^\infty\int_0^\infty \lambda_1 e^{-\lambda_1 x}\lambda_4 e^{-\lambda_4 y}\left(1 - e^{-\lambda_3\left(\frac{\theta x}{Q\alpha_2} + (\theta+1)y\right)}\right)^M dxdy \\ &= \lambda_1\lambda_4 \sum_{t=0}^{M} (-1)^t C_M^t \int_0^\infty\int_0^\infty e^{-\lambda_1 x} e^{-\lambda_4 y} e^{-\lambda_3\left(\frac{\theta x}{Q\alpha_2} + (\theta+1)y\right)t} dxdy \\ &= \lambda_1\lambda_4 \sum_{t=0}^{M} (-1)^t C_M^t \times \tfrac{Q\alpha_2}{\lambda_1 Q\alpha_2 + \lambda_3\theta t} \times \tfrac{1}{\lambda_4 + (\theta+1)\lambda_3 t}. \end{aligned} \tag{7.40}$$

The next, we calculate the SOP at destination node D_1 in the ST2 case in which the destination node D_1 does not receive signal safely from the source node S through the best relay R_{b2} under the malicious attempt of the eavesdropper E as follows

$$P_{\mathrm{ST2}}^{out\_D_1} = \Pr\left(SC_{R_{b_2}D_1}^{x_1} < SC_{th}\right) = \Pr\left(R_{R_{b_2}D_1}^{x_1} - R_{R_{b_2}E}^{x_1} \le SC_{th}\right). \tag{7.41}$$

By replacing the formulas (7.9) and (7.13) into (7.41), we have an expression of the $P_{\mathrm{ST2}}^{out\_D_1}$ as follow

$$\begin{aligned} P_{\mathrm{ST2}}^{out\_D_1} &= \Pr\left[\tfrac{1}{2}\log_2\left(1 + SINR_{R_{b_2}D_1}^{x_1}\right) < \tfrac{1}{2}\log_2\left(1 + SINR_{R_{b_2}E}^{x_1}\right) + SC_{th}\right] \\ &= \Pr\left[\tfrac{1}{2}\log_2\left(1 + \tfrac{P_R\alpha_1 g_{2b_2}}{P_R\alpha_2 g_{2b_2}+1}\right) < \tfrac{1}{2}\log_2\left(1 + \tfrac{P_R\alpha_1 g_{4b_2}}{P_R\alpha_2 g_{4b_2}+1}\right) + SC_{th}\right] \\ &= \Pr\left[\tfrac{P_R\alpha_1 g_{2b_2}}{P_R\alpha_2 g_{2b_2}+1} < \theta + (\theta+1)\left(\tfrac{P_R\alpha_1 g_{4b_2}}{P_R\alpha_2 g_{4b_2}+1}\right)\right]. \end{aligned} \tag{7.42}$$

We solve the probability $P_{\mathrm{ST2}}^{out\_D_1}$ similar to the probability $P_{\mathrm{ST1}}^{out\_D_1}$, we also consider the worst case in which the node E can wiretap the data x_1 with the best condition. Hence, the formula (7.42) rewrite an upper constraint of the $P_{\mathrm{ST2}}^{out\_D_1}$ as follows

$$P_{\mathrm{ST2}}^{out\_D_1} \leq P_{\mathrm{ST2}}^{out\_upper} = \Pr\left[\frac{P_R\alpha_1 g_{2b_2}}{P_R\alpha_2 g_{2b_2}+1} < \theta + (\theta+1)\left(P_R\alpha_1 g_{4b_2}\right)\right]. \tag{7.43}$$

After some algebra, the probability of the$P_{\mathrm{ST2}}^{out_D_1}$ can be shown as

$$P_{\mathrm{ST2}}^{out\_D_1} \leq P_{\mathrm{ST2}}^{out\_upper} = \begin{cases} 1 & ,\alpha_1 \leq \theta\alpha_2 \\ \frac{\lambda_2\psi}{(\lambda_1+\lambda_2\psi)} + \frac{\lambda_1\lambda_2 M}{\alpha_2 Q} \times \mathrm{I}_2 & ,\alpha_1 > \theta\alpha_2, \end{cases} \tag{7.44}$$

where $\mathrm{I}_2 = \int\limits_0^{\infty}\int\limits_{px}^{\infty}\left[\begin{array}{l} \exp\left(-\lambda_1 x + nx - \frac{\lambda_4 x}{(\theta+1)\alpha_2 Q} + \frac{\lambda_2 x}{\alpha_2 Q}\right) \\ \times \exp\int\limits_{px}^{\infty}\exp\left(\frac{\lambda_4 x^2}{(\theta+1)\alpha_2 Q\mathrm{z}} - \frac{\lambda_2 z}{\alpha_2 Q}\right) \end{array}\right] dzdx.$

From formulas (7.40) and (7.44), we calculate the sum SOPs of secrecy transmission in the ST2 case is constrained by the upper expression as

$$\begin{aligned} Sum\, P_{\mathrm{ST2}}^{out} &= P_{ST2}^{out\_D_1} + P_{ST2}^{out\_D_2} \\ &\leq \begin{cases} 1 + \left(\lambda_1\lambda_4 \sum\limits_{t=0}^{M}(-1)^t C_M^t \times \frac{Q\alpha_2}{\lambda_1 Q\alpha_2+\lambda_3\theta t} \times \frac{1}{\lambda_4+(\theta+1)\lambda_3 t}\right) & ,\alpha_1 \leq \theta\alpha_2 \\ \left(\frac{\lambda_2\psi}{(\lambda_1+\lambda_2\psi)} + \frac{\lambda_1\lambda_2 M}{\alpha_2 Q} \times \mathrm{I}_2\right) + \left(\lambda_1\lambda_4 \sum\limits_{t=0}^{M}(-1)^t C_M^t \times \frac{Q\alpha_2}{\lambda_1 Q\alpha_2+\lambda_3\theta t} \times \frac{1}{\lambda_4+(\theta+1)\lambda_3 t}\right) & ,\alpha_1 > \theta\alpha_2. \end{cases} \end{aligned} \tag{7.45}$$

7.3.3 The SOP of the secrecy transmission in the proposed UCCN-NOMA system with the best relay selection, called as ST3 case.

With this case, the best relay R_{b_3} based on calculating the minimum channel gain of the R_i-E link. The best relay selection is given as

$$R_{b_3} = \arg \underbrace{\min}_{m=1\ldots M} |h_{R_m E}|^2 = \underbrace{\min}_{m=1\ldots M} |h_{4i}|^2 = g_{4b_3} \tag{7.46}$$

The CDF and cdf of of the random variable g_{4b_3} is given as

$$\begin{aligned} F_{g_{4b_3}}(a) &= \Pr\left[\underbrace{\min}_{i=1\ldots M} g_{4i} < a\right] = 1 - \Pr\left[\underbrace{\min}_{i=1\ldots M} g_{4i} \geq a\right] \\ &= 1 - \prod_{i=1}^{M}\left[1 - F_{g_{4_i}}(a)\right] = \left(1 - e^{-\sum\limits_{i=1}^{M}\lambda_4 a}\right). \end{aligned} \tag{7.47}$$

$$f_{g_{4b_3}}(a) = \frac{\partial F_{g_{4b_3}}(a)}{\partial a} = M\lambda_4 e^{-\sum\limits_{i=1}^{M}\lambda_4 a}. \tag{7.48}$$

The SOP of D_1, D_2 in the ST3 case is performed similar to in two cases ST1 and ST2, and is shown by two math equation, respectively, as follows

$$P_{\text{ST3}}^{out\_D_2} = \Pr\left(SC_{R_{b_3}D_2}^{x_2} < SC_{th}\right) = \Pr\left(R_{R_{b_3}D_2}^{x_2} - R_{R_{b_3}E}^{x_2} \leq SC_{th}\right) \tag{7.49}$$

$$P_{\text{ST3}}^{out\_D_1} = \Pr\left(SC_{R_{b_3}D_1}^{x_1} < SC_{th}\right) = \Pr\left(R_{R_{b_3}D_1}^{x_1} - R_{R_{b_3}E}^{x_1} \leq SC_{th}\right) \tag{7.50}$$

With calculating the same way, finally, we can easily calculate the probability $P_{\text{ST3}}^{out\_D_2}$, $P_{\text{ST3}}^{out\_D_1}$, respectively as

$$P_{\text{ST3}}^{out\_D_2} = 1 \quad - \quad \frac{M\lambda_1\lambda_4}{\left(\lambda_1 + \frac{\lambda_2\theta}{Q\alpha_2}\right)(M\lambda_4 + \lambda_2(\theta+1))} \tag{7.51}$$

-When $\alpha_1 \leq \theta\alpha_2$

$$P_{\text{ST3}}^{out\_D_1} = \int_0^\infty f\gamma_{1i}(x)(1+0)dx = \int_0^\infty \lambda_1 e^{-\lambda_1 x}dx = 1 \tag{7.52a}$$

-When $\alpha_1 > \theta\alpha_2$

$$P_{\text{ST3}}^{out\_D_1} = \left(\frac{\psi\lambda_2}{\lambda_1 + \psi\lambda_2} + \frac{\lambda_1\lambda_2}{\alpha_2 Q} \times \mathrm{I}_3\right) \tag{7.52b}$$

where $\mathrm{I}_3 = \int_0^\infty \int_{px}^\infty \left[\begin{array}{l} \exp\left(-\lambda_1 x + \frac{M\lambda_4\theta}{(\theta+1)\alpha_1 Q}x - \frac{M\lambda_4 x}{(\theta+1)\alpha_2 Q} + \frac{\lambda_2 x}{\alpha_2 Q}\right) \\ \times \exp\int_{px}^\infty \exp\left(\frac{M\lambda_4 x^2}{(\theta+1)\alpha_2 Q\mathrm{z}} - \frac{\lambda_2 z}{\alpha_2 Q}\right) \end{array} \right] dtdx.$

From formulas (7.51), (7.52a) and (7.52b), the $Sum\, P_{\text{ST3}}^{out}$ is obtained as

$$\begin{aligned} Sum\, P_{\text{ST3}}^{out} &= P_{\text{ST3}}^{out\_D_1} + P_{\text{ST3}}^{out\_D_2} \\ &\leq \begin{cases} 1 + \left(1 \quad - \quad \frac{M\lambda_1\lambda_4}{\left(\lambda_1 + \frac{\lambda_2\theta}{Q\alpha_2}\right)(M\lambda_4 + \lambda_2(\theta+1))}\right) & , \alpha_1 \leq \theta\alpha_2 \\ \left(\frac{\psi\lambda_2}{\lambda_1 + \psi\lambda_2} + \frac{\lambda_1\lambda_2}{\alpha_2 Q} \times \mathrm{I}_3\right) + \left(1 \quad - \quad \frac{M\lambda_1\lambda_4}{\left(\lambda_1 + \frac{\lambda_2\theta}{Q\alpha_2}\right)(M\lambda_4 + \lambda_2(\theta+1))}\right) & , \alpha_1 > \theta\alpha_2. \end{cases} \end{aligned} \tag{7.53}$$

The integrals I_1 in (7.35), I_2 in (7.45) and I_3 in (7.53) are the complex, and solving of these integrals is not practical. However, we can use numerical methods to find value of I_1, I_2 and I_3.

7.4 Simulation Results

With system model, we analyzed and evaluated the sum SOPs of secrecy transmission in three cases, namely ST1, ST2, and ST3. The theoretical analyses results are verified by the

Monte Carlo simulations. In the two-dimensional plane, the coordinates of S, R_i, D_1, D_2, Pu and E are set as S(0, 0), R(x_R, 0), D_1(1,0), D_2(x_{D_2}, y_{D_2}), Pu(x_{Pu}, y_{Pu}), E(x_E, y_E) , respectively, satisfying ($0 < x_R, x_{D_2}, x_E$). Therefore $d_{SR_b} = x_R$, $d_{R_bD_1} = x_{D_1} - x_R$, $d_{R_bD_2} = \sqrt{(x_{D_2} - x_R)^2 + y_{D_2}^2}$, $d_{R_bPu} = \sqrt{(x_{Pu} - x_R)^2 + y_{Pu}^2}$ and $d_{R_bE} = \sqrt{(x_E - x_R)^2 + {y_E}^2}$. We assume that the target secrecy capacity and the path-loss exponent are set to constants, $SC_{th} = 1$ (bits/s/Hz) and $\beta = 3$. The value range of β can be from 2 to 7 which depends on the transmission environments. The parameters for simulating and analyzing are summarized in Table 1 as follow.

Tab. 7.1: Simulation parameters.

Symbols	**Parameter Names**	**Values**
β	Path-loss	3
M	Number of Relay	3
α_1,α_2	Power allocation coefficients	0.8;0.2
SC_{th}	Threshold	0.7,1(bit/s/Hz)
d_{R_bPu}	Distance of R_b-Pu link	1
$d_{R_bD_1}$	Distance of R_b-D_1 link	0.5
$d_{R_bD_2}$	Distance of R_b-D_2 link	0.6,1
d_{R_bE}	Distance of R_b-E link	1-3

Figure 7.3 shows the sum SOPs of secrecy transmission in three cases ST1, ST2 and ST3 versus Q(dB) when the symmetric network model is examined the parameters as M=3, $\alpha_1 = 0.8$, $\alpha_2 = 0.2$, $\beta = 3$, SC_{th}=1(bit/s/Hz), $d_{R_bPu} = 1$, $d_{R_bD_1} = 0.5$, $d_{R_bD_2} = 1$, $d_{R_bE} = 1$. With the results shown in Figure 7.3, we can see that the secrecy performance of the ST3 is good than the ST1 and ST2. Besides, the sum SOPs of the ST1, ST2 and ST3 decrease when the Q(dB) raise because of the increment of transmit powers. It can be explained by applying the NOMA technique and selecting the best relay method.

Figure 7.4 shows the security performance versus the position of the eavesdropper node E when the symmetric network model is performed with M=3, $\alpha_1 = 0.8$, $\alpha_2 = 0.2$, $\beta = 3$, Q(dB)=10dB, SC_{th}=1(bit/s/Hz) and d_{R_bE} changes from 1 to 3. As shown in Figure 7.4, the security performance of the ST3 case is also smaller than the ST1 and ST2 case. The simulation results and the theoretical results are reasonable. Furthermore, we can see that when the value d_{R_bE} increases, the security performance becomes good than in three cases. It means that the security of the system is very well when eavesdropper node E is far from the relays.

In Figure 7.5, shows the sum SOPs of secrecy transmission in three cases ST1, ST2 and ST3 versus Q(dB) when the symmetric network model is examined the parameters as M=3, $\alpha_1 = 0.8$, $\alpha_2 = 0.2$, $\beta = 3$, $d_{R_bPu} = 1$, $d_{R_bD_1} = 0.5$, $d_{R_bD_2} = 1$, $d_{R_bE} = 1$. We compare the secrecy performance in two cases of thresholds security capacity: SC_{th}=0.7(bit/s/Hz) and SC_{th}=1(bit/s/Hz). It is clear that the security capacity is the lower, the secrecy

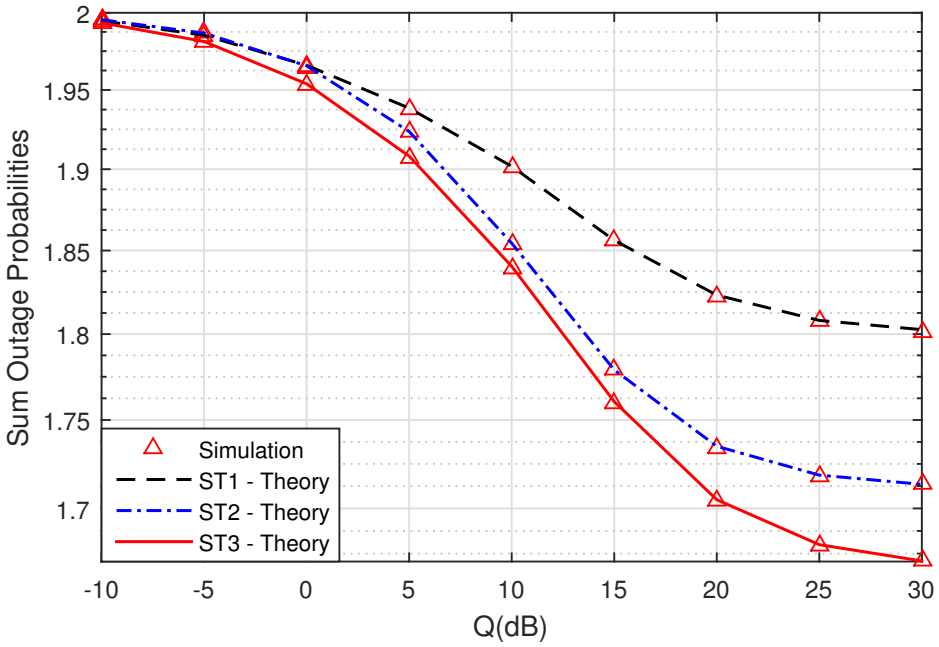

Figure 7.3: The sum SOPs of the UCCN-NOMA system versus Q(dB) when M=3, $\alpha_1 = 0.8$, $\alpha_2 = 0.2$, $\beta = 3$ and SC_{th}=1(bit/s/Hz).

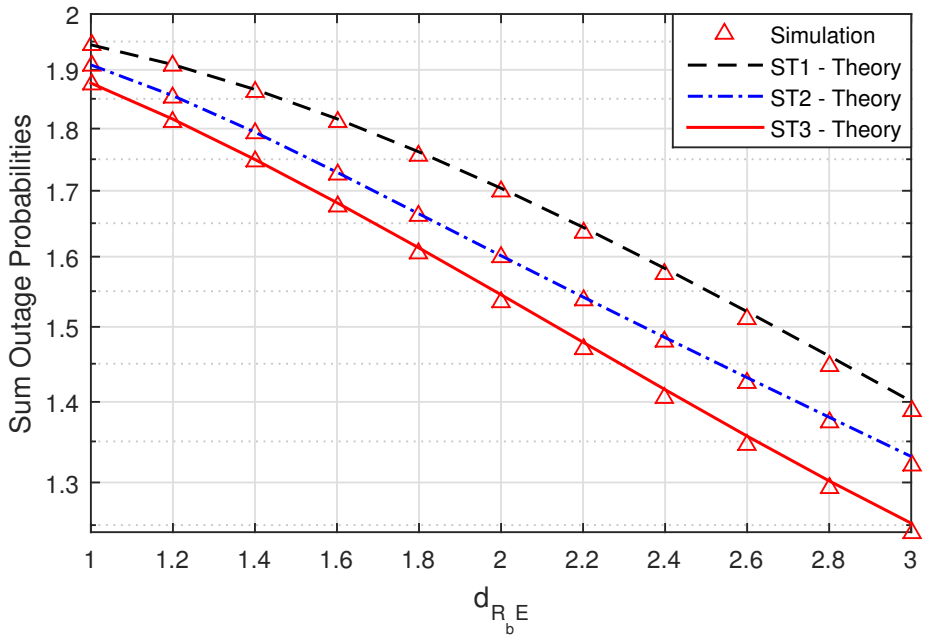

Figure 7.4: The sum SOPs of the UCCN-NOMA system versus d_{R_bE} when M=3, $\alpha_1 = 0.8$, $\alpha_2 = 0.2$, $\beta = 3$ and SC_{th}=1(bit/s/Hz).

performance becomes more efficient. In addition, as shown in Figure 7.5, the simulation results are suitable to the theoretical results in three cases of security transmission. .

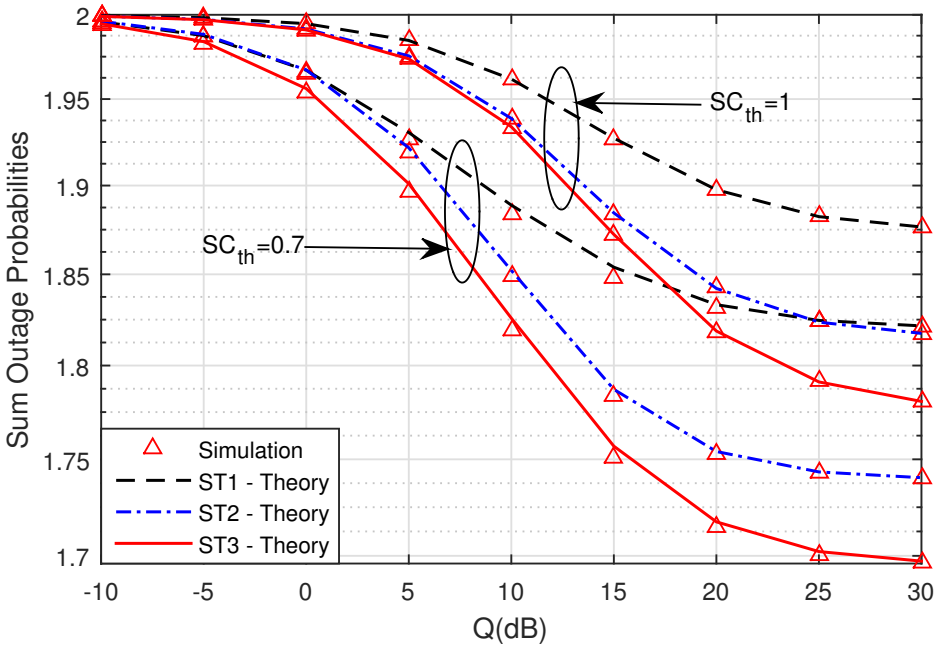

Figure 7.5: The sum SOPs of the UCCN-NOMA system versus Q(dB) when M=3, $\alpha_1 = 0.8$, $\alpha_2 = 0.2$, $\beta = 3$, SC$_{th}$=0.7(bit/s/Hz) and SC$_{th}$=1(bit/s/Hz).

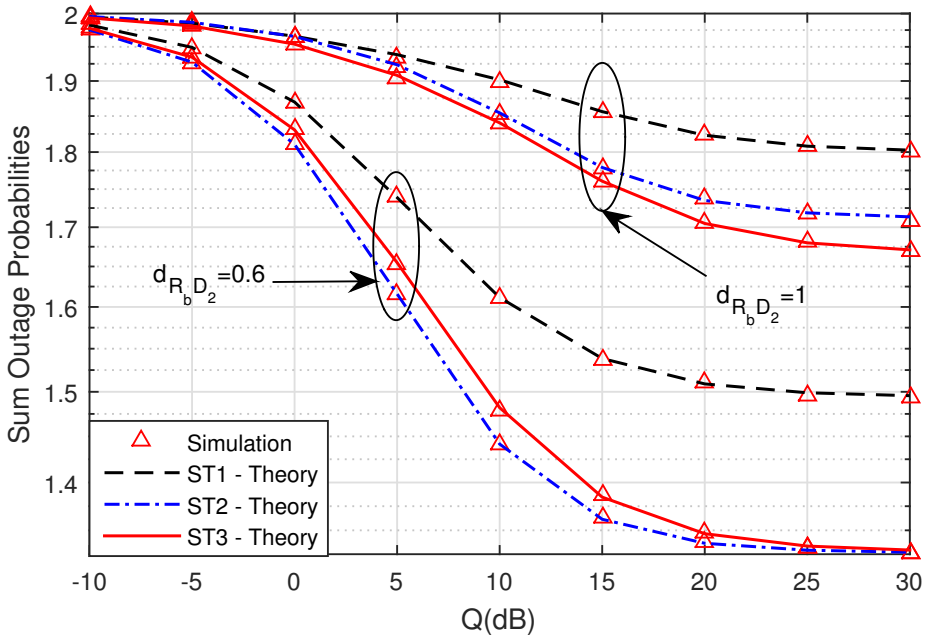

Figure 7.6: The sum SOPs of the UCCN-NOMA system versus Q(dB) when M=3, $\alpha_1 = 0.8$, $\alpha_2 = 0.2$, $\beta = 3$, SC$_{th}$=1(bit/s/Hz), $d_{R_bD_2} = 0.6$ and $d_{R_bD_2} = 1$.

Figure 7.6 represents the sum SOPs versus Q (dB) when M=3, $\alpha_1 = 0.8$, $\alpha_2 = 0.2$, $\beta = 3$, SC$_{th}$=1(bit/s/Hz), $d_{R_bD_2} = 0.6$ and $d_{R_bD_2} = 1$. The secrecy performance of the ST1, ST2,

and ST3 reduce at the higher Q(dB) regions. It means that the proposed UCCN system used NOMA solution, and apply PLS with the best relay selection, so achieves higher secrecy efficiency. Besides, we can see that when link distance $d_{R_bD_2} = 0.6$ is security performance of system good than the $d_{R_bD_2} = 1$.

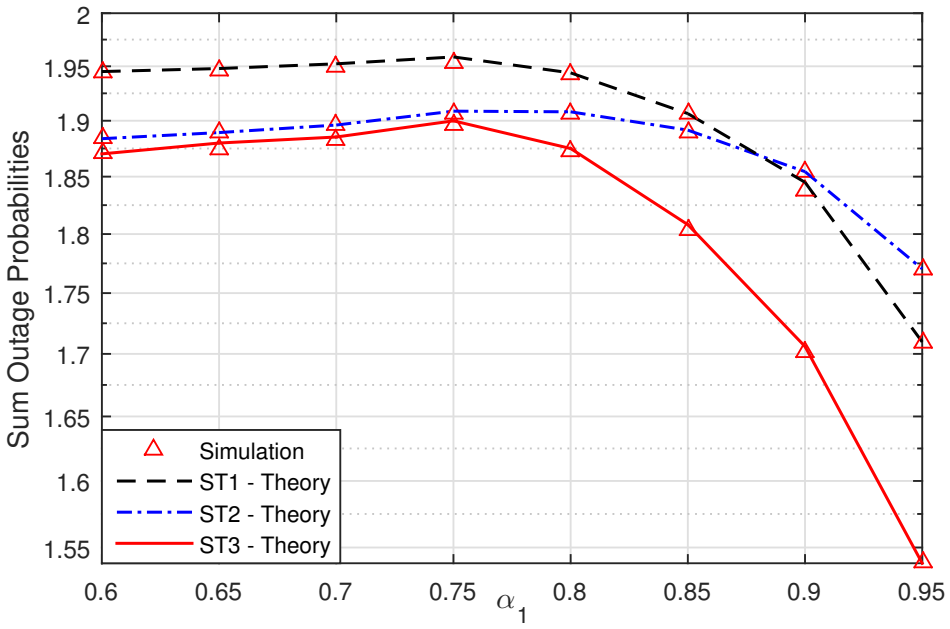

Figure 7.7: The sum SOPs of the UCCN-NOMA system versus α_1 when M=3, $\beta = 3$ and SC_{th}=1(bit/s/Hz).

In Figure 7.7, we shows the security performance of the UCCN system using the NOMA technology under the impact of power allocation coefficients. As illustrates in this figure, we consider the effects of varying α_1 and α_2 on system. When α_1 rises, the SOPs of the secrecy transmission of the signals x_1 and x_2 decrease and move to small values. We can see that the power allocation coefficients in Figure 7.7 can make significant capacity gains in the UCCN system using the NOMA and the best relay selection solution.

7.5 Conclusions

We investigated the secrecy for Underlay Cooperative Cognitive Network in which multiple relays using the NOMA technology. We researched the three strategies of relay selection. The first case and second case, the best relay was calculated base on the maximum channel of the link R_i-D_1 and R_i-D_2, respectively. In the third case, we found the best relay by calculating the minimum value of the channel gains from the R_i-E link. We analyzed and evaluated the secrecy performance of UCCN system using NOMA technology in terms of the secrecy outage probabilities based on Rayleigh fading channels. Besides, the proposed scheme using NOMA and PLS improved secrecy performances. In addition, the security

performance in the system model obtained better when the distance between eavesdropper E and the best relay was far together. Finally, theory analyses and the simulations results proved the tight accuracy.

8 CONCLUSIONS AND FUTURE WORK

The thesis considered potential benefits of cooperative relaying in conventional wireless and cognitive radio networks, include: Two-Way scheme, Multiple Relay scheme. Base on these scheme, we applied the methods such as AF, DF, Relay selection, EH and NOMA to propose the protocols to improve the reliability, throughput performance and enhance the data rate. In addition, the best important research work of this dissertation was to use the NOMA technique combine with PLS in the UCCN having many relays. The achieved results have shown that the proposed system model increase QoS , and security performance. Finally, we analyzed and evaluated the system performance in terms of exact closed-form outage probabilities over Rayleigh fading channels. Furthermore, the theoretical analyses were verified by performing Monte Carlo simulation results.

8.1 Summary of Results and Insights

There are three the main goals of the thesis as follows. Parts of the thesis, which are dedicated to the **Goal 1**, we can find in Chapter 4 and Chapter 5, where Two-Way Energy Harvesting cooperative relaying protocol and multi-relay cooperative protocols (EHAF, EHDF) with the best relay selection method in wireless communication networks were proposed and analyses. **Goal 2** was presented in Chapter 6, where the Two-Way NOMA cooperative relaying protocol to enhance transmission efficiency was investigated. **Goal 3** was presented in Chapter 7, where multiple relays NOMA scheme in Underlay Cooperative Cognitive Network for enhancing secrecy performances was studied.

All three goals of the thesis specified in Chapter 3 were fulfilled. **Goal 1** was published in [HTP02], [HTP03] and [HTP05] with Two-Way cooperative relaying scheme and multi-hop relaying scheme for enhancing throughput performance and improving the range of wireless communication. **Goal 2** was published in the articles [HTP04] and proposed with Two-Way NOMA protocol for enhancing the spectral performance and overcome the disadvantages of the fading environment. **Goal 3** was published in paper [HTP01] and proposed the security system for the UCCN using NOMA to improve the secrecy performance.

In light of the investigated obtained of this dissertation is the hypothesis given: It is possible to apply the NOMA technology for the development of 5G networks. Such application would contribute to the security efficiency of wireless communications.

8.2 Future Work

To finish the thesis, some works in the future are mentioned with the details as follows.

In this dissertation, we have investigated different cooperative methods in wireless communication networks, but each user has assumed only a private antenna. However,

in practice, each user can have many antennas for receiving and sending the signal. This problem will be interesting, and this is an attractive research topic.

As shown in Chapter 7. We have just only researched the NOMA in the one-way system with multi-relay. In order to enhance system reliability, the Two-Way scheme, in this case, needs to be researched and designed.

In this thesis, we only present the wireless cooperative network with assumption each node being stationary. However, in mobile ad-hoc networks, each node can move to different places, so the security system needs to thorough considered. So this problem will be one of our future researches.

REFERENCES

[1] Zhong and Z. Zhang, "Non-Orthogonal Multiple Access With Cooperative Full-Duplex Relaying," in *IEEE Communications Letters*, vol. 20, no. 12, pp. 2478-2481, Dec. 2016.

[2] Z. Ding, F. Adachi, and H. V. Poor, "The application of MIMO to non orthogonal multiple access," *IEEE Trans. Wireless Communications.*, vol. 15, no. 1, pp. 537–552, Jan 2016.

[3] S. Ali, E. Hossain and D. I. Kim, "Non-Orthogonal Multiple Access (NOMA) for Downlink Multiuser MIMO Systems: User Clustering, Beamforming, and Power Allocation," in *IEEE Access*, vol. 5, pp. 565-577, 2017.

[4] Z. Yang, J. A. Hussein, P. Xu, Z. Ding and Y. Wu, "Power Allocation Study for Non-Orthogonal Multiple Access Networks With Multicast-Unicast Transmission," in *IEEE Transactions on Wireless Communications*, vol. 17, no. 6, pp. 3588-3599, June 2018.

[5] Y. Wu, L. P. Qian, H. Mao, X. Yang, H. Zhou and X. Shen, "Optimal Power Allocation and Scheduling for Non-Orthogonal Multiple Access Relay-Assisted Networks," in *IEEE Transactions on Mobile Computing*, vol. 17, no. 11, pp. 2591-2606, 1 Nov. 2018.

[6] M. F. Sohail, C. Y. Leow and S. Won, "Non-Orthogonal Multiple Access for Unmanned Aerial Vehicle Assisted Communication," in *IEEE Access*, vol. 6, pp. 22716-22727, 2018.

[7] Z. Ding, M. Peng and H. V. Poor, "Cooperative Non-Orthogonal Multiple Access in 5G Systems," in *IEEE Communications Letters*, vol. 19, no. 8, pp. 1462-1465, Aug. 2015.

[8] S. M. R. Islam, N. Avazov, O. A. Dobre and K. Kwak, "Power-Domain Non-Orthogonal Multiple Access (NOMA) in 5G Systems: Potentials and Challenges," in *IEEE Communications Surveys Tutorials*, vol. 19, no. 2, pp. 721-742, Secondquarter 2017.

[9] L. Dai, B. Wang, Z. Ding, Z. Wang, S. Chen and L. Hanzo, "A Survey of Non-Orthogonal Multiple Access for 5G," in *IEEE Communications Surveys Tutorials*, vol. 20, no. 3, pp. 2294-2323, thirdquarter 2018.

[10] K. J. R. Liu et al., "Cooperative Communication and Networking," *New York: Cambridge University Press*, 2009.

[11] P. N. Son and H. Y. Kong, "Cooperative communication with energy-harvesting relays under physical layer security," in *IET Communications*, vol. 9, no. 17, pp. 2131-2139, 11 26 2015.

[12] K. Xie, X. Wang, X. Liu, J. Wen and J. Cao, "Interference-Aware Cooperative Communication in Multi-Radio Multi-Channel Wireless Networks," in *IEEE Transactions on Computers*, vol. 65, no. 5, pp. 1528-1542, 1 May 2016.

[13] L. C. Tran, A. Mertins, X. Huang and F. Safaei, "Comprehensive Performance Analysis of Fully Cooperative Communication in WBANs," in *IEEE Access*, vol. 4, pp. 8737-8756, 2016.

[14] J. W. Raymond, T. O. Olwal and A. M. Kurien, "Cooperative Communications in Machine to Machine (M2M): Solutions, Challenges and Future Work," in *IEEE Access*, vol. 6, pp. 9750-9766, 2018.

[15] H. Cui, L. Song, and B. Jiao, "Multi-Pair Two-Way Amplify-and-Forward Relaying with Very Large Number of Relay Antennas," *IEEE Transactions on Wireless Communications*, vol. 13, pp. 2636-2645, 2014.

[16] S. Luo and K. C. Teh, "Amplify-and-Forward Based Two-Way Relay ARQ System With Relay Combination," in *IEEE Communications Letters*, vol. 19, no. 2, pp. 299-302, Feb. 2015.

[17] D. Li, "Amplify-and-Forward Relay Sharing for Both Primary and Cognitive Users, " *IEEE Transactions on Vehicular Technology*, vol. 65, no, 4, pp. 2796-2801, 2016.

[18] S. H. Alvi, S. Wyne," Error analysis of fixed-gain AF relaying with MRC over Nakagami-m fading channels," *Radioengineering*, vol. 25, no. 1, pp. 106–113,2016.

[19] Y. Dong, M. J. Hossain and J. Cheng, "Performance of Wireless Powered Amplify and Forward Relaying Over Nakagami-m Fading Channels With Nonlinear Energy Harvester," in *IEEE Communications Letters*, vol. 20, no. 4, pp. 672-675, April 2016.

[20] S. Li et al., "Full-Duplex Amplify-and-Forward Relaying: Power and Location Optimization," in *IEEE Transactions on Vehicular Technology*, vol. 66, no. 9, pp. 8458-8468, Sept. 2017.

[21] K. M. Rabie and B. Adebisi, "Enhanced Amplify-and-Forward Relaying in Non-Gaussian PLC Networks," in *IEEE Access*, vol. 5, pp. 4087-4094, 2017.

[22] M. R. Bhatnagar, R. K. Mallik and O. Tirkkonen, "Performance Evaluation of Best-Path Selection in a Multihop Decode-and-Forward Cooperative System," in *IEEE Transactions on Vehicular Technology*, vol. 65, no. 4, pp. 2722-2728, April 2016.

[23] Y. Gu and A. S, "RF-Based Energy Harvesting in Decode-and-Forward Relaying Systems: Ergodic and Outage Capacities," *IEEE Transactions on Wireless Communications*, vol. 14, pp. 6425-6434, 2015.

[24] G. T. Djordjevic, K. Kansanen and A. M. Cvetkovic, "Outage Performance of Decode-and-Forward Cooperative Networks Over Nakagami- m Fading With Node Blockage," in *IEEE Transactions on Wireless Communications*, vol. 15, no. 9, pp. 5848-5860, Sept. 2016.

[25] T. T. Duy and H. Y. Kong, "Performance analysis of mixed amplify-and-forward and decode-and-forward protocol in underlay cognitive networks," in *China Communications*, vol. 13, no. 3, pp. 115-126, March 2016.

[26] H. Liu, Z. Ding, K. J. Kim, K. S. Kwak and H. V. Poor, "Decode-and-Forward Relaying for Cooperative NOMA Systems With Direct Links," in *IEEE Transactions on Wireless Communications*, vol. 17, no. 12, pp. 8077-8093, Dec. 2018.

[27] R. Fan, S. Atapattu, W. Chen, Y. Zhang and J. Evans, "Throughput Maximization for Multi-Hop Decode-and-Forward Relay Network With Wireless Energy Harvesting," in *IEEE Access*, vol. 6, pp. 24582-24595, 2018.

[28] O. M. Kandelusy and S. M. H. Andargoli, "Outage performance of decode-and-forward (DF)-based multiuser spectrum sharing relay system with direct link in the presence of primary users' power," in *IET Communications*, vol. 12, no. 3, pp. 246-254, 20 2 2018.

[29] E. Li, X. Wang, Z. Wu, S. Hao and Y. Dong, "Outage Analysis of Decode-and-Forward Two-Way Relay Selection With Different Coding and Decoding Schemes," in *IEEE Systems Journal*, vol. 13, no. 1, pp. 125-136, March 2019.

[30] P. N. Son and H. Y. Kong, "Exact outage probability of two-way decode-and-forward scheme with opportunistic relay selection under physical layer security," *Wireless personal communications*, vol. 77, pp. 2889-2917, 2014.

[31] K. Tutuncuoglu, B. Varan and A. Yener, "Throughput Maximization for Two-Way Relay Channels With Energy Harvesting Nodes: The Impact of Relaying Strategies," in *IEEE Transactions on Communications*, vol. 63, no. 6, pp. 2081-2093, June 2015.

[32] Q. F. Zhou, W. H. Mow, S. Zhang and D. Toumpakaris, "Two-Way Decode-and-Forward for Low-Complexity Wireless Relaying: Selective Forwarding Versus One-Bit Soft Forwarding," in *IEEE Transactions on Wireless Communications*, vol. 15, no. 3, pp. 1866-1880, March 2016.

[33] W. Li, M. Ku, Y. Chen and K. J. Ray Liu, "On Outage Probability for Two-Way Relay Networks With Stochastic Energy Harvesting," in *IEEE Transactions on Communications*, vol. 64, no. 5, pp. 1901-1915, May 2016.

[34] X. Jia, C. Zhang and I. Kim, "Optimizing Wireless Powered Two-Way Communication System With EH Relays and Non-EH Relays," in *IEEE Transactions on Vehicular Technology*, vol. 67, no. 11, pp. 11248-11252, Nov. 2018.

[35] K. Belbase, C. Tellambura and H. Jiang, "Two-Way Relay Selection for Millimeter Wave Networks," in *IEEE Communications Letters*, vol. 22, no. 1, pp. 201-204, Jan. 2018.

[36] A. Koc, I. Altunbas and E. Basar, "Two-Way Full-Duplex Spatial Modulation Systems With Wireless Powered AF Relaying," in IEEE Wireless Communications Letters, vol. 7, no. 3, pp. 444-447, June 2018.

[37] S. Modem and S. Prakriya, "Optimization of Two-Way Relaying Networks With Battery-Assisted EH Relays," in *IEEE Transactions on Communications*, vol. 66, no. 10, pp. 4414-4430, Oct. 2018.

[38] C. Kong, C. Zhong, M. Matthaiou, E. Björnson and Z. Zhang, "Multipair Two-Way Half-Duplex DF Relaying With Massive Arrays and Imperfect CSI," in *IEEE Transactions on Wireless Communications*, vol. 17, no. 5, pp. 3269-3283, May 2018.

[39] K. Lee, J. Hong, H. Choi and T. Q. S. Quek, "Wireless-Powered Two-Way Relaying Protocols for Optimizing Physical Layer Security," in IEEE Transactions on Information Forensics and Security, vol. 14, no. 1, pp. 162-174, Jan. 2019.

[40] C. Ren, H. Zhang, J. Wen, J. Chen and C. Tellambura, "Successive Two-Way Relaying for Full-Duplex Users With Generalized Self-Interference Mitigation," in *IEEE Transactions on Wireless Communications*, vol. 18, no. 1, pp. 63-76, Jan. 2019.

[41] K. H. Liu, "Performance Analysis of Relay Selection for Cooperative Relays Based on Wireless Power Transfer With Finite Energy Storage," *IEEE Transactions on Vehicular Technology*, vol. 65, pp. 5110-5121, 2016.

[42] Y. Wu, L. p. Qian, L. Huang and X. Shen, "Optimal Relay Selection and Power Control for Energy-Harvesting Wireless Relay Networks," in IEEE Transactions on Green Communications and Networking, vol. 2, no. 2, pp. 471-481, June 2018.

[43] F. Wang, S. Guo, Y. Yang and B. Xiao, "Relay Selection and Power Allocation for Cooperative Communication Networks With Energy Harvesting," in *IEEE Systems Journal*, vol. 12, no. 1, pp. 735-746, March 2018.

[44] M. G. Khafagy, M. Alouini and S. Aïssa, "Full-Duplex Relay Selection in Cognitive Underlay Networks," in *IEEE Transactions on Communications*, vol. 66, no. 10, pp. 4431-4443, Oct. 2018.

[45] P. Xu, Z. Yang, Z. Ding and Z. Zhang, "Optimal Relay Selection Schemes for Cooperative NOMA," in *IEEE Transactions on Vehicular Technology*, vol. 67, no. 8, pp. 7851-7855, Aug. 2018.

[46] S. Chu, "Secrecy Analysis of Modify-and-Forward Relaying With Relay Selection," in *IEEE Transactions on Vehicular Technology*, vol. 68, no. 2, pp. 1796-1809, Feb. 2019.

[47] Y. Feng, S. Yan, C. Liu, Z. Yang and N. Yang, "Two-Stage Relay Selection for Enhancing Physical Layer Security in Non-Orthogonal Multiple Access," in IEEE Transactions on Information Forensics and Security, vol. 14, no. 6, pp. 1670-1683, June 2019.

[48] A. Nasir, X. Zhou, S. Durrani, and R. A. Kennedy, "Relaying Protocols for Wireless Energy Harvesting and Information Processing," *IEEE Transactions on Wireless Communications*, vol. 12, pp. 3622-3636, 2013.

[49] S. Q Nguyen, H.Y. KONG, "Generalized diversity combining of energy harvesting multiple antenna relay networks: outage and throughput performance analysis". Annals of Telecommunications , vol. 71, no. 5, pp. 265-277, 2016.

[50] R. Vahidnia, A. Anpalagan, and J. Mirzaei, "Achievable Rate Region for Energy Harvesting Asynchronous Two-Way Relay Networks," *IEEE Access*, vol. 4, pp. 951-958, 2016.

[51] H. Chen, G. Li, and J. Cai, "Spectral–Energy Energy Efficiency Tradeoff in Full-Duplex Two-Way Relay Networks," *IEEE Systems Journal*, vol. PP, pp. 1-10, 2015.

[52] O. Ozel, S. Ulukus and P. Grover, "Energy Harvesting Transmitters That Heat Up: Throughput Maximization Under Temperature Constraints," in *IEEE Transactions on Wireless Communications*, vol. 15, no. 8, pp. 5440-5452, Aug. 2016.

[53] S. Atapattu and J. Evans, "Optimal Energy Harvesting Protocols for Wireless Relay Networks," in *IEEE Transactions on Wireless Communications*, vol. 15, no. 8, pp. 5789-5803, Aug. 2016.

[54] L. Lei, Y. Kuang, X. S. Shen, K. Yang, J. Qiao and Z. Zhong, "Optimal Reliability in Energy Harvesting Industrial Wireless Sensor Networks," in *IEEE Transactions on Wireless Communications*, vol. 15, no. 8, pp. 5399-5413, Aug. 2016.

[55] L. Zhang, J. Liu, M. Xiao, G. Wu, Y. C. Liang and S. Li, "Performance Analysis and Optimization in Downlink NOMA Systems With Cooperative Full-Duplex Relaying," in *IEEE Journal on Selected Areas in Communications*, vol. 35, no. 10, pp. 2398-2412, Oct. 2017.

[56] Z. Zhou, M. Peng, Z. Zhao, W. Wang and R. S. Blum, "Wireless-Powered Cooperative Communications: Power-Splitting Relaying With Energy Accumulation," in *IEEE Journal on Selected Areas in Communications*, vol. 34, no. 4, pp. 969-982, April 2016.

[57] F. Fang, H. Zhang, J. Cheng, S. Roy and V. C. M. Leung, "Joint User Scheduling and Power Allocation Optimization for Energy-Efficient NOMA Systems With Imperfect CSI," in *IEEE Journal on Selected Areas in Communications*, vol. 35, no. 12, pp. 2874-2885, Dec. 2017.

[58] M. Noor-A-Rahim, M. O. Khyam and Y. L. Guan, "Energy harvesting two-way relaying with antenna selection scheme," in *IET Communications*, vol. 13, no. 2, pp. 198-204, 2019.

[59] F. Delgosha and F. Fekri, "Public-key cryptography using paraunitary matrices," IEEE Transactions on Signal Processing, vol. 54, no. 9, pp. 3489-3504,Sept 2006.

[60] T. Q. Duong, T. M. Hoang, C. Kundu, M. Elkashlan and A. Nallanathan, "Optimal Power Allocation for Multiuser Secure Communication in Cooperative Relaying Networks," in IEEE Wireless Communications Letters, vol. 5, no. 5, pp. 516-519, Oct. 2016.

[61] F. Pan, Y. Jiang, H. Wen, R. Liao and A. Xu, "Physical Layer Security Assisted 5G Network Security," 2017 IEEE 86th Vehicular Technology Conference (VTC-Fall), Toronto, ON, 2017, pp. 1-5.

[62] L. Sun and Q. Du, "Physical layer security with its applications in 5G networks: A review," in *China Communications*, vol. 14, no. 12, pp. 1-14, December 2017.

[63] Y. Wu, A. Khisti, C. Xiao, G. Caire, K. Wong and X. Gao, "A Survey of Physical Layer Security Techniques for 5G Wireless Networks and Challenges Ahead," in *IEEE Journal on Selected Areas in Communications*, vol. 36, no. 4, pp. 679-695, April 2018.

[64] H. Wang, L. Xu, W. Lin, P. Xiao and R. Wen, "Physical Layer Security Performance of Wireless Mobile Sensor Networks in Smart City," in *IEEE Access*, vol. 7, pp. 15436-15443, 2019.

[65] K. Ho-Van, "Outage Analysis of Opportunistic Relay Selection in Underlay Cooperative Cognitive Networks Under General Operation Conditions," in *IEEE Transactions on Vehicular Technology*, vol. 65, no. 10, pp. 8145-8154, Oct. 2016.

[66] C. Zhang et al., "Secrecy Outage Analysis on Underlay Cognitive Radio System With Full-Duplex Secondary User," in *IEEE Access*, vol. 5, pp. 25696-25705, 2017.

[67] B. Zhong and Z. Zhang, "Opportunistic Two-Way Full-Duplex Relay Selection in Underlay Cognitive Networks," in *IEEE Systems Journal*, vol. 12, no. 1, pp. 725-734, March 2018.

[68] S. Lee, T. Q. Duong, D. B. da Costa, D. Ha and S. Q. Nguyen, "Underlay cognitive radio networks with cooperative non-orthogonal multiple access," in *IET Communications*, vol. 12, no. 3, pp. 359-366, 20 2 2018.

[69] P. N. Son and T. T. Duy, "Performance analysis of Underlay Cooperative Cognitive Full-duplex Networks with Energy-Harvesting Relay," *Computer Communications,* vol. 2018, no. 122, pp. 9-19, March 2018.

[70] A. Bletsas, H. Shin and M. Z. Win, "Outage optimality of opportunistic amplify-and-forward relaying," in *IEEE Communications Letters*, vol. 11, no. 3, pp. 261-263, March 2007.

[71] S. Wyne, S. Alvi, "On amplify-and-forward relaying over Hyper-Rayleigh fading channels," *Radioengineering* ,vol.23, no.4, p. 1226-1233,2014.

[72] N. Nguyen, T. Q. Duong, H. Q. Ngo, Z. Hadzi-Velkov and L. Shu, "Secure 5G Wireless Communications: A Joint Relay Selection and Wireless Power Transfer Approach," in *IEEE Access*, vol. 4, pp. 3349-3359, 2016.

[73] Y. Liu, L. Wang, M. Elkashlan, T. Q. Duong and A. Nallanathan, "Two-way relay networks with wireless power transfer: design and performance analysis," in *IET Communications*, vol. 10, no. 14, pp. 1810-1819, 20 9 2016.

[74] A. Minasian, S. ShahbazPanahi and R. S. Adve, "Energy Harvesting Cooperative Communication Systems," in *IEEE Transactions on Wireless Communications*, vol. 13, no. 11, pp. 6118-6131, Nov. 2014.

[75] Z. Ding, S. M. Perlaza, I. Esnaola and H. V. Poor, "Power Allocation Strategies in Energy Harvesting Wireless Cooperative Networks," in *IEEE Transactions on Wireless Communications*, vol. 13, no. 2, pp. 846-860, February 2014.

[76] P. Mekikis, A. S. Lalos, A. Antonopoulos, L. Alonso and C. Verikoukis, "Wireless Energy Harvesting in Two-Way Network Coded Cooperative Communications: A Stochastic Approach for Large Scale Networks," in *IEEE Communications Letters*, vol. 18, no. 6, pp. 1011-1014, June 2014.

[77] T. Li, P. Fan and K. B. Letaief, "Outage Probability of Energy Harvesting Relay-Aided Cooperative Networks Over Rayleigh Fading Channel," in *IEEE Transactions on Vehicular Technology*, vol. 65, no. 2, pp. 972-978, Feb. 2016.

[78] C. Zhai, J. Liu, " Cooperative wireless energy harvesting and information transfer in stochastic networks," *EURASIP Journal on Wireless Communications and Networking*, vol. 2015, no.1, p.44, 2015.

[79] Z. Hadzi-Velkov, N. Zlatanov, T. Q. Duong and R. Schober, "Rate Maximization of Decode-and-Forward Relaying Systems With RF Energy Harvesting," in *IEEE Communications Letters*, vol. 19, no. 12, pp. 2290-2293, Dec. 2015.

[80] P.N. Son, H.Y. Kong, "Exact outage analysis of energy harvesting underlay cooperative cognitive networks," *IEICE Transactions on Communications*, Vol. 98, no. 4, p. 661-672. 2015.

[81] D. Zwillinger, "Table of integrals, series, and products, " *Academic Press*, 2014.

[82] J. Li, M. Matthaiou and T. Svensson, "I/Q Imbalance in Two-Way AF Relaying," in *IEEE Transactions on Communications*, vol. 62, no. 7, pp. 2271-2285, July 2014.

[83] J. Qi, S. Aïssa and M. Alouini, "Impact of I/Q imbalance on the performance of two-way CSI-assisted AF relaying," 2013 *IEEE Wireless Communications and Networking Conference (WCNC)*, Shanghai, pp. 2507-2512, 2013.

[84] N. T. Do, V. N. Q. Bao and B. An, "A relay selection protocol for wireless energy harvesting relay networks," 2015 *International Conference on Advanced Technologies for Communications (ATC)*, Ho Chi Minh City, pp. 243-247, 2015,

[85] E.K.P. Chong, S.H. Zak," An Introduction to Optimization, " *Wiley, United States*, 2nd ed, 2001.

[86] C. Zhang, J. Ge, J. Li, Y. Rui, and M. Guizani, "A Unified Approach for Calculating the Outage Performance of Two-Way AF Relaying Over Fading Channels," *IEEE Transactions on Vehicular Technology*, vol. 64, no. 3, pp. 1218-1229, Mar. 2015.

[87] P. N. Son, H. Y. Kong, "Improvement of the two-way decode-and-forward scheme by energy harvesting and digital network coding relay," *Transactions on Emerging Telecommunications Technologies (ETT)*, vol. 28, no. 3, pp. 1-14, March 2017.

[88] J. B. Kim and I. H. Lee, "Capacity Analysis of Cooperative Relaying Systems Using Non-Orthogonal Multiple Access," *IEEE Communications Letters*, vol. 19, no. 11, pp. 1949-1952, Nov. 2015.

[89] R. Jiao, L. Dai, J. Zhang, R. MacKenzie, and M. Hao, "On the Performance of NOMA-Based Cooperative Relaying Systems over Rician Fading Channels," *IEEE Transactions on Vehicular Technology* , vol.PP, no.99, pp.1-1, Jul. 2017.

[90] S. Lee, D. Benevides da Costa and T. Q. Duong, "Outage probability of non-orthogonal multiple access schemes with partial relay selection," 2016 *IEEE 27th*

Annual International Symposium on Personal, Indoor, and Mobile Radio Communications (PIMRC), pp. 1-6, Valencia, 2016.

[91] A. Jeffrey, D. Zwillinger, "Table of integrals, series, and products," *Academic Press*, 2007.

[92] T. Srivantana, K.Maichalernnukul, "Two-Way Multi-Antenna Relaying with Simultaneous Wireless Information and Power Transfer," *Symmetry*, 9, 42. 2017.

[93] Wu, F.; Xiao, L.; Yang, D.; Cuthbert, L.; Liu, X. Transceiver Design and Power Allocation for SWIPT in MIMO Cognitive Radio Systems. *Symmetry* 2018, 10, 647.

[94] Z. Ding, X. Lei, G. K. Karagiannidis, R. Schober, J. Yuan and V. K. Bhargava, "A Survey on Non-Orthogonal Multiple Access for 5G Networks: Research Challenges and Future Trends," in *IEEE Journal on Selected Areas in Communications*, vol. 35, no. 10, pp. 2181-2195, Oct. 2017.

[95] T.T.H. Ly, H.S. Nguyen, T. S. Nguyen, V. V. Huynh, T. L. Nguyen, M. Voznak," Outage Probability Analysis in Relaying Cooperative Systems with NOMA Considering Power Splitting," *Symmetry*, 11, 72. 2019.

[96] Y. Liu, Z. Ding, M. Elkashlan and H. V. Poor, "Cooperative Non-orthogonal Multiple Access With Simultaneous Wireless Information and Power Transfer," in *IEEE Journal on Selected Areas in Communications*, vol. 34, no. 4, pp. 938-953, April 2016.

[97] S. Lee, D. B. da Costa, Q. Vien, T. Q. Duong and R. T. de Sousa, "Non-orthogonal multiple access schemes with partial relay selection," in *IET Communications*, vol. 11, no. 6, pp. 846-854, 20 4 2017.

[98] T. T. Duy, T. Q. Duong, T. L. Thanh and V. N. Q. Bao, "Secrecy performance analysis with relay selection methods under impact of co-channel interference," in *IET Communications*, vol. 9, no. 11, pp. 1427-1435, 23 7 2015.

[99] B. Maide, C. Riccardo, F. Luigi, F. Mattia, R. Alessandro," Does chaos work better than noise?," *CircuitsCircuits Syst.* Mag, 2, 4–19, 2003.

[100] P. Arena, S. Fazzino, L. Fortuna, P. Maniscalco," Game theory and non-linear dynamics: The Parrondo Paradox case study," *Chaos Solitons Fract*, vol 17, pp. 545–555, 2003.

[101] L. Fan, X. Lei, N. Yang, T. Q. Duong and G. K. Karagiannidis, "Secrecy Cooperative Networks With Outdated Relay Selection Over Correlated Fading Channels," in *IEEE Transactions on Vehicular Technology*, vol. 66, no. 8, pp. 7599-7603, Aug. 2017.

[102] B. He, A. Liu, N. Yang and V. K. N. Lau, "On the Design of Secure Non-Orthogonal Multiple Access Systems," in *IEEE Journal on Selected Areas in Communications*, vol. 35, no. 10, pp. 2196-2206, Oct. 2017.

[103] J. Chen, L. Yang and M. Alouini, "Physical Layer Security for Cooperative NOMA Systems," in *IEEE Transactions on Vehicular Technology*, vol. 67, no. 5, pp. 4645-4649, May 2018.

[104] X. Liu, Y. Wang, S. Liu and J. Meng, "Spectrum Resource Optimization for NOMA-Based Cognitive Radio in 5G Communications," in *IEEE Access*, vol. 6, pp. 24904-24911, 2018.

[105] L. Lv, J. Chen and Q. Ni, "Cooperative Non-Orthogonal Multiple Access in Cognitive Radio," in *IEEE Communications Letters*, vol. 20, no. 10, pp. 2059-2062, Oct. 2016.

[106] S. Lee, T. Q. Duong, D. B. da Costa, D. Ha, S.Q. Nguyen," Underlay cognitive radio networks withcooperative non-orthogonal multiple access," *IET Communications*, vol 12, 359–366, 2018.

[107] L. Lv, J. Chen, Q. Ni and Z. Ding, "Design of Cooperative Non-Orthogonal Multicast Cognitive Multiple Access for 5G Systems: User Scheduling and Performance Analysis," in *IEEE Transactions on Communications*, vol. 65, no. 6, pp. 2641-2656, June 2017.

[108] X. Ding, T. Song, Y. Zou and X. Chen, " Relay selection for secrecy improvement in cognitive amplify-and-forward relay networks against multiple eavesdroppers," in *IET Communications*, vol. 10, no. 15, pp. 2043-2053, 13 10 2016.

[109] Y. Liu, L. Wang, T. T. Duy, M. Elkashlan and T. Q. Duong, " Relay Selection for Security Enhancement in Cognitive Relay Networks," in *IEEE Wireless Communications Letters*, vol. 4, no. 1, pp. 46-49, Feb. 2015.

[110] B. Li, X. Qi, K. Huang, Z. Fei, F. Zhou and R. Q. Hu, "Security-Reliability Tradeoff Analysis for Cooperative NOMA in Cognitive Radio Networks," in *IEEE Transactions on Communications*, vol. 67, no. 1, pp. 83-96, Jan. 2019.

[111] P.N. Son, D. Har, N. I. Cho, H. Y. Kong, " Optimal Power Allocation of Relay Sensor Node Capable of Energy Harvesting in Cooperative Cognitive Radio Network," *Sensors* vol 17, 648, 2017.

[112] I. S. Gradshteyn, I. M. Ryzhik, A. Jerey, and D. Zwillinger, Table of integrals, series and products, 7th ed. Amsterdam Boston: Elsevier, 2007.

CANDIDATE'S RESEARCH CITED IN THE THESIS

Articles in journals indexed in WoS/Scopus

[HTP01] **Tan-Phuoc Huynh**, P.N. Son, M. Voznak, "Secrecy Performance of Underlay Cooperative Cognitive Network Using Non-Orthogonal Multiple Access with Opportunistic Relay Selection," *Symmetry*, vol. 11, no. 3, March. 2019. DOI: 10.3390/sym11030385.

[HTP02] **Tan-Phuoc Huynh**, P.N. Son, M. Voznak "Exact Throughput Analyses of Energy-Harvesting Cooperation Scheme with Best Relay Selections Under I/Q Imbalance," *Advances in Electrical and Electronic Engineering (AEEE)*, vol. 15, no. 4, pp. 585-590, Nov. 2017. DOI: 10.15598/aeee.v15i4.2302.

Other papers in proceedings of conferences indexed in WoS/Scopus

[HTP03] **Tan-Phuoc Huynh**, T. N. Kieu, T. D. Dinh, M. Voznak and D. Uhrin, "A performance analysis about impact of I/Q imbalance in AF two-hop relay system,"*XI International Symposium on Telecommunications (BIHTEL 2016)*", pp. 1-4, Sarajevo, 2016.

[HTP04] **Tan-Phuoc Huynh**, P.N. Son, M. Voznak, "Exact Outage Probability of Two-Way Decode-and-Forward NOMA Scheme with digital network coding," *The 2nd International Conference on Recent Advances in Signal Processing, Telecommunications Computing (SigTelCom 2018)*, pp. 102-106, Ho Chi Minh City, Vietnam, 2018.

[HTP05] **Tan-Phuoc Huynh**, P.N. Son, M. Voznak," Exact Outage Probability of Two-Way Decode-and-Forward Scheme with Energy Harvesting from Intermediate Relaying Station," *the 3rd EAI International Conference on Industrial Networks and Intelligent Systems (INISCOM 2017)*, Ho Chi Minh City, Vietnam, September 4–6, 2017.

LIST OF CANDIDATE'S RESEARCH RESULTS AND ACTIVITIES

Publication activities

I provide the following list indexed results in relevant scientific databases, in order to document my research activities within the entire period of my doctoral study:

- articles indexed in **WoS/Scopus**: 2 articles
- conference papers indexed in **WoS/Scopus**: 5 papers

Project memberships and participations

- Specific research, SGS FEI VSB-TU Ostrava, project SP2018/170, **Knowledge retrieval in communications networks, modelling and simulation - II**.
- Specific research, SGS FEI VSB-TU Ostrava, project SP2017/82, **Knowledge retrieval in communications networks, modelling and simulation - I**.

Other results indexed in conference proceedings of WoS, Scopus, IEEE-Xplore (2 publications: [HTP06], [HTP07])

In addition, I also have achieved the results not directly related to my thesis and They have indexed in conference proceedings of WoS, Scopus, IEEE-Xplore.

[HTP06] **Tan-Phuoc Huynh**, Hoang-Sy Nguyen, Dinh-Thuan Do, Miroslav Voznak, "Impact of hardware impairments in AF relaying network for WIPT: TSR and performance analysis," *Jan 2016 International Conference on Electronics, Information, and Communications (ICEIC)*, 2016.

[HTP07] Hoang-S.N, Hai Nguyen, Sau Dang-Sau, M. Voznak, **Tan-Phuoc Huynh**, "Impact of hardware impairments for power splitting relay with wireless information and EH", *Jan 2016 International Conference on Electronics, Information, and Communications (ICEIC)*, 2016.

APPENDIX A

A1. Proof of the Lemma 1 - Solving formula (7.23)

From formula (7.27), we calculate A_1 as follows

$$\begin{aligned}\mathrm{A}_1 &= \mathrm{P}_\mathrm{r}\left[\frac{g_{2b_1}x}{(\theta+1)\left(Qg_{2b_1}\alpha_2+x\right)} \leq \frac{\theta x}{(\theta+1)Q\alpha_1}\right] \\ &= \mathrm{P}_\mathrm{r}\left[\frac{g_{2b_1}(\theta+1)Q\alpha_1}{(\theta+1)\left(Qg_{2b_1}\alpha_2+x\right)\theta} \leq 1\right] = \mathrm{P}_\mathrm{r}\left[g_{2b_1}Q\left(\alpha_1-\theta\alpha_2\right) \leq x\theta\right] \\ &= \begin{cases} 1 & ,\alpha_1 \leq \alpha_2\theta \\ F_{g_{2b_1}}\left[\frac{x\theta}{Q(\alpha_1-\alpha_2\theta)}\right] & ,\alpha_1 > \alpha_2\theta \end{cases}\end{aligned} \tag{A.1}$$

Applying the CDF of the RV g_{2b_1} (7.17) into (A.1), A.1 is solved in a closed-form expression as

$$A_1 = \begin{cases} 1 & ,\alpha_1 \leq \alpha_2\theta \\ \left(1-e^{-\lambda_2\psi x}\right)^M & ,\alpha_1 > \alpha_2\theta \end{cases} \tag{A.2}$$

where $\psi = \frac{\theta}{Q(\alpha_1-\theta\alpha_2)}$

.

Hence, Appendix A1 is proven completely.

A2. Proof of Lemma 2 - Solving formula (7.24)

To solve Lemma 2, we calculate A_2 in (7.22) as follows

$$\begin{aligned}\mathrm{A}_2 &= \Pr\left[g_{4b_1} > \frac{g_{2b_1}x}{(\theta+1)\left(\alpha_2Qg_{2b_1}+x\right)} - \frac{\theta x}{(\theta+1)Q\alpha_1}, \frac{g_{2b_1}x}{(\theta+1)\left(\alpha_2Qg_{2b_1}+x\right)} > \frac{\theta x}{(\theta+1)Q\alpha_1}\right] \\ &= \Pr\left[g_{4b_1} > \frac{g_{2b_1}x}{(\theta+1)\left(\alpha_2Qg_{2b_1}+x\right)} - \frac{\theta x}{(\theta+1)\alpha_1Q}, Qg_{2b_1}\left(\alpha_1-\theta\alpha_2\right) > \theta x\right] \\ &= \begin{cases} 0, \alpha_1 \leq \theta\alpha_2 \\ \int\limits_{\psi x}^{\infty} f_{g_{2b_1}}(y) P_r\left[g_{4b_1} > \frac{xy}{(\theta+1)(\alpha_2Qy+x)} - \frac{\theta x}{(\theta+1)\alpha_1Q}\right] dy, \alpha_1 > \theta\alpha_2 \end{cases}\end{aligned} \tag{A.3}$$

Solving (A.3) by using the pdf of the random variable g_{2b_1} and the CDF of the random variable g_{4b_1}, A.3 is obtained as

$$\mathrm{A}_2 = \begin{cases} 0 & ,\alpha_1 \leq \theta\alpha_2 \\ \int\limits_{\psi x}^{\infty} f_{g_{2b_1}}(y)\, e^{-\lambda_4\left(\frac{xy}{(\theta+1)(\alpha_2Qy+x)} - \frac{\theta x}{(\theta+1)Q\alpha_1}\right)} dxdy & ,\alpha_1 > \theta\alpha_2. \end{cases} \tag{A.4}$$

Hence, Appendix A2 is proven completely.